Ion Cyclotron Resonance Studies of Inorganic Molecules in the Gas Phase. I. Organotransition Metal Complexes. II. Chain Reactions Involving Ionic Intermediates.

Thesis by

Reed Roeder Corderman

In Partial Fulfillment of the Requirements

for the Degree of

Doctor of Philosophy

California Institute of Technology

Pasadena, California

1977

(Submitted May 9, 1977)

ACKNOWLEDGMENTS

I wish to thank my advisor, Professor J. L. Beauchamp, for his continuing guidance, assistance, and especially encouragement during the course of my graduate studies at Caltech.

I take great pleasure in acknowledging the many contributions, both great and small, of my friend Ralph H. Staley to my graduate education. I have greatly enjoyed our many camping trips in the mountains and deserts of California.

Many of my fellow colleagues have been of much assistance to me at various stages of this work. Several in particular whom I would like to thank include Richard L. Woodin, Sally A. Sullivan, Michael S. Foster, Ashley D. Williamson, and D. Wayne Berman. A collective acknowledgment is made to many others, and especially to Joyce L. Lundstedt, who contributed magnificently by her technical assistance.

Finally, I express my appreciation to the California Institute of Technology for financial support during the term of my graduate studies.

ABSTRACT

A brief introduction (Chapter I) gives a general overview of the results presented in this thesis, and is followed by five chapters which concern ion cyclotron resonance spectroscopy (ICR) studies of transition metal complexes, trifluorophosphine, and methylsilanes in the gas phase. An ancillary study on the photoionization mass spectrometry (PIMS) of the methylsilanes is also included.

Chapter II discusses the gas phase ion chemistry of $(\eta^5\text{-}C_5H_5)NiNO$. The dissociative bond energies, $D(B\text{–}CpNi^+)$ $[Cp \equiv \eta^5\text{–}C_5H_5]$, are obtained by measuring equilibrium constants for reactions involving $CpNi^+$ transfer between appropriate base pairs. A wide variety of reactions effected by $CpNi^+$, including dehydrohalogenation, dehydration, dehydrogenation, decarbonylation, and alkylation processes are observed, and reaction mechanisms proposed.

Chapter III presents a detailed study of the sequential alkylation of $CpNi^+$ and $CpFe^+$ by d_3-methyl bromide. A reaction mechanism involving oxidative addition of the metal to the weak carbon-bromine σ-bond is presented.

The first observed example of a ligand displacement reaction involving an anionic transition metal complex, in which PF_3 displaces CO from $CpCo(CO)^-$, is reported in Chapter IV. This result leads directly to the conclusion that PF_3 is a stronger π-acceptor ligand than CO towards $CpCo^-$ in the gas phase. Additionally, the negative ion chemistry of $CpCo(CO)_2$ both alone and in mixtures with various

ligands is presented.

The gas phase basicity, or proton affinity, of phosphorus trifluoride is determined in Chapter V. The results are discussed in terms of contributions from inductive and hyperconjugative interactions involving $p_\pi - d_\pi$ bonding in HPF_3^+. Ion-molecule reactions of mixtures of PF_3 with SiF_4, BF_3, SF_6, NF_3, CH_3F, and $(CH_3)_2CO$ are briefly considered; various thermochemical considerations are used to determine the energetics of formation of the PF_2^+, PF_4^+, and $CH_3PF_3^+$ ions observed in these mixtures.

Several examples of gas phase chain reaction which proceed through ionic intermediates are presented in Chapter VI. Chain propagation reactions involve hydride and fluoride transfer between pairs of siliconium ions R_1^+ and carbonium ions R_2^+, for which $D(R_1^+-F^-) \geq D(R_2^+-F^-)$ and $D(R_1^+-H^-) \leq D(R_2^+-H^-)$.

Photoionization efficiency for the low energy fragment ions $(P-H)^+$, $(P-H_2)^+$, and $(P-CH_4)^+$ for the series of methylsilanes, $(CH_3)_nH_{4-n}Si$ (n = 0-3), are reported in Chapter VII. Appearance potentials for the $(P-H)^+$ siliconium ion fragments afford accurate calculation of the hydride affinities, $D(R_3Si^+-H^-)$ of these species.

TABLE OF CONTENTS

CHAPTER I

INTRODUCTION

While the ion-molecule reactions of both organic and non-metallic inorganic species in the gas phase have received much attention in the past twenty-five years,[1-6] only recently has investigation of the ion chemistry of compounds containing transition metal elements commenced.[7-15] The techniques of ion cyclotron resonance mass spectroscopy (ICR),[6] in particular, are proving to be invaluable in the study of the ion chemistry of organotransition metal complexes.[6-13] ICR experiments are performed at low pressures ($\approx 10^{-6}$ Torr) in the gas phase and provide quantitative information relating to the intrinsic properties and reactivity of the species considered, in the absence of complicating solvation phenomena. Mechanistic studies involving the use of deuterium labelled isotopes are readily implemented, and serve to elucidate reaction mechanisms which may have solution analogs. ICR studies of organotransition complexes may be especially valuable in providing insights into the energetics and mechanisms of reaction which may be important in further understanding processes that involve homogeneous[16] and heterogeneous catalysis.[17]

Foster and Beauchamp were the first to bring attention to the potential of ICR mass spectroscopy for the study of transition metal complexes in a communication on the ion-molecule reactions of $Fe(CO)_5$.[7] This study demonstrated that polynuclear metal clusters

are copiously produced, that rapid displacement of CO by a variety of n- and π-donor, mono- and polydentate ligands occurs, and, most interestingly, that oxidative-addition reactions are facile (eq. 1).

$$(CH_3)_2F^+ + Fe(CO)_5 \begin{cases} \longrightarrow CH_3Fe(CO)_5^+ + CH_3F & (1) \\ \longrightarrow CH_3Fe(CO)_4^+ + CO + CH_3F & (2) \end{cases}$$

Several other investigations of organotransition metal complexes have recently been reported,[11-15] and additional processes in which oxidative insertion of a transition metal cation into a polar C–X bond (X = H, Cl, Br, I, OH) occurs are known.[12,15]

Chapters II and III describe many such oxidative insertion reactions which are effected by the $CpNi^+$($Cp \equiv \eta^5$-C_5H_5) cation. These reactions include dehydrohalogenation, dehydration, dehydrogenation, decarbonylation,[10] and alkylation processes; reaction mechanisms for each case are proposed and discussed.

A second objective of the ICR study of organotransition metal ions is the quantitative determination of metal-ligand bond strengths. Binding energies of $CpNi^+$ to 31 n-donor ligands are obtained by measuring equilibrium constants for reactions involving $CpNi^+$ transfer between appropriate base pairs (eq. 2).[9] Measurement of

$$CpNiB_1^+ + B_2 \overset{K_{eq}}{\rightleftharpoons} CpNiB_2^+ + B_1 \qquad (2)$$

these K_{eq} (eq. 2) yields the relative free energy difference of binding B_1 and B_2 to $CpNi^+$ through the use of eq. 3, and subsequently

$$\Delta G = -RT\ell nK_{eq} \qquad (3)$$

$D(B\text{-}CpNi^+)$, by assuming that ΔS is zero except for small corrections due to changes in symmetry numbers.[18] A scale of $D(B\text{-}CpNi^+)$ is thus obtained, with reference to $D(NO\text{-}CpNi^+) = 45.9$ Kcal/mol, determined from photoionization mass spectrometric (PIMS) measurement of IP(CpNiNO) and $AP(CpNi^+)$. Most significantly, the results of Chapter II provide the first direct measurements of the relative contributions of σ- and π-bonding interactions to the strengths of transition metal-ligand bonds.[9]

Chapter IV reports the first observed example of a ligand displacement reaction involving an anionic transition metal complex, in which PF_3 displaces CO from $CpCo(CO)^-$. This result leads directly to the conclusion that PF_3 is a stronger π-acceptor ligand than CO towards $CpCo^-$ in the gas phase. While equilibrium ligand exchange processes analogous to eq. 2 are not observed, these results suggest that by starting with a metal anion with weakly bound π-acceptor ligands [e.g., $CpCo(PMe_3)^-$ or $Fe(CO)_3(PMe_3)^-$], a quantitative scale of π-acceptor ability can be measured using ICR techniques, as such scales for H^+,[19] Li^+,[20] and $CpNi^+$[9] have been constructed.

A study ancillary to the results of Chapters II-IV is presented in Chapter V of the ion chemistry and gas phase basicity, or proton affinity, of phosphorus trifluoride. In mixtures of PF_3 with CH_3F, the $CH_3PF_3^+$ ion is observed, and may have either the protonated methylene phosphorane[21] or difluorophosphine methyl fluoronium ion[22] structures. The energetics of formation of HPF_3^+, $CH_3PF_3^+$,

PF_2^+, and PF_4^+ are discussed.

Only a very few non-branching chain reactions which proceed through ionic intermediates have been characterized in the gas phase,[23,24] in vivid contrast to solution, where such processes are important in the Ziegler-Natta polymerization of ethylene.[25] Aside from their intrinsic interest, ionic chain reactions might have significant chemical applications, for example: (1) detection of ionizing radiation, (2) detection of the initially ionized neutral species in the event that it forms or is itself the chain carrier, and (3) detection of a species which interrupts the chain process. During the course of recent studies of the fluoromethyl silanes,[26] it became evident that there may be a large number of chain reactions generalized in equation 4 in which Si–H and C–F bonds are interconverted to Si–F

$$\equiv Si{-}H + \equiv C{-}F \rightarrow \equiv Si{-}F + \equiv C{-}H \qquad (4)$$

and C–H bonds. Several examples of gas phase reactions which proceed through ionic intermediates in mixtures of methylsilanes, $(CH_3)_nH_{4-n}Si$ (n = 0-3) with fluorocarbons are presented in Chapter VI. Chain propagation reactions involve hydride and fluoride transfer between pairs of siliconium ions R_1^+ and carbonium ions R_2^+, for which $D(R_1^+-F^-) \geq D(R_2^+-F^-)$ and $D(R_1^+-H^-) \leq D(R_2^+-H^-)$, such that the overall process is represented by equation 4.

Photoionization efficiency curves for the low energy fragment ions $(P-H)^+$, $(P-H_2)^+$, and $(P-CH_4)^+$ for the methylsilanes are reported in Chapter VII. Appearance potentials for the $(P-H)^+$

siliconium ion fragments afford accurate calculation of the hydride affinities, $D(R_3Si^+-H^-)$, of these species, and are important to the interpretation of data presented in Chapter VI.

References and Notes

(1) P. Ausloos, Ed. "Ion-Molecule Reaction in the Gas Phase", Advances in Chemistry Series, No. 58, Amer. Chem. Soc., Washington, D. C., 1966.

(2) J. H. Futrell and T. O. Tiernan in "Fundamental Processes in Radiation Chemistry", P. Ausloos, Ed., Wiley, New York, N.Y., 1968, Chapter 4.

(3) E. W. McDaniel, V. Čermák, A. Dalgarno, E. E. Ferguson, and L. Friedman, "Ion-Molecule Reactions", Wiley-Interscience, New York, N.Y., 1970.

(4) J. L. Franklin, Ed., "Ion-Molecule Reactions", v. 1 and 2, Plenum Press, New York, N.Y., 1972.

(5) S. G. Lias and P. Ausloos, "Ion-Molecule Reactions. Their Role in Radiation Chemistry", Amer. Chem. Soc., Washington, D.C., 1975.

(6) For recent reviews of ion cyclotron resonance spectroscopy see J. L. Beauchamp, Annu. Rev. Phys. Chem., 22, 527 (1971); T. A. Lehman and M. M. Bursey, "Ion Cyclotron Resonance Spectrometry", Wiley, New York, N.Y., 1976.

(7) M. S. Foster and J. L. Beauchamp, J. Am. Chem. Soc., 93, 4924 (1971).

(8) M. S. Foster and J. L. Beauchamp, J. Am. Chem. Soc., 97, 4808, 4814 (1975); R. R. Corderman and J. L. Beauchamp, Inorg. Chem., 15, 665 (1976).

(9) R. R. Corderman and J. L. Beauchamp, J. Am. Chem. Soc.,

98, 3998 (1976).

(10) R. R. Corderman and J. L. Beauchamp, J. Am. Chem. Soc., 98, 5700 (1976).

(11) R. D. Bach, A. T. Weibel, J. Patane, and L. Kevan, J. Am. Chem. Soc., 98, 6237 (1970); R. D. Bach, J. Gauglhofer, and L. Kevan, ibid., 94, 6860 (1972); R. D. Bach, J. Patane, and L. Kevan, J. Org. Chem., 40, 257 (1975).

(12) J. Allison and D. P. Ridge, J. Organomet. Chem., 99, C11 (1975); J. Allison and D. P. Ridge, J. Am. Chem. Soc., 98, 7445 (1976); J. Allison and D. P. Ridge, ibid., 99, 35 (1977); G. H. Weddle, J. Allison, and D. P. Ridge, ibid., 99, 105 (1977).

(13) R. C. Dunbar, J. F. Ennever, and J. P. Fackler, Jr., Inorg. Chem., 12, 2734 (1973); R. C. Dunbar and B. B. Hutchinson, J. Am. Chem. Soc., 96, 3816 (1974); P. P. Dymerski, R. C. Dunbar, and J. V. Dugan, Jr., J. Chem. Phys., 61, 298 (1974); J. H. Richardson, L. M. Stephenson, and J. I. Brauman, J. Am. Chem. Soc., 96, 3671 (1974).

(14) S. M. Schildcrout, J. Phys. Chem., 80, 2834 (1976); S. M. Schildcrout, J. Am. Chem. Soc., 95, 3845 (1973); J. L. Garnett, I. K. Gregor, and D. Nelson, Inorg. Chim. Acta, 18, L12 (1976); E. Schumacher and R. Taubenest, Helv. Chim. Acta, 47, 1525 (1964); G. D. Flesch, R. M. White, and H. J. Svec, Int. J. Mass Spectrom. Ion Phys., 3, 339 (1969); W. P. Anderson, N. Hsu, C. W. Stanger, Jr., and

B. Munson, J. Organomet. Chem., 69, 249 (1974); J. R. Gilbert, W. P. Leach, and J. R. Miller, ibid., 56, 295 (1973); D. F. Hunt, J. W. Russell, and R. L. Torian, ibid., 43, 175 (1972).

(15) J. Müller, Adv. Mass Spectrom., 6, 823 (1974) and references contained therein.

(16) A. L. Robinson, Science, 194, 1150, 1261 (1976).

(17) J. H. Sinfelt, Science, 195, 641 (1977); J. H. Sinfelt, Acc. Chem. Res., 10, 15 (1977).

(18) S. W. Benson, J. Am. Chem. Soc., 80, 5151 (1958).

(19) J. F. Wolf, R. H. Staley, I. Koppel, M. Taagepera, R. T. McIver, Jr., J. L. Beauchamp, and R. W. Taft, J. Am. Chem. Soc., submitted for publication; P. Kebarle, R. Yamdagni, K. Hiraoka, and T. B. McMahon, Int. J. Mass Spectrom. Ion Phys., 19, 71 (1976).

(20) R. H. Staley and J. L. Beauchamp, J. Am. Chem. Soc., 97, 5920 (1975).

(21) H. Lischka, J. Am. Chem. Soc., 99, 353 (1977).

(22) The $F_2PFCH_3^+$ ion is isoelectronic with F_2POCH_3 [D. R. Martin and P. J. Pizzolato, J. Am. Chem. Soc., 72, 4584 (1950)].

(23) K. Bansal and G. R. Freeman, Radiat. Res. Rev., 3, 209 (1971).

(24) T. B. McMahon, R. J. Blint, D. P. Ridge, and J. L. Beachamp, J. Am. Chem. Soc., 94, 8934 (1972); R. J. Blint, T. B. McMahon, and J. L. Beauchamp, ibid., 96, 1269 (1974); J. L. Beauchamp and J. Y. Park, J. Phys. Chem., 80, 575 (1976).

(25) R. T. Morrison and R. N. Boyd, "Organic Chemistry", 2nd ed., Allyn and Bacon, Boston, MA, 1966, p. 266.

(26) M. K. Murphy and J. L. Beauchamp, J. Am. Chem. Soc., 98, 5781 (1976).

CHAPTER II

Properties and Reactions of $(\eta^5\text{-}C_5H_5)NiNO$ by Ion Cyclotron Resonance Spectroscopy. Quantitative Metal-Ligand Bond Dissociation Energies and Oxidative Addition Reactions of $(\eta^5\text{-}C_5H_5)Ni^+$ With Organic Molecules

Reed R. Corderman and J. L. Beauchamp

Contribution No. 5577 from the Arthur Amos Noyes Laboratory of Chemical Physics, California Institute of Technology, Pasadena, California 91125

ABSTRACT

The gas-phase ion chemistry of (η^5-cyclopentadienyl) nickel nitrosyl (CpNiNO) is studied using the techniques of ion cyclotron resonance spectroscopy. Photoionization efficiency curves for ions derived from CpNiNO have been recorded. The ionization potential of the molecule is determined to be 8.21 ± 0.03 eV. The lowest energy fragmentation process involves loss of NO to give $CpNi^+$ with an ionization threshold of 10.20 ± 0.03 eV, leading to $D(NO-CpNi^+)$ = 45.9 ± 1.0 kcal/mol. Total rate constants and product distributions for reaction of the molecular ion and of the major fragment ions formed at 70 eV electron energy are determined using trapped-ion methods. Binding energies of $CpNi^+$ to 31 n-donor bases are obtained by measuring equilibrium constants for reactions involving transfer of this ion between appropriate base pairs. An excellent correlation of proton and $CpNi^+$ base strengths is observed, except for those molecules which are expected to have substantial π-bonding ability to nickel. A wide variety of reactions are effected by interaction of $CpNi^+$ with organic molecules, usually involving oxidative addition to σ-bonds. Observed processes include dehydrohalogenation, dehydration, dehydrogenation, decarbonylation, and alkylation reactions. Reaction mechanisms for these processes are proposed and discussed in detail. The gas phase basicity or proton affinity of CpNiNO is determined to be 198 ± 4 kcal/mole relative to $PA(NH_3)$ = 202.3 ± 2.0 kcal/mol. The site of protonation is most likely on the cyclopentadienyl ring. The base strength of CpNiNO toward CH_3^+ as a reference acid is briefly considered.

Introduction

The investigation of the ion chemistry of metals and organometallic complexes by ion cyclotron resonance spectroscopy (ICR) serves not only to characterize the nature and strengths of metal-ligand bonds,[1-5] but also reveals a rich chemistry associated with the chemical transformation of organic molecules effected by their interaction with metal complexes.[1-10] The first extensive ICR study[11] of an organometallic complex, $Fe(CO)_5$,[1,2] demonstrated that polynuclear metal clusters $Fe_n(CO)_m^+$ (n = 1-4; m = 0-12) are produced, that rapid displacement of CO by a variety of n- and π-donor, mono- and polydentate bases occurs, and that oxidation of the transition metal cation is a facile process. So copious is the production of polynuclear metal species and ligand displacement product ions, that no quantitative data relating to transition metal-ligand bond dissociation energies could be obtained for this system.[1,2] In ICR investigations of ferrocene[12] and nickelocene,[13] reaction sequences in which significant quantities of acid-base complexes with σ- and π-donor bases such as H_2O, NH_3, and benzene were not observed. Presumably this is due to the inherent stability which results from strong interaction of metal centers with cyclopentadienyl rings. Thus both $Fe(CO)_5$ and the metallocenes Cp_2Fe and Cp_2Ni are poor choices for studies in which the objective is to determine metal-ligand bond strengths. Such studies require a system in which condensation reactions leading to polynuclear complexes are slow, and which, for simplicity, has a single exchangeable weakly bound ligand. An attractive candidate is (η^5–cyclopentadienyl) nickel

nitrosyl (CpNiNO), which Müller has already shown, using high pressure mass spectrometry, to participate in reaction sequences leading to the formation of ions $CpNiB^+$ in the presence of σ- and π-donor ligands, B.[11, 14]

In the present study, the positive ion chemistry of CpNiNO, both alone and in mixtures with a wide variety of organic compounds, is examined, substantially expanding results previously reported.[5, 6] The energetics of molecular and fragment ion formation from CpNiNO are examined using photoionization mass spectrometry, leading to an accurate value for the bond dissociation energy $D(NO-CpNi^+)$. This value serves as the reference for the values $D(B-CpNi^+)$ determined for 31 n-donor bases by measuring equilibrium constants for reactions involving transfer of $CpNi^+$ between appropriate base pairs.

A variety of interesting reactions are initiated by interaction of the abundant fragment ion $CpNi^+$ with organic molecules. Observed transformations include sequential alkylation of the reactant ion, decarbonylation of aldehydes,[6] and elimination reactions (Scheme I).

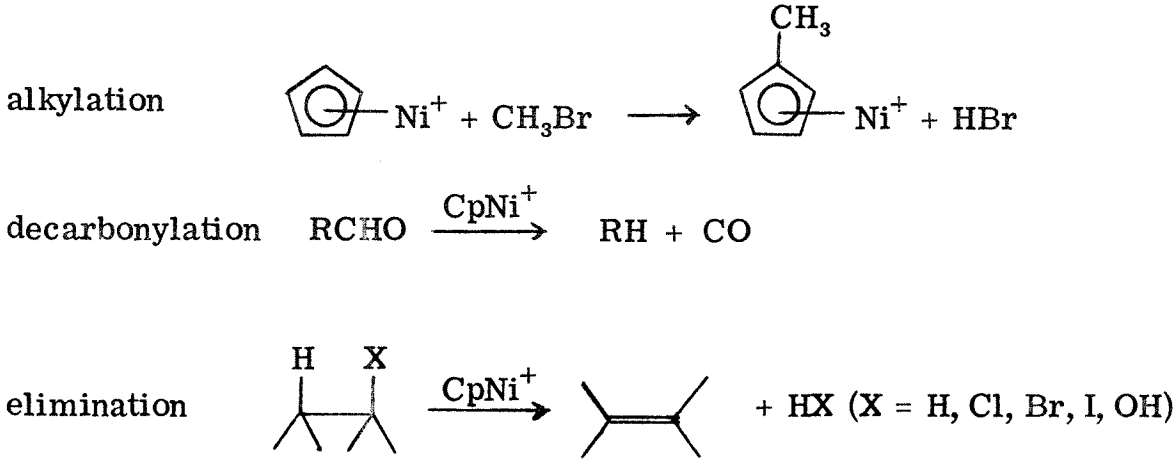

Scheme I

Studies of the mechanism of these processes suggest in every case an initial step involving oxidative insertion of $CpNi^+$ into polar C–X bonds (X = H, Cl, Br, I, OH).[15] In the case of the decarbonylation and elimination reactions, the more basic product remains bound to the metal center in $CpNi^+$. The gas phase basicity of CpNiNO towards both H^+ and CH_3^+ as reference acids is determined. Previous reports of the ion chemistry of CpNiNO using high pressure mass spectrometry,[14] the He(I) photoelectron spectrum of CpNiNO,[16] and ab initio calculations of the electronic structures of CpNiNO[16, 17] and CpNi·[18] are useful in the interpretation of the present results.

Experimental Section

The theory and instrumentation of ICR mass spectrometry have been previously described.[19-21] This work employed an instrument constructed at the California Institute of Technology equipped with a 15-inch electromagnet capable of a maximum field strength of 23.4 kG.

Cyclopentadienyl nickel nitrosyl was obtained commercially (Strem Chemicals Inc., Danvers, Mass.) and used without further purification; no impurities were observed in the ICR mass spectrum. Because of the high vapor pressure of CpNiNO at 25 °C (mp = 41 °C, bp_{15} = 47-48 °C[22]), the sample was kept in an ice water bath during use to prevent it from condensing in the spectrometer inlet. All other chemicals used in this study were readily available from commercial sources. Before use, each sample was degassed by repeated freeze-pump-thaw cycles.

Pressures were measured with a Schulz-Phelps type ion gauge calibrated against an MKS Baratron Model 90H1-E capacitance manometer in a manner previously described.[23] The estimated uncertainty in absolute pressures, and thus in all rate constants reported, is ± 20%. All experiments were performed at ambient temperature (20-25°C). CpNiNO is well-behaved in the ICR spectrometer and no experimental difficulties were encountered.

The California Institute of Technology-Jet Propulsion Laboratory photoionization mass spectrometer used in this study has been described in detail elsewhere.[24] Pertinent operating conditions include: source temperature, ambient (20-25°C); sample pressure, 1×10^{-4} Torr; resolution, 2 Å; repeller field, 0.3 V cm^{-1}; ion energy for mass analysis, 9.2 eV. The hydrogen many-line spectrum was utilized in the wavelength range examined (1550-1150 Å).

Data reported in tables and figures represent total nickel content, with ^{58}Ni through ^{64}Ni abundances summed. Throughout this work, isotopic nickel containing species were observed in their natural abundance ratios.[25]

Results

Mass Spectrometry of CpNiNO. The 70 eV positive ion ICR mass spectrum of CpNiNO at 1.5×10^{-7} Torr is in good agreement with a previously reported mass spectrum.[14] The ions observed and their relative abundances are $CpNiNO^+$ (28%), $CpNi^+$ (41%), $C_3H_3Ni^+$ (11%), and Ni^+ (20%). Unlike $(\eta^5-C_5H_5)_2Ni$,[13] CpNiNO does not attach low energy electrons as prominent negative ion formation is not observed

over a range of electron energies and pressures.

Photoionization efficiency curves for the molecular ion and the lowest energy fragment $CpNi^+$ for photon energies between 8.0 and 10.7 eV are shown in Figure 1. The onset of $CpNiNO^+$ formation occurs at 1509 Å, giving a value of 8.21 ± 0.03 eV for the adiabatic ionization potential of CpNiNO. This compares with IP(CpNiNO) = 8.29 ± 0.05 eV obtained from He(I) photoelectron spectroscopy.[16] Fragmentation producing $CpNi^+$ by loss of NO from $CpNiNO^+$ exhibits an onset at 1215 Å, corresponding to an appearance potential of 10.20 ± 0.03 eV. The difference between IP(CpNiNO) and AP($CpNi^+$) gives D(NO–$CpNi^+$) = 1.99 ± 0.04 eV = 45.9 ± 1.0 kcal/mol, in excellent agreement with Müller's value of D(NO–$CpNi^+$) = 46 ± 5 kcal/mol derived from similar but less accurate electron impact studies.

Ion Chemistry of CpNiNO. Figures 2 and 3 present the temporal variation of relative ion abundance for CpNiNO at 2.7×10^{-7} Torr following a 70 eV, 10 ms electron beam pulse. Double resonance experiments[19-20] identify reactions 1-9 as occurring in this system.[26]

$$CpNiNO^+ + CpNiNO \longrightarrow Cp_2Ni_2NO^+ + NO \quad (1)$$

$$CpNi^+ + CpNiNO \xrightarrow{82\%} Cp_2Ni_2^+ + NO \quad (2)$$

$$CpNi^+ + CpNiNO \xrightarrow{16\%} CpNiNO^+ + CpNi \quad (3)$$

$$CpNi^+ + CpNiNO \xrightarrow{2\%} Cp_2Ni^+ + NiNO \quad (4)$$

$$C_3H_3Ni^+ + CpNiNO \longrightarrow CpNi_2(C_3H_3)^+ + NO \quad (5)$$

$$Ni^+ + CpNiNO \longrightarrow CpNi_2NO^+ \quad (6)$$

FIGURE 1

Apparent photoionization efficiency curves for $CpNiNO^+$ and $CpNi^+$. Data were recorded at 2 Å intervals with the hydrogen many-line spectrum.

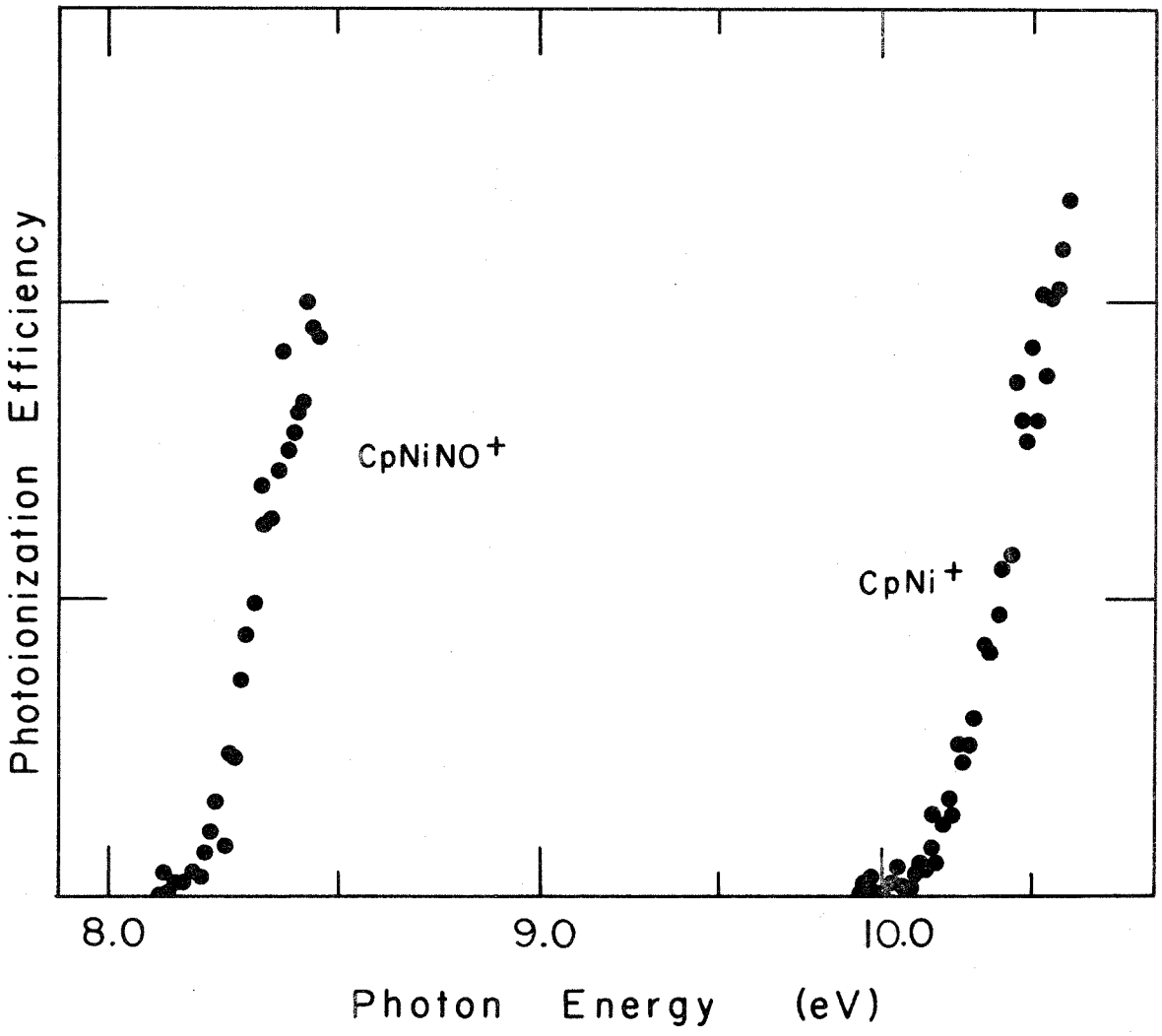
Photoionization Efficiency
CpNiNO+
CpNi+
8.0
9.0
10.0
Photon Energy (eV)

$$Cp_2Ni_2^+ + CpNiNO \longrightarrow Cp_3Ni_2^+ + NiNO \quad (7)$$

$$CpNi_2(C_3H_3)^+ + CpNiNO \longrightarrow Cp_2Ni_3(C_3H_3)NO^+ \quad (8)$$

$$CpNi_2NO^+ + CpNiNO \longrightarrow Cp_2Ni_3(NO)_2^+ \quad (9)$$

As expected from the reaction scheme, eq 1-6, abundances of the $CpNiNO^+$, $CpNi^+$, $C_3H_3Ni^+$, and Ni^+ ions decrease exponentially with time. From limiting slopes for decay of the reactant ions shown in Figures 2 and 3 and the known pressure of CpNiNO, total rate constants are calculated and summarized in Table I. The parent ion, $CpNiNO^+$, reacts slowly in a process where CpNiNO appears to displace NO (eq 1) producing $Cp_2Ni_2NO^+$. This suggests that $D(CpNiNO-CpNi^+) > D(NO-CpNi^+) = 45.9$ kcal/mol. The $CpNi^+$ cation reacts predominantly to form $Cp_2Ni_2^+$ (reaction 2), and to a lesser extent via charge exchange to produce $CpNiNO^+$ (reaction 3). The $CpNi^+$ ions involved in reaction 3 most likely possess excess internal excitation since charge exchange should be endothermic [IP(CpNi) = 7.8 eV[27] < IP(CpNiNO) = 8.21 eV]. Both $C_3H_3Ni^+$ and Ni^+ react with CpNiNO to produce higher mass condensation products (eq 5 and 6) which react further (eq 8 and 9). Interestingly, while Ni^+ reacts with nickelocene exclusively via charge exchange,[13] Ni^+ directly attaches to CpNiNO to produce $CpNi_2NO^+$ (eq 6). These observations are not unexpected since the ionization potential of nickel (7.64 eV)[28] is between IP(Cp_2Ni) = 6.2 eV[29] and IP(CpNiNO) = 8.21 eV. The present results are in agreement with the conclusions of Müller and Goll regarding the secondary ion mass spectrum of CpNiNO.[14, 30]

FIGURE 2

Temporal variation of ion abundance in CpNiNO at 2.7×10^{-7} Torr following ionization by a 70 eV, 10 ms electron beam pulse. Major ions.

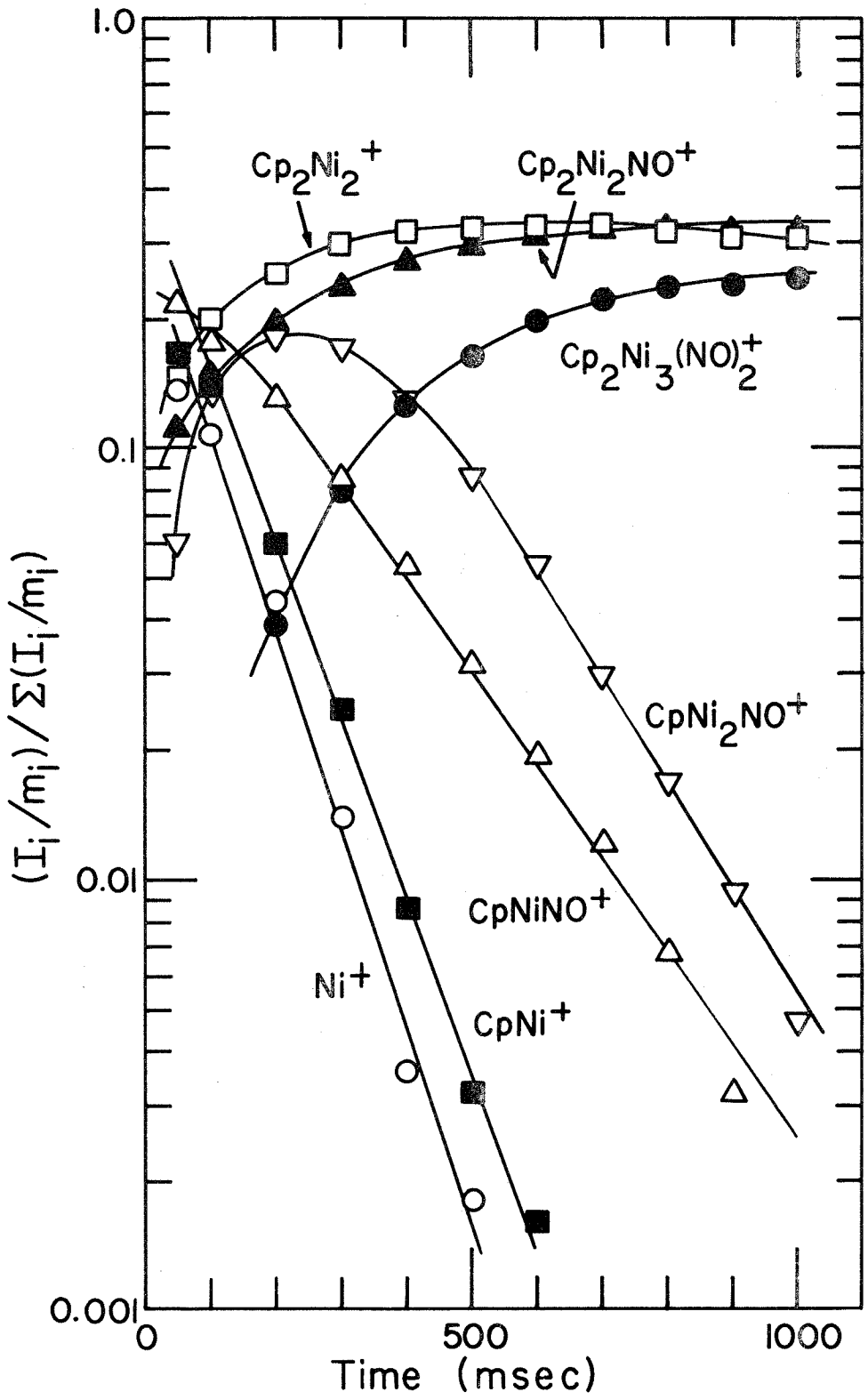
1.0
0.1
0.01
0.001
0
500
1000
Time (msec)
$(I_i/m_i)/\Sigma(I_i/m_i)$
$Cp_2Ni_2^+$
$Cp_2Ni_2NO^+$
$Cp_2Ni_3(NO)_2^+$
$CpNi_2NO^+$
$CpNiNO^+$
$CpNi^+$
Ni^+

FIGURE 3

Temporal variation of ion abundance in CpNiNO at 2.7×10^{-7} Torr following ionization by a 70 eV, 10 ms electron beam pulse. Minor ions.

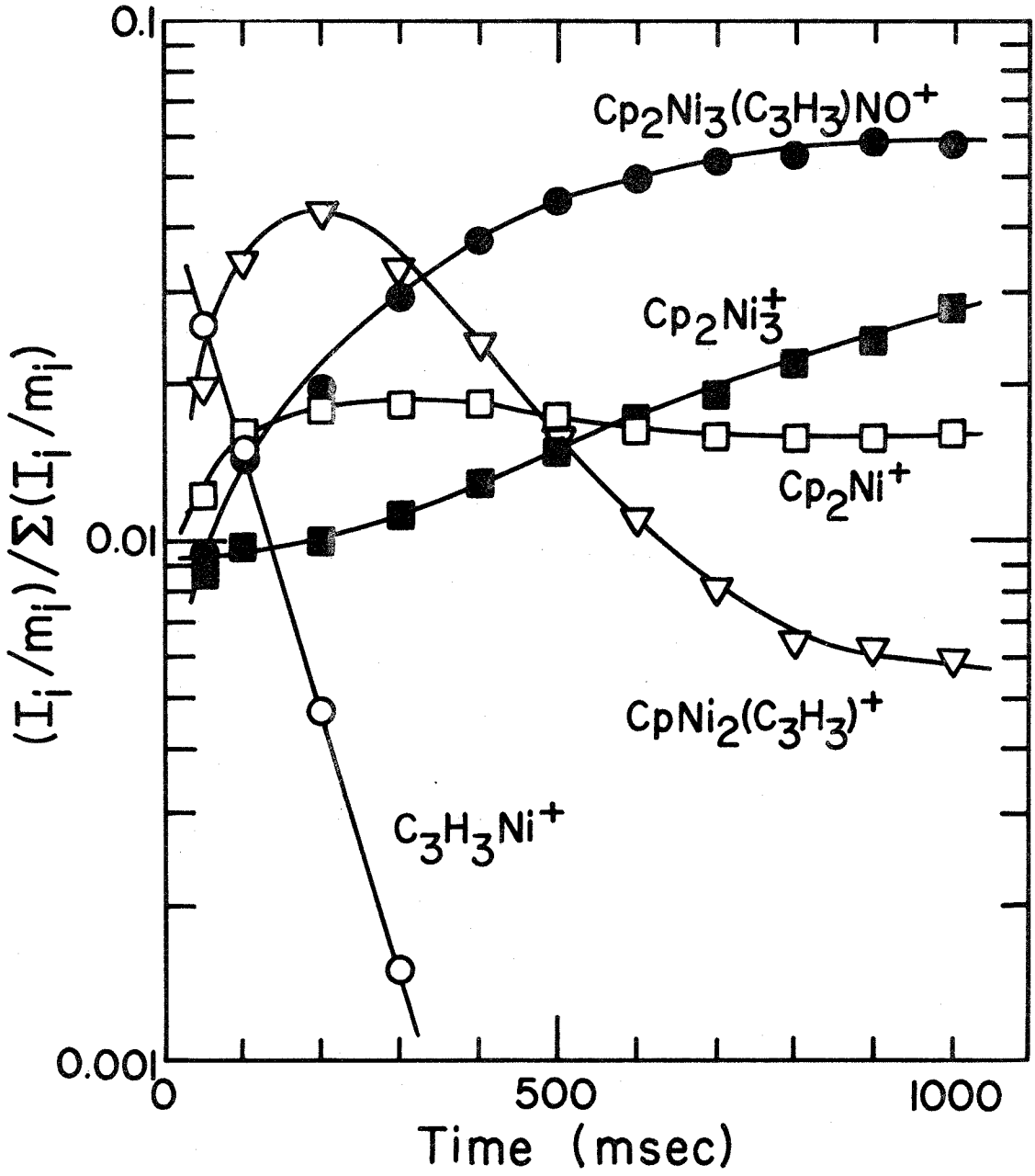
0.1
0.01
0.001
0
500
1000
Time (msec)
$(I_i/m_i)/\Sigma(I_i/m_i)$
$Cp_2Ni_3(C_3H_3)NO^+$
$Cp_2Ni_3^+$
Cp_2Ni^+
$CpNi_2(C_3H_3)^+$
$C_3H_3Ni^+$

Table I. Ion-Molecule Reactions and Rate Constants for CpNiNO

Reaction	k^a
$CpNiNO^+ + CpNiNO \rightarrow Cp_2Ni_2NO^+ + NO$	5.8 ± 1.0
$CpNi^+ + CpNiNO \rightarrow Cp_2Ni_2^+ + NO$	8.6 ± 1.0
$CpNi^+ + CpNiNO \rightarrow CpNiNO^+ + CpNi$	1.7 ± 1.0
$CpNi^+ + CpNiNO \rightarrow Cp_2Ni^+ + NiNO$	0.2 ± 1.0
$C_3H_3Ni^+ + CpNiNO \rightarrow CpNi_2(C_3H_3)^+ + NO$	14.1 ± 2.0
$Ni^+ + CpNiNO \rightarrow CpNi_2NO^+$	12.0 ± 2.0
$Cp_2Ni_2^+ + CpNiNO \rightarrow Cp_3Ni_2^+ + NiNO$	0.10 ± 0.05
$CpNi_2(C_3H_3)^+ + CpNiNO \rightarrow Cp_2Ni_3(C_3H_3)NO^+$	4.5 ± 1.0
$CpNi_2NO^+ + CpNiNO \rightarrow Cp_2Ni_3(NO)_2^+$	6.4 ± 1.0

[a]Total rate constants in units of 10^{-10} $cm^3 molecule^{-1} s^{-1}$ measured for disappearance of the reactant ion.

At higher pressures ($\sim 10^{-5}$ - 10^{-4} Torr), additional trinuclear nickel product ions are observed in the 70 eV ICR single resonance spectrum of CpNiNO, reactions 10-12. Observation of these product

$$Cp_2Ni_2^+ + CpNiNO \rightarrow Cp_3Ni_3NO^+ \quad (10)$$

$$CpNi_2(C_3H_3)^+ + CpNiNO \rightarrow Cp_2Ni_3(C_3H_3)^+ + NO \quad (11)$$

$$CpNi_2NO^+ + CpNiNO \rightarrow Cp_2Ni_3NO^+ + NO \quad (12)$$

ions, and determination of their precursors using double resonance techniques,[19, 20] indicates that under these conditions the only binuclear product ion not to react further is $Cp_2Ni_2NO^+$, formed by reaction of the molecular cation (eq 1).

Ligand Displacement Reactions. In the presence of an n-donor base, B, ligand displacement reactions, such as generalized in eq 13,

$$CpNiNO^+ + B \rightarrow CpNiB^+ + NO \quad (13)$$

are observed in those cases where $D(B-CpNi^+) > D(NO-CpNi^+) = 45.9$ kcal/mol. The ability of different bases to effect substitution is indicated in Table II. Exemplifying these studies are the data shown in Figure 4, which indicates the temporal variation of ion abundance in a 1.4:1 mixture of MeCHO and CpNiNO following a 12 eV, 10 ms electron beam pulse at a total pressure of 5.7×10^{-7} Torr.[31] From the slope of the exponential decrease of $CpNiNO^+$ ion abundance and the pressures of CpNiNO and MeCHO, the rate constant for production of the ligand displacement product $CpNi(MeCHO)^+$ (eq 13, B = MeCHO) is calculated to be $k = 8.5 \times 10^{-10}$ cm^{3}molecule^{-1}s^{-1}. At long times

Table II. Ligand Displacement Reactions Involving $CpNiNO^+$[a]

Ligands which displace NO and exchange rapidly:

PH_3, MeOH, ethylene oxide, NO, Me_2O, 1, 4-dioxane, MeCHO, MeSH, EtOH, HCN, EtCHO, iPrCHO, C_2H_3CHO, iPrOH, tBuCHO, tetrahydropyran, Me_2CO, tetrahydrofuran, tBuOH, MeOAc, Et_2O, Me_2S, NH_3, MeCN, iPr_2O, $MeNH_2$, Me_3N, Me_2NH, Me_3As, MeNC, Me_3P

Ligands which do not displace NO:

H_2, O_2, N_2, C_2H_4, CO, CH_3F, CH_3Br, CH_3Cl, PF_3, C_2H_4, H_2O, H_2S, H_2CO, $CH_3CH_2CH_3$, AsH_3

Ligands which displace NO and exchange slowly, if at all:

benzene, isobutene, butadiene, pyridine

[a]All ligands listed in increasing proton affinity order (references 19 and 34).

FIGURE 4

Temporal variation of relative ion abundance in a 1.4:1 mixture of MeCHO and CpNiNO following a 12 eV, 10 ms electron beam pulse at 5.7×10^{-7} Torr total pressure.

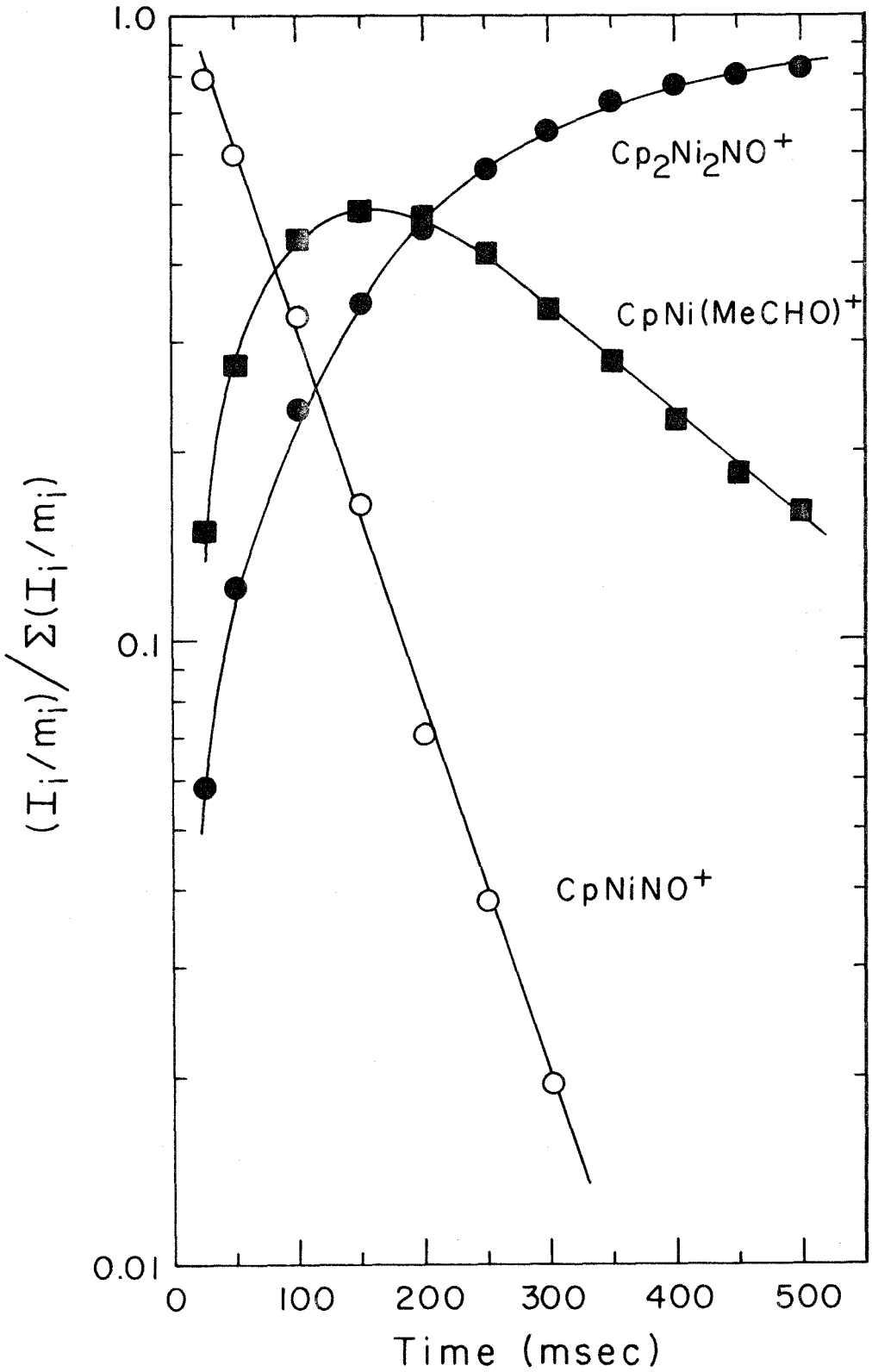
1.0
0.1
0.01
0
100
200
300
400
500
Time (msec)
$(I_i/m_i)/\Sigma(I_i/m_i)$
$Cp_2Ni_2NO^+$
$CpNi(MeCHO)^+$
$CpNiNO^+$

(> 200 ms), the ion abundance of $CpNi(MeCHO)^+$ gradually decreases to produce $Cp_2Ni_2NO^+$ (eq 14; for B = MeCHO, $k = 5.0 \times 10^{-10}$ cm^3 molecule^{-1}s^{-1}). Reaction 14 involves $CpNi^+$ transfer from B to

$$CpNiB^+ + CpNiNO \rightarrow Cp_2Ni_2NO^+ + B \qquad (14)$$

CpNiNO and for B = MeCHO indicates that $D(CpNiNO{-}CpNi^+) > D(MeCHO{-}CpNi^+)$. Reaction 14 is not observed for n-donor bases with proton affinity greater than NH_3 (Table II), which suggests that $D(CpNiNO{-}CpNi^+) < D(NH_3{-}CpNi^+)$.

In a mixture containing an excess of two bases, B_1 and B_2 with CpNiNO, the equilibrium indicated in eq 15 is established rapidly in

$$CpNiB_1^+ + B_2 \rightleftharpoons CpNiB_2^+ + B_1 \qquad (15)$$

relation to any further reactions of the complexes with the neutrals present. Table II lists those bases for which equilibria are observed. Figure 5 shows equilibrium $CpNi^+$ transfer between Me_3As and $MeNH_2$ (eq 16). The apparent ion loss at long ion trapping times results from

$$CpNiNH_2Me^+ + AsMe_3 \underset{k_r}{\overset{k_f}{\rightleftharpoons}} CpNiAsMe_3^+ + NH_2Me \qquad (16)$$

the displacement of the base in $CpNiB^+$ by CpNiNO (eq 14). Double resonance ion ejection results[19, 32] for the $AsMe_3{-}NH_2Me$ equilibrium are shown in Figure 6. From these results, $k_f = 3.0 \times 10^{-10}$ cm^3 molecule^{-1}s^{-1} and $k_r = 5.7 \times 10^{-11}$ cm^{3}molecule^{-1}s^{-1}, giving $K_{eq} = 5.3$, to be compared with the data shown in Figure 5, which yield $K_{eq} \cong 5.2$.

The relative free energy of binding B_1 and B_2 to $CpNi^+$ can be determined from the equilibrium constant observed for process 15

FIGURE 5

Temporal variation of $CpNiAsMe_3^+$ and $CpNiNH_2Me^+$ signal intensities following a 12 eV, 10 ms electron beam pulse in a 4.3:1 mixture of NH_2Me and $AsMe_3$ at 6.0×10^{-7} Torr pressure.

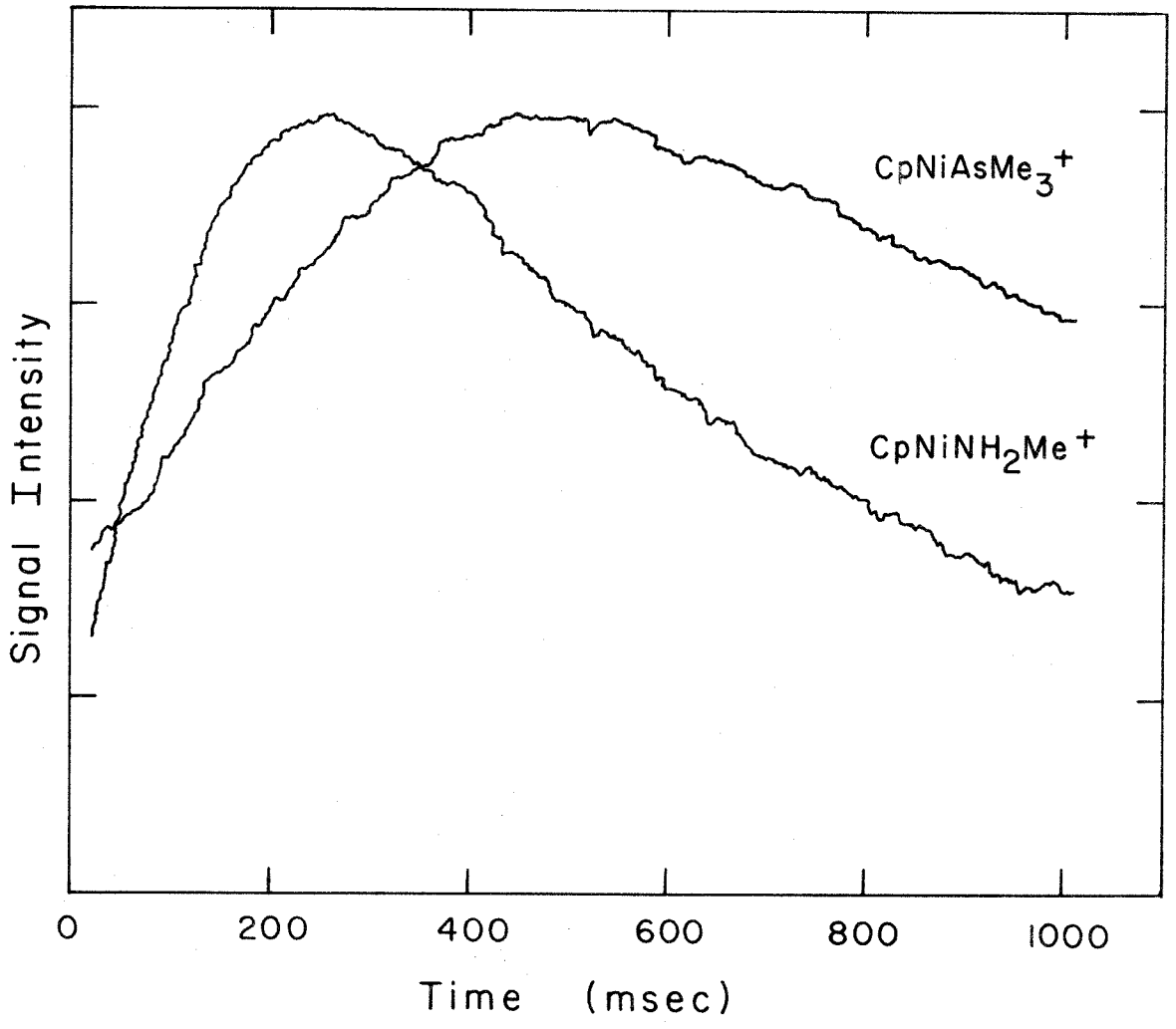
Signal Intensity
CpNiAsMe3+
CpNiNH2Me+
0
200
400
600
800
1000
Time (msec)

FIGURE 6

Logarithmic plot of relative signal intensities for $CpNiAsMe_3^+$ and $CpNiNH_2Me^+$ following continuous ejection after 600 ms. The slopes of these lines and the known pressures of the neutral species give the forward and reverse rate constants for ligand exchange.

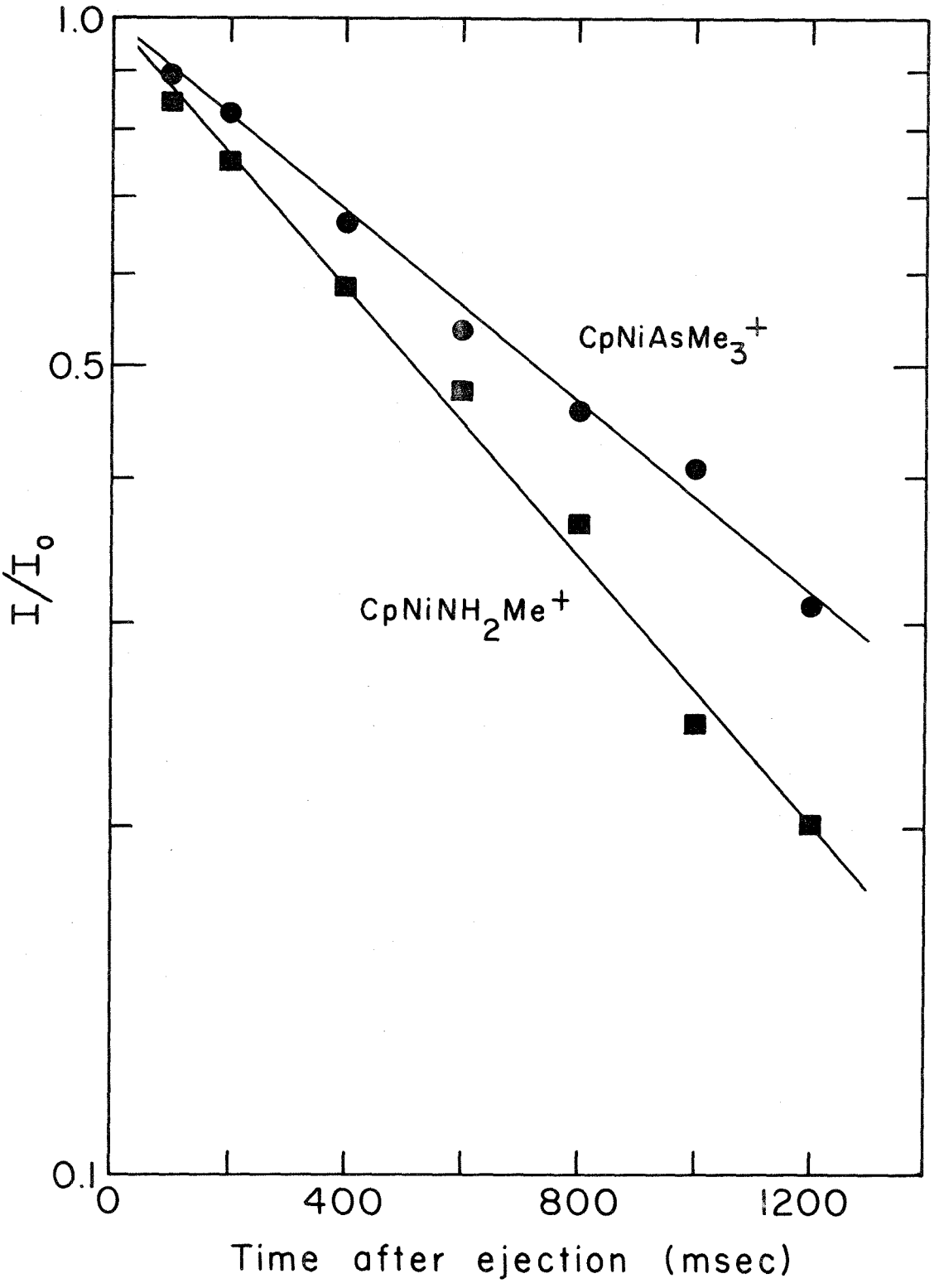
1.0
0.5
0.1
I/I₀
CpNiAsMe₃⁺
CpNiNH₂Me⁺
0
400
800
1200
Time after ejection (msec)

with an accuracy of ± 0.2 kcal/mol for $\Delta G \leq 3$ kcal/mol. These data are converted to enthalpies by assuming ΔS is zero except for small corrections due to changes in symmetry numbers.[33] The assumption is made that there is no rotation about the nickel-ligand bond [e.g., for B = NH_3, $\sigma(CpNiNH_3^+) = 1$]. Data for 31 n-donor bases relative to NH_3 are summarized in Figure 7 and Table III. Included for comparison in Table III are the proton affinities, $D(B-H^+)$,[19, 34] and values of $D(B-Li^+)$[35, 36] for the same series of bases, also relative to NH_3. Absolute values of $D(NH_3-CpNi^+)$ = 52.3 ± 2 kcal/mol,[37] $D(NH_3-H^+)$ = 202.3 ± 2 kcal/mol,[34] and $D(NH_3-Li^+)$ = 39.1 ± 2 kcal/mol,[36] are assigned using available literature data.

Unlike the n-donor bases, for which ligand exchange is rapid ($5\text{-}10 \times 10^{-10}$ $cm^3 molecule^{-1} s^{-1}$), displacement reactions involving propylene and isobutylene are observed to be very slow. Consequently, double resonance techniques[19, 20] rather than equilibrium methods are used to bracket[38] $D(B-CpNi^+)$ for these species. The results indicate that $D(C_3H_6-CpNi^+)$ = 44 ± 5 kcal/mol (approximately equal to MeOH) and $D(C_4H_8-CpNi^+)$ = 49 ± 7 kcal/mol (approximately equal to iPrCHO).

Reactions of $CpNi^+$ with Organic Molecules. During the course of examining the ligand displacement processes described above, many product ions which result from reactions of $CpNi^+$ with various organic species were observed. These reactions include dehydrohalogenation, dehydration, dehydrogenation, decarbonylation, and alkylation processes, and in many instances are analogous to the observed solution chemistry of organotransition metal complexes. Table IV lists

FIGURE 7

Ligand-$CpNi^+$ binding energies relative to ammonia at $D(NH_3-CpNi^+) = 52.3 \pm 2.0$ kcal/mol.

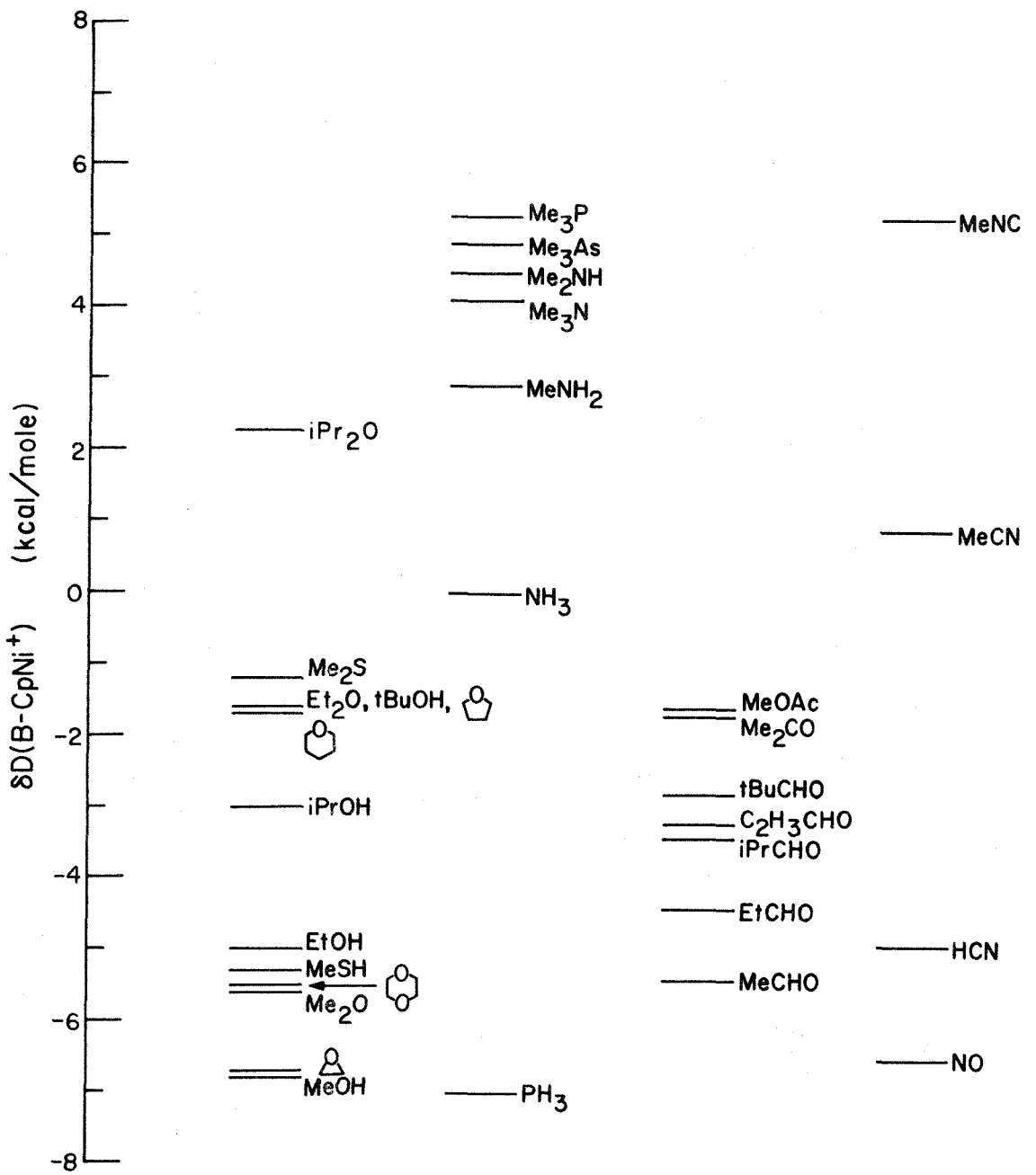
8
6
4
2
0
-2
-4
-6
-8
δD(B-CpNi+) (kcal/mole)
Me3P
Me3As
Me2NH
Me3N
MeNH2
iPr2O
NH3
Me2S
Et2O, tBuOH,
iPrOH
EtOH
MeSH
Me2O
MeOH
PH3
MeNC
MeCN
HCN
NO
MeOAc
Me2CO
tBuCHO
C2H3CHO
iPrCHO
EtCHO
MeCHO

Table III. Relative Gas Phase Ligand Binding Energies, $\delta D(B\text{-}CpNi^+)$, $\delta D(B\text{-}H^+)$, and $D(B\text{-}Li^+)$[a]

Base	$\delta D(B\text{-}H^+)$[b]	$\delta D(B\text{-}CpNi^+)$	$\delta D(B\text{-}Li^+)$[c]	Base	$\delta D(B\text{-}H^+)$[b]	$\delta D(B\text{-}CpNi^+)$	$\delta D(B\text{-}Li^+)$[c]
PH_3	-15.0	-6.8		tetra-hydropyran	- 5.2	-1.6	
MeOH	-20.1	-6.7	-1.0	Me_2CO	- 8.4	-1.6	+6.2
ethylene oxide	-16.8[d]	-6.6		tetra-hydrofuran	- 5.9	-1.5	
NO	-75[e]	-6.4		tBuOH	1.5[i]	-1.5	
Me_2O	-12.2	-5.4	+0.4	MeOAc	- 6.9	-1.4	
1,4-dioxane	-11.4	-5.4		Et_2O	- 4.9	-1.4	
MeCHO	-17.3	-5.3	+1.3[f]	Me_2S	- 4.7	-1.2	-6.5[f]
MeSH	-16.4	-5.2		NH_3	0.0[j]	0.0[k]	0.0[c]
EtOH	-15.6	-4.8		MeCN	-15.3	0.9	+4.5[f]
HCN	-27.8	-4.7	-2.7	iPr_2O	+ 2.3	+1.2	
EtCHO	-14.3	-4.2		$MeNH_2$	8.9	2.9	+2.0
iPrCHO	-11.7	-3.2		Me_3N	19.2	4.1	+3.0
C_2H_3CHO	-11.3[g]	-3.0		Me_2NH	15.1	4.5	+3.1
iPrOH	- 7.5[h]	-2.8		Me_3As	8.3[l]	4.9	
tBuCHO	- 9.5	-2.7		MeNC	- 3.3[m]	5.3	
				Me_3P	21.0[n]	5.3	

[a]All values in kcal/mol. [b]Unless otherwise noted, all $\delta D(B\text{-}H^+)$ are from reference 34.

[c]$D(NH_3\text{-}Li^+) = 39.1 \pm 2.0$ kcal/mol; unless otherwise noted all values of $\delta D(B\text{-}Li^+)$ are from reference 36.

[d]R. H. Staley, R. R. Corderman, M. S. Foster, and J. L. Beauchamp, J. Am. Chem. Soc., 96, 1260 (1974). [e]A. E. Roche, M. M. Sutton, D. K. Bohme, and H. I. Schiff, J. Chem. Phys., 55, 5480 (1971). [f]Reference 35. [g]B. S. Freiser and J. L. Beauchamp, unpublished results. [h]R. T. McIver, Jr., unpublished results. [i]J. L. Beauchamp and M. C. Caserio, J. Am. Chem. Soc., 94, 2638 (1972). [j]$D(NH_3\text{-}H^+)$ = 202.3 ± 2.0 kcal/mol, reference 34. [k]$D(NH_3\text{-}CpNi^+)$ = 52.3 ± 2.0 kcal/mol is obtained from the PIMS value of $D(NO\text{-}CpNi^+)$ = 45.9 ± 1.0 kcal/mol and the measured value of $\delta D(NO\text{-}CpNi^+)$ = -6.4 kcal/mol, reference 5. [ℓ]R. V. Hodges and J. L. Beauchamp, Inorg. Chem., 14, 2887 (1975). [m]J. F. Vogt and J. L. Beauchamp, unpublished results. [n]R. H. Staley and J. L. Beauchamp, J. Am. Chem. Soc., 96, 6252 (1974).

Table IV. Reaction Enthalpies for Processes Effected by $(\eta^5\text{-}C_5H_5)Ni^+$

Reaction	ΔH(kcal/mol)
$EtBr \rightarrow C_2H_4 + HBr$	18.9
$EtCl \rightarrow C_2H_4 + HCl$	16.5
$iPrCl \rightarrow C_3H_6 + HCl$	16.4
$tBuCl \rightarrow C_3H_6 + CH_3Cl$	27.9
$tBuCl \rightarrow C_4H_8 + HCl$	17.4
$EtOH \rightarrow C_2H_4 + H_2O$	10.9
$iPrOH \rightarrow C_3H_6 + H_2O$	12.2
$tBuOH \rightarrow C_4H_8 + H_2O$	12.7
$CH_3COOH \rightarrow CH_2CO + H_2O$	34.1
$c\text{-}C_6H_{12} \rightarrow c\text{-}C_6H_{10} + H_2$	28.4
$c\text{-}C_6H_{10} \rightarrow c\text{-}C_6H_8 + H_2$	26.5
$c\text{-}C_6H_8 \rightarrow c\text{-}C_6H_6 + H_2$	- 5.6
$c\text{-}C_5H_{10} \rightarrow c\text{-}C_5H_8 + H_2$	26.2
$c\text{-}C_5H_8 \rightarrow c\text{-}C_5H_6 + H_2$	24.2
$c\text{-}C_4H_8 \rightarrow c\text{-}C_4H_6 + H_2$	30.7
$n\text{-}C_6H_{14} \rightarrow n\text{-}2\text{-}C_6H_{12} + H_2$	27.0
$n\text{-}2\text{-}C_6H_{12} \rightarrow n\text{-}1,3\text{-}C_6H_{10} + H_2$	33.0
$n\text{-}C_4H_{10} \rightarrow n\text{-}1\text{-}C_4H_8 + H_2$	30.2
$n\text{-}C_4H_{10} \rightarrow n\text{-}2\text{-}C_4H_8 + H_2$	27.4
$n\text{-}1\text{-}C_4H_8 \rightarrow 1,3\text{-}C_4H_6 + H_2$	26.3
$n\text{-}2\text{-}C_4H_8 \rightarrow 1,3\text{-}C_4H_6 + H_2$	29.1
$C_3H_8 \rightarrow C_3H_6 + H_2$	29.5

Table IV. (Continued)

Reaction		ΔH(kcal/mol)
Et_3N	→ $Et_2N(C_2H_3) + H_2$	28.0
Et_2NH	→ $EtNH(C_2H_3) + H_2$	30.8
$EtNH_2$	→ $(C_2H_3)NH_2 + H_2$	31.0
Et_2O	→ $EtO(C_2H_3) + H_2$	26.6
AsH_3	→ $AsH + H_2$	38.2
MeCHO	→ $CH_4 + CO$	- 4.6
EtCHO	→ $C_2H_6 + CO$	2.0
iPrCHO	→ $C_3H_8 + CO$	4.1
tBuCHO	→ $iC_4H_{10} + CO$	1.6
CH_2CHCHO	→ $C_2H_4 + CO$	9.1
$CH_2C(CH_3)CHO$	→ $C_3H_6 + CO$	5.5
C_6H_6CHO	→ $C_6H_6 + CO$	3.9

the reaction enthalpies for many of the processes that are observed using standard sources of thermochemical data.[28, 39-41]

Dehydrohalogenation Reactions. $CpNi^+$ readily dehydrohalogenates ethyl chloride, producing $CpNi(HCl)^+$ (eq 17) and $CpNi(C_2H_4)^+$ (eq 18). Both HCl and C_2H_4 are displaced in subsequent reactions of

$$CpNi^+ + C_2H_5Cl \xrightarrow{39\%} CpNi(HCl)^+ + C_2H_4 \quad (17)$$

$$CpNi^+ + C_2H_5Cl \xrightarrow{61\%} CpNi(C_2H_4)^+ + HCl \quad (18)$$

these product ions with C_2H_5Cl and CpNiNO (eq 14). Processes analogous to reactions 17 and 18 are observed for a variety of alkyl halides including EtBr, iPrCl, and tBuCl (Table V). In proceeding from EtCl to tBuCl, the product CpNi (alkene)$^+$ becomes more abundant relative to $CpNi(HCl)^+$, consistent with the expectation that $D(\text{alkene-}CpNi^+) > D(HCl\text{-}CpNi^+)$. Other metal ion species which react similarly include Li^+,[35, 42] Fe^+, Co^+, and Ni^+.[3, 8]

Dehydration Reactions. $CpNi^+$ is observed to effect the dehydration of alcohols ROH = EtOH, iPrOH, and tBuOH, yielding product ions with either H_2O or the appropriate alkene bonded to $CpNi^+$, as illustrated for iPrOH in eq 19 and 20. As for the dehydrohalogenation

$$CpNi^+ + iPrOH \xrightarrow{41\%} CpNi(OH_2)^+ + C_3H_6 \quad (19)$$

$$CpNi^+ + iPrOH \xrightarrow{59\%} CpNi(C_3H_6)^+ + H_2O \quad (20)$$

reactions, a constant increase in the abundance of CpNi(alkene)$^+$

Table V. Dehydrohalogenation and Dehydration Reactions Effected by $CpNi^+$

Reactant	Species Bound to $CpNi^+$	Product Distribution (%)
EtCl	HCl	0.39
	C_2H_4	0.61
iPrCl	HCl	0.19
	C_3H_6	0.81
tBuCl	HCl	< 0.02
	C_3H_6	0.46
	C_4H_8	0.54
EtBr	HBr	0.78
	C_2H_4	0.22
EtOH	H_2O	1.00
	C_2H_4	0.00
iPrOH	H_2O	0.41
	C_3H_6	0.59
tBuOH	H_2O	0.27
	C_4H_8	0.73
CH_3COOH	H_2O	0.71
	CH_2CO	0.29

relative to $CpNi(OH_2)^+$ is observed as ROH progresses from EtOH to tBuOH. These results are in good agreement with similar observations by Allison and Ridge of the dehydration of alcohols by bare transition metal cations including Fe^+, Co^+, and Ni^+ (for iPrOH: $Ni(OH_2)^+$ = 67% and $(C_3H_6)Ni^+$ = 33%).[8] Acetic acid is dehydrated to yield ketene (reactions 21 and 22). The ketene containing product ion,

$$CpNi^+ + CH_3COOH \xrightarrow{71\%} CpNi(OH_2)^+ + CH_2CO \quad (21)$$

$$CpNi^+ + CH_3COOH \xrightarrow{29\%} CpNi(CH_2CO)^+ + H_2O \quad (22)$$

$CpNi(CH_2CO)^+$, is less abundant than $CpNi(OH_2)^+$, which is consistent with oxygen, but not carbon binding to $CpNi^+$.[43]

Dehydrogenation Reactions. Several examples of dehydrogenation reactions effected by $CpNi^+$ were observed (Table VI). $CpNi^+$ dehydrogenates cyclopentane to both cyclopentene and cyclopentadiene (eq 23 and 24). When a 2.4:1 mixture of cyclopentane and CpNiNO at

$$CpNi^+ + c\text{-}C_5H_{10} \xrightarrow{49\%} CpNi(c\text{-}C_5H_8)^+ + H_2 \quad (23)$$

$$CpNi^+ + c\text{-}C_5H_{10} \xrightarrow{51\%} CpNi(c\text{-}C_5H_6)^+ + 2H_2 \quad (24)$$

a total pressure of 7.8×10^{-7} Torr is examined using trapped ion techniques[19, 21] following a 20 eV, 10 ms electron beam pulse, the ion-molecule reactions 2, 23 and 24 are initiated by $CpNi^+$ and account for the temporal variation of ion abundance illustrated in Figure 8.[44]

Table VI. $CpNi^+$ Dehydrogenation Reactions

Reaction	Product Distribution (%) This Work	Ref. 14
$CpNi^+ + c\text{-}C_6H_{12} \rightarrow CpNi(c\text{-}C_6H_{10})^+ + H_2$	0.68	0.49
$CpNi^+ + c\text{-}C_6H_{12} \rightarrow CpNi(c\text{-}C_6H_8)^+ + 2H_2$	0.26	0.33
$CpNi^+ + c\text{-}C_6H_{12} \rightarrow CpNi(c\text{-}C_6H_6)^+ + 3H_2$	0.06	0.19
$CpNi^+ + c\text{-}C_6H_{10} \rightarrow CpNO(c\text{-}C_6H_8)^+ + H_2$	0.61	0.77
$CpNi^+ + c\text{-}C_6H_{10} \rightarrow CpNi(c\text{-}C_6H_6)^+ + 2H_2$	0.39	0.23
$CpNi^+ + c\text{-}1,3\text{-}C_6H_8 \rightarrow CpNi(c\text{-}C_6H_6)^+ + N_2$	1.00	1.00
$CpNi^+ + c\text{-}1,4\text{-}C_6H_8 \rightarrow CpNi(c\text{-}C_6H_6)^+ + N_2$	1.00	- -
$CpNi^+ + c\text{-}C_5H_{10} \rightarrow CpNi(c\text{-}C_5H_8)^+ + H_2$	0.49	- -
$CpNi^+ + c\text{-}C_5H_{10} \rightarrow CpNi(c\text{-}C_5H_6)^+ + 2H_2$	0.51	- -
$CpNi^+ + c\text{-}C_4H_8 \rightarrow CpNi(c\text{-}C_4H_6)^+ + H_2$	1.00	- -
$CpNi^+ + n\text{-}C_6H_{14} \rightarrow CpNi(C_6H_{12})^+ + H_2$	0.76	1.00
$CpNi^+ + n\text{-}C_6H_{14} \rightarrow CpNi(C_6H_{10})^+ + 2H_2$	0.24	0.00
$CpNi^+ + n\text{-}C_4H_{10} \rightarrow CpNi(C_4H_8)^+ + H_2$	0.92	- -
$CpNi^+ + n\text{-}C_4H_{10} \rightarrow CpNi(C_4H_6)^+ + 2H_2$	0.08	- -
$CpNi^+ + C_3H_8 \rightarrow CpNi(C_3H_6)^+ + H_2$	1.00	- -
$CpNi^+ + C_2H_6 \rightarrow$ no reaction	- -	- -

Table VI. (Continued)

Reaction	Product Distribution (%) This Work	Ref. 14
$CpNi^+ + Et_3N \rightarrow CpNi[(C_2H_3)Et_2N]^+ + H_2$	1.00	- -
$CpNi^+ + Et_2NH \rightarrow CpNi[(C_2H_3)EtNH]^+ + H_2$	0.79	0.80
$CpNi^+ + Et_2NH \rightarrow CpNi[(C_2H_3)_2NH]^+ + 2H_2$	0.21	0.20
$CpNi^+ + EtNH_2 \rightarrow CpNi(C_2H_3NH_2)^+ + H_2$	0.61	- -
$CpNi^+ + EtNH_2 \rightarrow CpNi(C_2HNH_2)^+ + 2H_2$	0.39	- -
$CpNi^+ + Et_2O \rightarrow CpNi[(C_2H_3)EtO]^+ + H_2$	1.00	1.00
$CpNi^+ + AsH_3 \rightarrow CpNiAsH^+ + H_2$	1.00	- -

FIGURE 8

Temporal variation of relative ion abundance in a 2.4:1 mixture of cyclopentane and CpNiNO at a total pressure of 7.8×10^{-7} Torr following a 20 eV, 10 ms electron beam pulse.

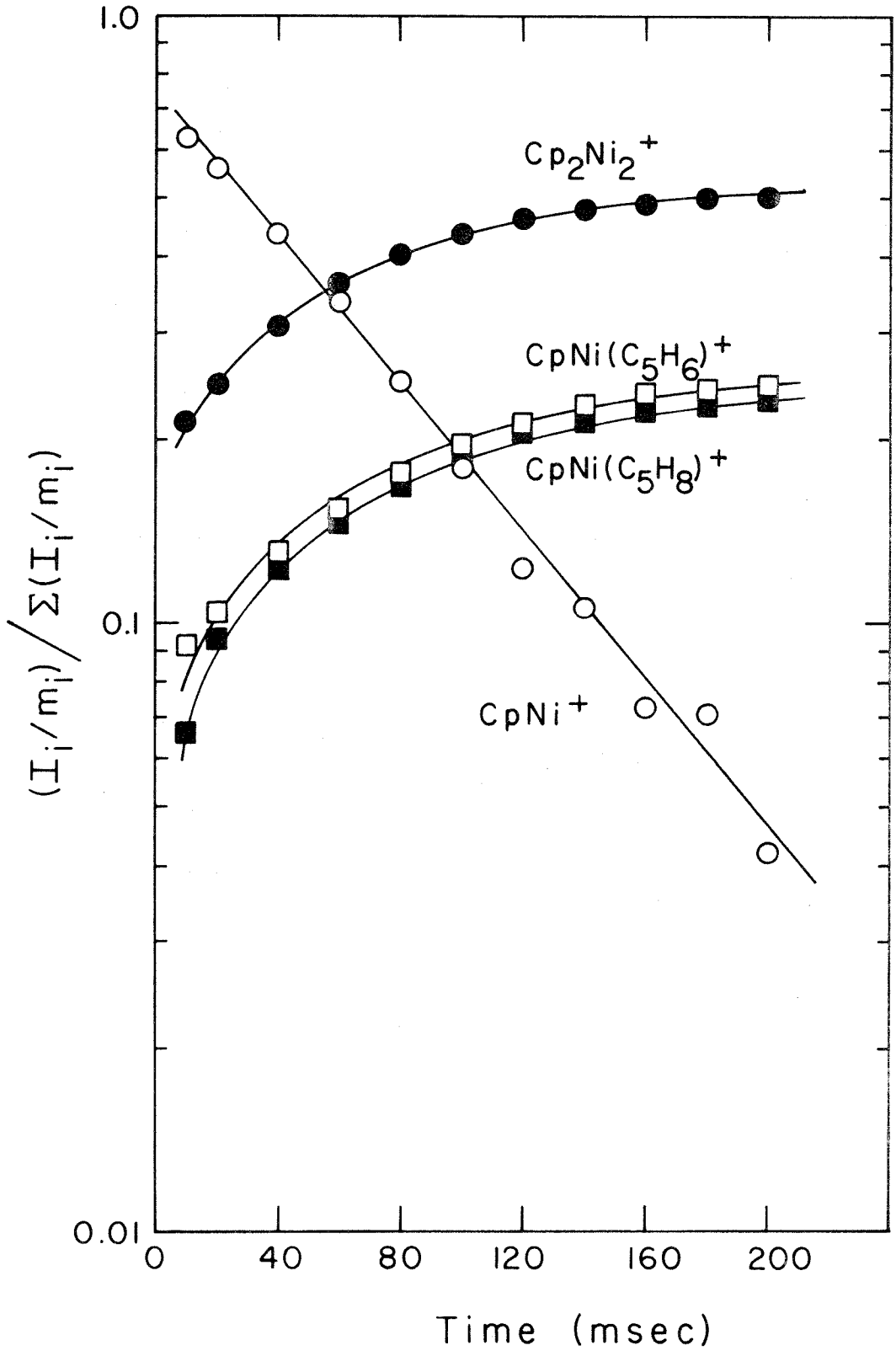
1.0
0.1
0.01
0
40
80
120
160
200
Time (msec)
$(I_i/m_i)/\Sigma(I_i/m_i)$
$Cp_2Ni_2^+$
$CpNi(C_5H_6)^+$
$CpNi(C_5H_8)^+$
$CpNi^+$

Similarly, $CpNi^+$ reacts with ethylamines, $(C_2H_5)_nNH_{3-n}$ (n = 1-3), and diethyl ether to produce species which are presumably both σ- and π-bonded to nickel.[14] Müller and Goll observed the dehydrogenation of several of these species using high pressure mass spectrometry;[14] their product yields are included in Table V for comparison. Müller suggests that $CpNiNO^+$ dehydrogenates both saturated and olefinic hydrocarbons, (e.g., cyclohexane, eq 25) and concludes from

$$CpNiNO^+ + c\text{-}C_6H_{14} \rightarrow CpNi(c\text{-}C_5H_{10})^+ + NO + H_2 \qquad (25)$$

appearance potential measurements that for such reactions, activation energies of $\approx$ 35 kcal/mol are necessary.[14] Results of ICR double resonance experiments[19, 38] are in only partial agreement with these conclusions. Figure 9 presents two sets of ICR double resonance spectra at low irradiating RF field amplitude (90 mV cm^{-1}) for the dehydrogenation product ions of cyclohexane and cyclopentane. While an intense negative double resonance signal is always observed for $CpNi^+$ effected dehydrogenation reactions, only for processes 26 and 27 are strong positive double resonance signals observed, indicative of

$$CpNiNO^+ + c\text{-}C_6H_{12} \rightarrow CpNi(c\text{-}C_6H_8)^+ + 2H_2 + NO \qquad (26)$$

$$CpNiNO^+ + c\text{-}C_6H_{12} \rightarrow CpNi(c\text{-}C_6H_6)^+ + 3H_2 + NO \qquad (27)$$

endothermic reactions.[19, 38] In neither system is there evidence that thermal energy $CpNiNO^+$ molecular ions dehydrogenate $c\text{-}C_6H_{12}$ or $c\text{-}C_5H_{10}$. Müller's result is presumably due to the higher kinetic energy of reactant ions in the high pressure mass spectrometer.[14]

FIGURE 9

ICR double resonance spectra for the dehydrogenation product ions of cyclohexane and cyclopentane.

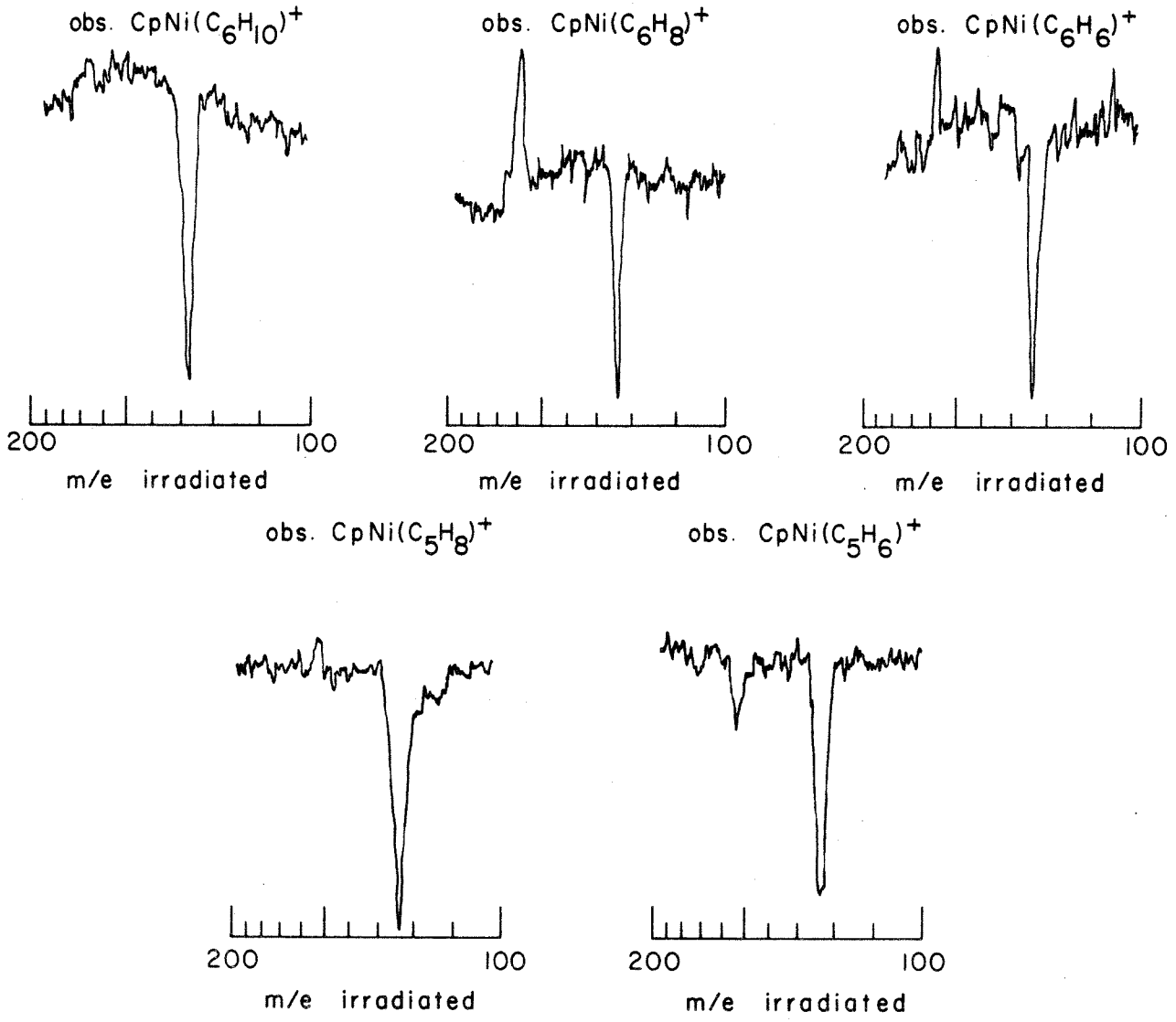
obs. CpNi(C_6H_{10})$^+$
200
100
m/e irradiated
obs. CpNi(C_6H_8)$^+$
200
100
m/e irradiated
obs. CpNi(C_6H_6)$^+$
200
100
m/e irradiated
obs. CpNi(C_5H_8)$^+$
200
100
m/e irradiated
obs. CpNi(C_5H_6)$^+$
200
100
m/e irradiated

The dehydrogenation of arsine (Table V) is not unexpected due to the low enthalpy for the reaction $AsH_3 \rightarrow AsH + H_2$ (38.2 kcal/mol).[45]

Decarbonylation Reactions. Perhaps the most intriguing of the reactions observed for $CpNi^+$ is the decarbonylation of aldehydes to hydrocarbons and CO, generalized in eq 28 and 29.

$$CpNi^+ + RCHO \rightarrow CpNiCO^+ + RH \quad (28)$$

$$CpNi^+ + RCHO \rightarrow CpNiRH^+ + CO \quad (29)$$

When a 1.4:1 mixture of CpNiNO and benzaldehyde at 3.4×10^{-7} Torr total pressure is examined using trapped ion ICR techniques[19, 21] with an ionizing energy of 20 eV, the sequence of reactions 1-4 and 30 and 31 is initiated by $CpNiNO^+$ and $CpNi^+$ and accounts for

$$CpNiNO^+ + C_6H_5CHO \rightarrow CpNi(C_6H_5CHO)^+ + NO \quad (30)$$

$$CpNi^+ + C_6H_5CHO \rightarrow CpNi(C_6H_6)^+ + CO \quad (31)$$

the temporal variation of ion abundance illustrated in Figure 10. The addition of C_6H_5CHO modifies the series of reactions observed in CpNiNO alone at 20 eV (eq 1-4) by the inclusion of reactions 30 and 31. The product of the decarbonylation reaction 31 reacts slowly, if at all, with CpNiNO (Table II), and reaches a maximum abundance of 14.5%. Ion ejection techniques[32] indicate that the rate of reaction 31 is $k = 9.6 \times 10^{-10}$ $cm^3 molecule^{-1} s^{-1}$, which is approximately equal to the collision rate.

Further observations with a variety of alkyl, alkenyl, and aryl aldehydes reveal the two reaction channels, eq 28 and 29, for

FIGURE 10

Temporal variation of relative ion abundance in a 1.4:1 mixture of CpNiNO and C_6H_5CHO following a 20 eV, 10 ms electron beam pulse at 3.4×10^{-7} Torr total pressure.

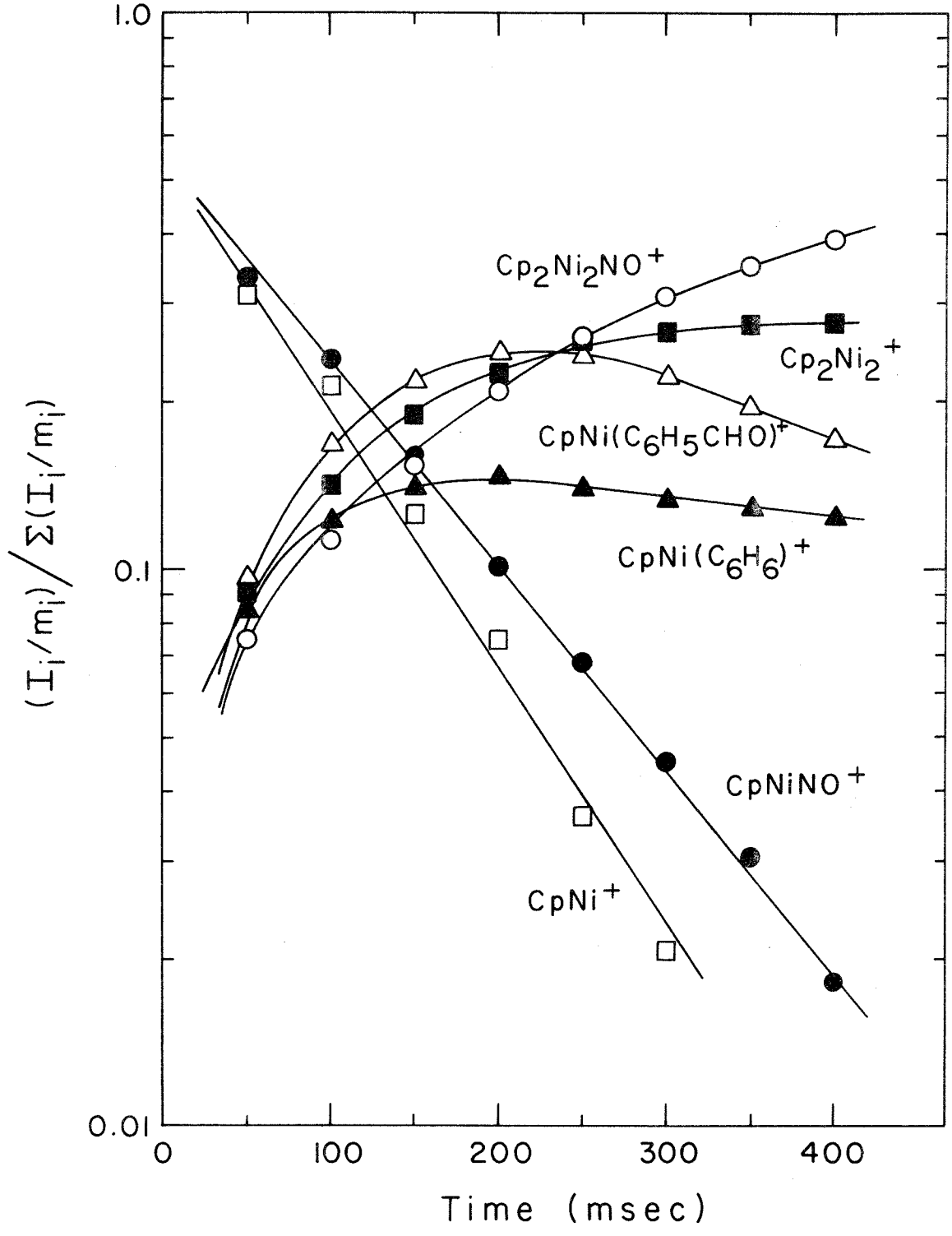
1.0
0.1
0.01
0
100
200
300
400
Time (msec)
$(I_i/m_i)/\Sigma(I_i/m_i)$
$Cp_2Ni_2NO^+$
$Cp_2Ni_2^+$
$CpNi(C_6H_5CHO)^+$
$CpNi(C_6H_6)^+$
$CpNiNO^+$
$CpNi^+$

decarbonylation. Reaction 28 is observed for RCHO = MeCHO, EtCHO, iPrCHO, and tBuCHO. $CpNiRH^+$ is observed with RCHO = 3-methyl acrolein and benzaldehyde. For RCHO = acrolein, product ions of equal mass result, making channels 28 and 29 indistinguishable. Decarbonylation reactions are not observed for H_2CO, CF_3CHO, CH_3COCl, CH_3COBr, Me_2CO, and MeOAc.

Sequential Alkylation Reactions. Another interesting example of an oxidative addition reaction is found in the reaction of methyl bromide with the $CpNi^+$ ion.[46] ICR studies using CD_3Br show that reaction 32 involves sequential alkylation of the cyclopentadienyl ring. Figure 11

$$(CD_3)_nC_5H_{5-n}Ni^+ + CD_3Br \rightarrow (CD_3)_{n+1}C_5H_{4-n}Ni^+ + HBr \qquad (n = 0\text{-}3) \qquad (32)$$

illustrates the temporal variation of relative ion abundance in a 1:3 mixture of CpNiNO and CD_3Br at a total pressure of 1.3×10^{-6} Torr following a 20 eV, 10 ms electron beam pulse [exclusive of ions from CpNiNO (Figures 2 and 3) and CD_3Br[47] alone]. Double resonance experiments[19, 20] clearly demonstrate the sequential nature of reaction 32, with each product ion having double resonance signals from each of its precursor ions. Species containing five CD_3 groups are not observed, even at high CD_3Br pressures or long ion trapping times.

Proton Transfer Reactions Involving CpNiNO. Several different proton transfer reactions are identified in mixtures of CpNiNO with various organic bases, B. For each of the bases AsH_3, C_6H_6, EtOH, MeCN, HCO_2Me, C_2H_3CHO, iPrCHO, $CH_2C(Me)CHO$, tBuCHO, iPrOH,

FIGURE 11

Temporal variation of relative ion abundance in a 1:3 mixture of CpNiNO and CD_3Br following a 20 eV, 10 ms electron beam pulse at 1.3×10^{-6} Torr total pressure. Ions from the reactions of CpNiNO alone (Figs. 2 and 3) and CD_3Br alone are excluded from the normalization.

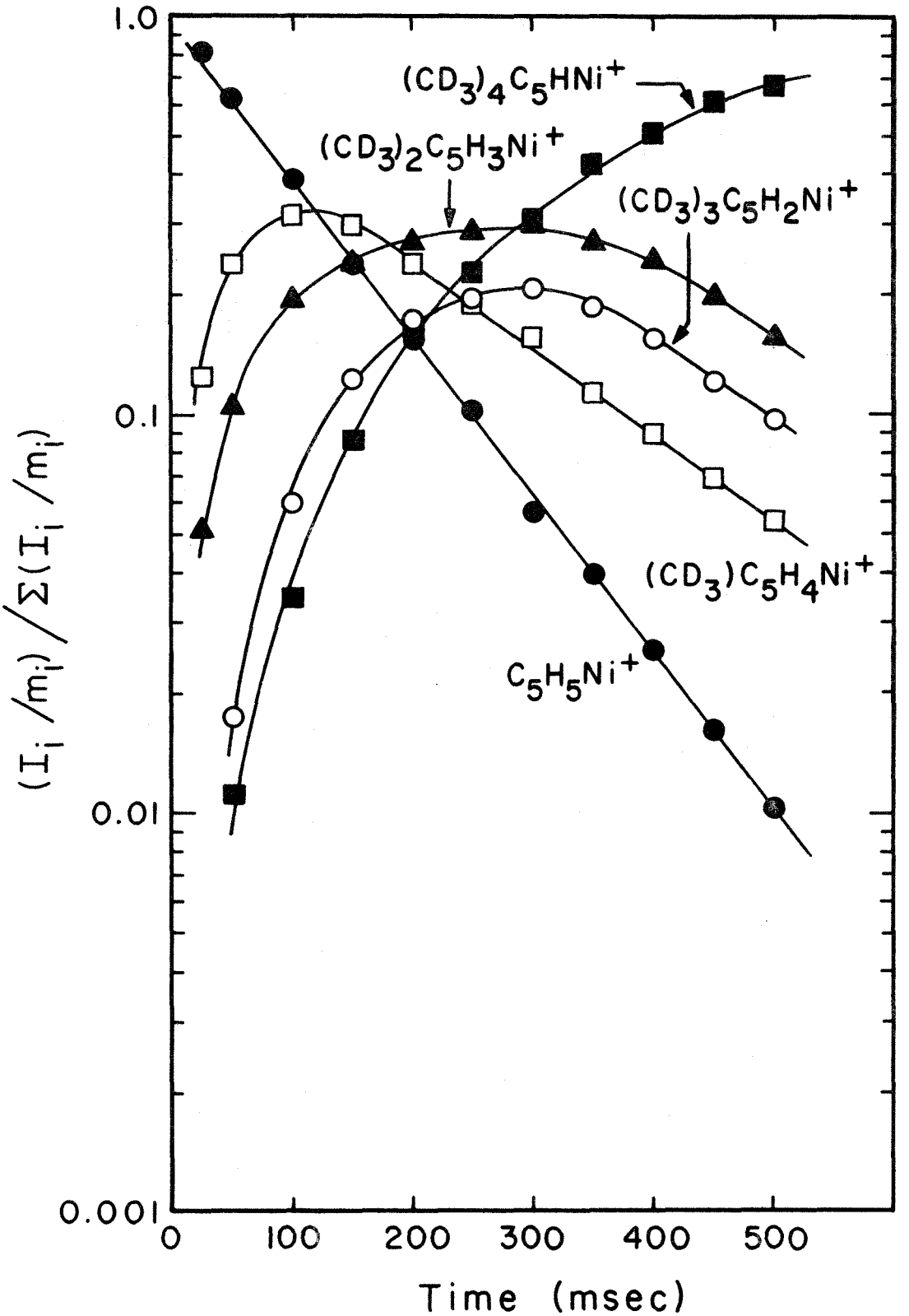
1.0
0.1
0.01
0.001
0
100
200
300
400
500
Time (msec)
$(I_i/m_i)/\Sigma(I_i/m_i)$
$(CD_3)_4C_5HNi^+$
$(CD_3)_2C_5H_3Ni^+$
$(CD_3)_3C_5H_2Ni^+$
$(CD_3)C_5H_4Ni^+$
$C_5H_5Ni^+$

Me_2CO, MeOAC, and $(MeO)_2CO$, proton transfer occurs exclusively to produce $(CpNiNO)H^+$ (eq 33). For Et_2O and Me_2S, reversible proton

$$BH^+ + CpNiNO \rightarrow (CpNiNO)H^+ + B \quad (33)$$

transfer produces both $(CpNiNO)H^+$ and BH^+ (eq 34), while for

$$BH^+ + CpNiNO \rightleftharpoons (CpNiNO)H^+ + B \quad (34)$$
$$(B = Et_2O,\ Me_2S)$$

$CF_3CH_2NH_2$, NH_3, iPr_2O, and $MeNH_2$, proton transfer occurs to produce BH^+ only (eq 35). Thermochemical data relevant to these

$$(CpNiNO)H^+ + B \rightarrow BH^+ + CpNiNO \quad (35)$$
$$(B = CF_3CH_2NH_2,\ NH_3,\ iPr_2O,\ MeNH_2)$$

observations are presented in Table VII, from which the proton affinity of CpNiNO is established as PA(CpNiNO) = 198 ± 4 kcal/mol, corresponding to $\Delta H_f[(CpNiNO)H^+] = 266 \pm 5$ kcal/mol using data given in the Appendix.

For all of the bases mentioned above, the protonated species BH^+ and $(CpNiNO)H^+$ react with the neutral gas present to produce $(B)NiNO^+$ ions, in which cyclopentadiene is displaced (eq 36 and 37).

$$BH^+ + CpNiNO \rightarrow (B)NiNO^+ + C_5H_6 \quad (36)$$

$$(CpNiNO)H^+ + B \rightarrow (B)NiNO^+ + C_5H_6 \quad (37)$$

This result is consistent with the weak bond strength of cyclopentadiene to $NiNO^+$, $D(C_5H_6\text{–}NiNO^+) \approx 10$ kcal/mol (see Appendix), while

Table VII. Proton Transfer Reactions Involving CpNiNO

Reaction Observed			PA(CpNiNO)[a]
Me_2COH^+ + CpNiNO	→	$(CpNiNO)H^+$ + Me_2CO	> 193.9
$MeOAcH^+$ + CpNiNO	→	$(CpNiNO)H^+$ + MeOAc	> 195.4
Et_2OH^+ + CpNiNO	⇌	$(CpNiNO)H^+$ + Et_2O	≈ 197.4
$(CpNiNO)H^+$ + Me_2S	⇌	Me_2SH^+ + CpNiNO	≈ 197.6
$(CPNiNO)H^+$ + $CF_3CH_2NH_2$	→	$CF_3CH_2NH_3^+$ + CpNiNO	< 200.3
$(CpNiNO)H^+$ + NH_3	→	NH_4^+ + CpNiNO	< 202.3

[a]All values in kcal/mol relative to $PA(NH_3)$ = 202.3 ± 2.0 kcal/mol (reference 34).

$D(B-NiNO^+)$ is approximately 50 kcal/mol, and strongly suggests that the site of protonation is on the cyclopentadienyl ring in reactions 36 and 37, while protonation may occur on the NiNO moiety in reactions 33 and 34. In an attempt to confirm this, mixtures of CpNiNO with a 16-fold excess of D_2O were examined using ICR trapped-ion techniques.[19, 21] Abundant $(CpNiNO)D^+$ ions result from the sequence of reactions 38 and 39, but no further incorporation of deuterium was

$$D_2O^+ + D_2O \rightarrow D_3O^+ + D \quad (38)$$

$$D_3O^+ + CpNiNO \rightarrow (CpNiNO)D^+ + D_2O \quad (39)$$

observed. In other cases it has been observed that protonation of aromatic species can lead to rapid exchange of ring hydrogens in the presence of D_2O.[48] Furthermore, the thermoneutral exchange reaction (eq 40), which would be indicative of ring protonation,[13] is

$$(C_5H_5D)NiNO^+ + CpNiNO \rightarrow (C_5H_6)NiNO^+ + (C_5H_4D)NiNO \quad (40)$$

not observed. A possible complication occurs in both the exchange with D_2O and the failure to observe thermoneutral proton transfer, however, because the labile <u>endo</u> and <u>exo</u> methylene hydrogens on the protonated cyclopentadienyl ring are not equivalent.[13]

A small amount of Et_3N was added to the mixture of CpNiNO and D_2O to remove either a proton or a deuteron from $(CpNiNO)D^+$ by proton (deuteron) transfer, producing $Et_3N(H, D)^+$ as shown in reactions 41 and 42. The results indicate that deuteron transfer predominates

$$(CpNiNO)D^+ + Et_3N \xrightarrow{86\%} Et_3ND^+ + CpNiNO \quad (41)$$

$$(CpNiNO)D^+ + Et_3N \xrightarrow{14\%} Et_3NH^+ + (C_5H_4D)NiNO \quad (42)$$

(86%) over proton transfer (14%), contrary to the expectation for statistical D^+ and H^+ transfer (17% and 83%, respectively). These results suggest that protonation either occurs on the NiNO moiety, or that scrambling of hydrogens on the cyclopentadienyl ring does not occur rapidly compared to the deprotonation rate.

The homolytic bond dissociation energy, $D(H-M^+)$, is defined as the enthalpy change for the reaction $MH^+ \rightarrow M^+ + H$ and is related to the proton affinity of M by eq 43, where the indicated ionization

$$PA(M) - D(H-M^+) = IP(H) - IP(M) \quad (43)$$

potentials refer to the adiabatic values. Combining the PIMS result of IP(CpNiNO) = 8.21 ± 0.03 eV with PA(CpNiNO) = 198 ± 4 kcal/mol gives $D(H-CpNiNO^+)$ = 76 ± 4 kcal/mol. This is remarkably close to $D(H-C_5H_5)$ = 81.1 ± 1.2 kcal/mol for cyclopentadiene.[49]

Methyl Cation Affinity of CpNiNO. Both $(CH_3)_2F^+$ and $(CH_3)_2Cl^+$ formed by reactions 44 and 45 transfer CH_3^+ to CpNiNO (reaction 46).

$$CH_3X^+ + CH_3X \rightarrow CH_3XH^+ + CH_2X \quad (44)$$

$$CH_3XH^+ + CH_3X \rightarrow (CH_3)_2X^+ + HX \quad (45)$$

$$(CH_3)_2X^+ + CpNiNO \rightarrow (CpNiNO)CH_3^+ + CH_3X \quad (X = F, Cl) \quad (46)$$

No reaction is observed for $(CH_3)_2Br^+$ or $(CH_3)_2I^+$. These results indicate that $D(CH_3Br-CH_3^+) > D(CpNiNO-CH_3^+) > D(CH_3Cl-CH_3^+)$, or that 51 kcal/mol < $D(CpNiNO-CH_3^+)$ < 56 kcal/mol.[47]

Discussion

CpNiNO is a diamagnetic,[50] 18-electron organometallic complex. Upon ionization, the 17-electron molecular ion, $CpNiNO^+$, is produced (eq 47), from which the three-electron donor ligand NO is readily displaced by those bases, B, where $D(B-CpNi^+) > D(NO-CpNi^+)$ = 45.9 kcal/mol, producing the 16-electron complex $CpNiB^+$ (eq 48).

$$CpNiNO + e^- \rightarrow CpNiNO^+ + 2e^- \quad (47)$$

$$CpNiNO^+ + B \rightarrow CpNiB^+ + NO \quad (48)$$

In a mixture of an excess of two bases with CpNiNO, equilibrium $CpNi^+$ transfer between B_1 and B_2 (eq 49) is observed to be rapid in comparison

$$CpNiB_1^+ + B_2 \rightleftharpoons [CpNiB_1B_2^+]^* \rightleftharpoons CpNiB_2^+ + B_1 \quad (49)$$

to any further reactions of the complexes with the neutrals present. The rapid exchange of monodentate n-donor ligands is promoted by the coordination vacancy of the 16-electron complexes, $CpNiB_1^+$ and $CpNiB_2^+$, which facilitates binding of a second pair donor to form the 18-electron intermediate indicated in eq 49.

The displacement of a monodentate ligand by a π-bonding ligand (e.g., propylene, isobutylene, butadiene, benzene, and pyridine) results in the formation of a complex which reacts very slowly, if at all, in further ligand exchange. For propylene and isobutylene this may be due to the formation of metallocycle complexes, 1, in which both σ- and π-bonding effects are important, as for cyclic bromonium ions 2.[51] Significant distortion of the alkene may accompany binding,

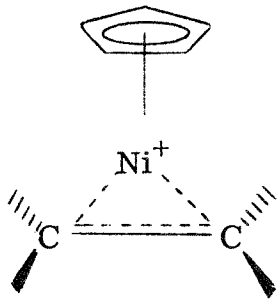

1

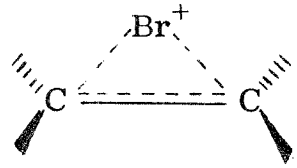

2

which would also seem to render exchange with other ligands less facile.[52] $D(B-CpNi^+)$ for the multidentate ligands butadiene, benzene, and pyridine are probably much larger than for n-donor bases (> 60 kcal/mol) and so these ligands are not displaced from $CpNi^+$. Illustrative of the larger metal-ligand bond strengths in metal sandwich compounds are $D(C_6H_6-CpMn^+)$ = 122 kcal/mol[53] and $D(C_5H_6-CpNi^+)$ = 115 kcal/mol.[13]

The data in Figure 7 reveal several trends in metal-ligand bond dissociation energies, $D(B-CpNi^+)$. First, $D(B-CpNi^+)$ generally increases with increasing substitution of alkyl groups for H on the basic site ($Me_3P > PH_3$, $Me_2O > MeOH > H_2O$, $Me_2S > MeSH > H_2S$). Also, $D(B-CpNi^+)$ increases with increasing methyl substitution on the carbon α to the basic site ($Me_3COH > Me_2CHOH > EtOH > MeOH$, $iPr_2O > Et_2O > Me_2O$, $MeCN > HCN$) and on carbon remote from the basic site ($Me_3CCHO > Me_2CHCHO > MeCH_2CHO > CH_3CHO$). Finally, $D(B-CpNi^+)$ is greater for second-row n-donor ligands than for first-row species ($Me_3P > Me_3N > Me_2S > Me_2O$). This is in direct contrast to Li^+ binding, for which $D(B-Li^+)$ is greater for first-row species than second-row n-donor bases ($MeCl < MeF$, $Me_2S < Me_2O$).[35]

Interestingly, the $D(B-CpNi^+)$ ordering of the alkyl amines is irregular, with $Me_2NH > Me_3N > MeNH_2 > NH_3$, similar to the behavior the amines exhibit towards Li^+.[36] While the experimental data (free energies) clearly indicate that $\Delta G(Me_3N-CpNi^+) > \Delta G(Me_2NH-CpNi^+)$, the entropy terms reverse this order, making $D(Me_2NH-CpNi^+) > D(Me_3N-CpNi^+)$ by 0.4 kcal/mol. A careful calculation of the entropy terms, using expressions derived from the partition functions for translation, rotation, vibration, and electronic states,[36, 54] gives results very close to those obtained using symmetry numbers.[33]

The measured metal-ligand bond energies are most striking in their comparison to proton affinities, Figure 12. Excluding the molecules NO, HCN, MeCN, MeNC, and Me_3As, a surprisingly good linear correlation is found between $D(B-H^+)$ and $D(B-CpNi^+)$. A least-squares analysis[55] gives a correlation coefficient of 0.964 and yields the linear relation (eq 50), where the errors quoted are standard

$$\delta D(R-CpNi^+) = (0.296 \pm 0.017)\, \delta D(B-H^+) - (0.453 \pm 0.213) \qquad (50)$$

deviations. The correlation may be of predictive value, e.g., from $D(H_2O-H^+) = 170.3$ kcal/mol,[34] $D(H_2O-CpNi^+) = 42.4 \pm 2.0$ kcal/mol is obtained. The excluded molecules all exhibit a greater preference for bonding $CpNi^+$ than predicted by eq 50, in accord with the expectation that all should have moderate π-bonding ability to nickel. For MeNC, the deviation from eq 50 is 6.7 kcal/mol, or only 12% of the total bond dissociation energy, $D(MeNC-CpNi^+) = 57.6 \pm 2.0$ kcal/mol

FIGURE 12

Comparison of two scales of molecular basicity; binding energies of molecules to H^+, $\delta D(B-H^+)$, and to $CpNi^+$, $\delta D(B-CpNi^+)$.

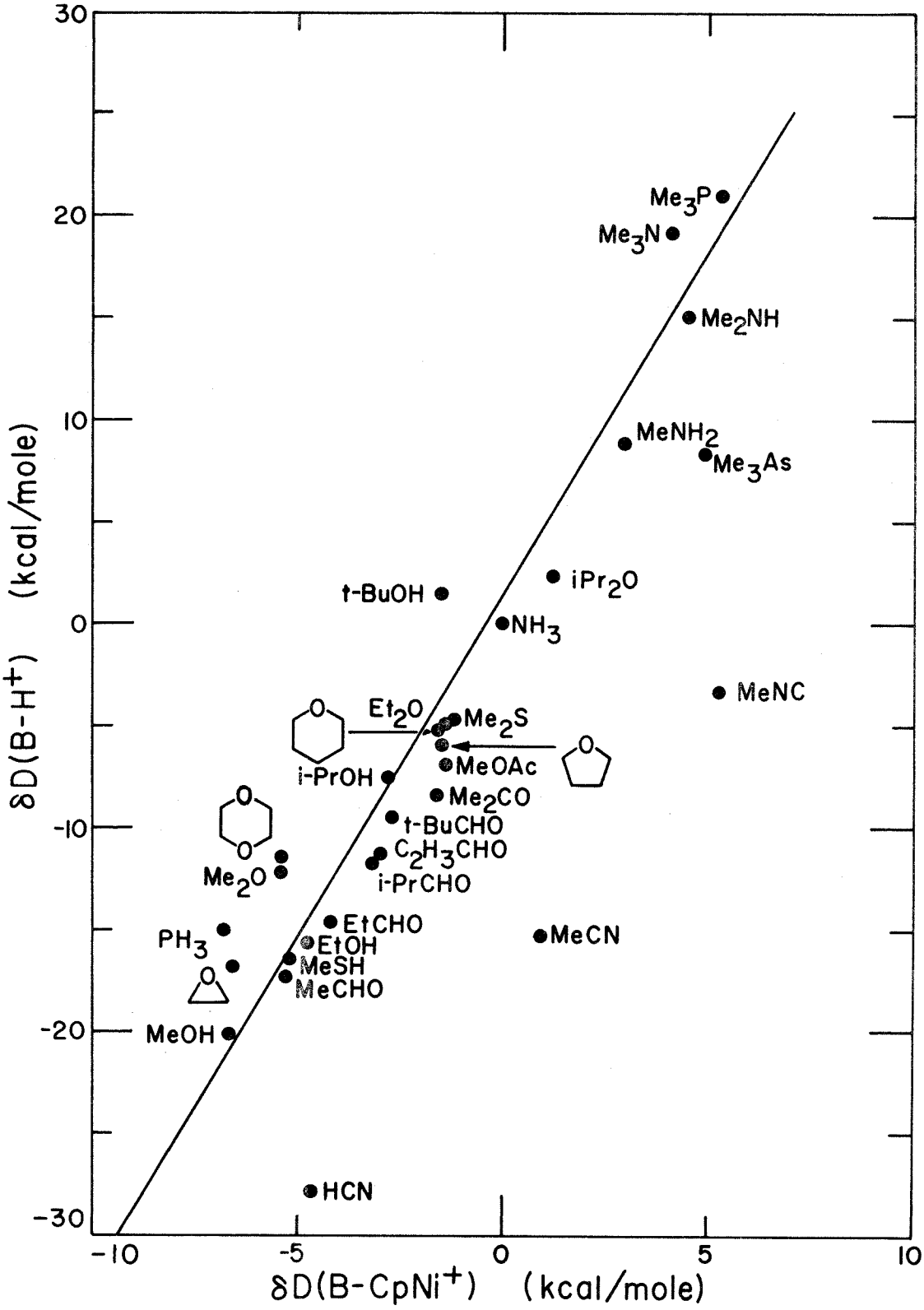
30
20
10
0
-10
-20
-30
-10
-5
0
5
10
δD(B-H+) (kcal/mole)
δD(B-CpNi+) (kcal/mole)
Me3P
Me3N
Me2NH
MeNH2
Me3As
iPr2O
t-BuOH
NH3
MeNC
Et2O
Me2S
MeOAc
i-PrOH
Me2CO
t-BuCHO
C2H3CHO
i-PrCHO
Me2O
EtCHO
PH3
EtOH
MeCN
MeSH
MeCHO
MeOH
HCN

(Table III). The enhancement of D(MeNC–$CpNi^+$) due to π-bonding effects is seen to be important, however, since it is comparable to the total range of D(B–$CpNi^+$) values measured in this study from 45.3 to 57.6 kcal/mol, or 12.3 kcal/mole.[5] The result that phosphorus compounds, with empty 3d orbitals (π-acceptors), fit the correlation reasonably well, suggests that metal-ligand donation is unimportant. This may, however, result from a stronger π-bond approximately cancelling the effects of a weaker σ-bond to $CpNi^+$.[56-58]

Recent semiempirical molecular orbital calculations of the electronic structure of $M(CH)_n$ (n = 3-8) and $M(CO)_3$ fragments[59] lead to a qualitative description of the bonding in $CpNi^+$ and $CpNiB^+$ species. Figure 13 presents a qualitative interaction diagram for the construction of the molecular orbitals of $CpNiB^+$ from the $CpNi^+$ and n-donor base, B, molecular orbitals. For clarity, only the highest occupied molecular orbitals of $CpNi^+$ and B are illustrated; the orbitals not displayed include the cyclopentadienyl a_1 and e_1 π-orbitals, and the nonbonding metal e_2 (d_{xy}, $d_{x^2-y^2}$) and a_1 (d_{z^2}) orbitals. For $CpNiB^+$, bonding occurs primarily through ligand-to-metal σ donation. This result is consistent with the observed trends in D(B–$CpNi^+$) (Figure 7), which suggest that the strength of the metal-ligand bond is directly proportional to the σ-donor ability of B. For those ligands with filled π orbitals (NO, HCN, MeCN, MeNC, and Me_3As), delocalization of the ligand π electrons into the empty metal e_1 (d_{xz} and d_{yz}) orbitals may occur, stabilizing the charge on nickel and leading to a stronger metal-ligand bond.

FIGURE 13

Qualitative interaction diagram for construction of the molecular orbitals of $CpNiB^+$ from the $CpNi^+$ and B molecular orbitals. Not shown are the filled low-lying cyclopentadienyl a_1 and e_1 π-orbitals and the metal e_2 and a_1 d-orbitals.

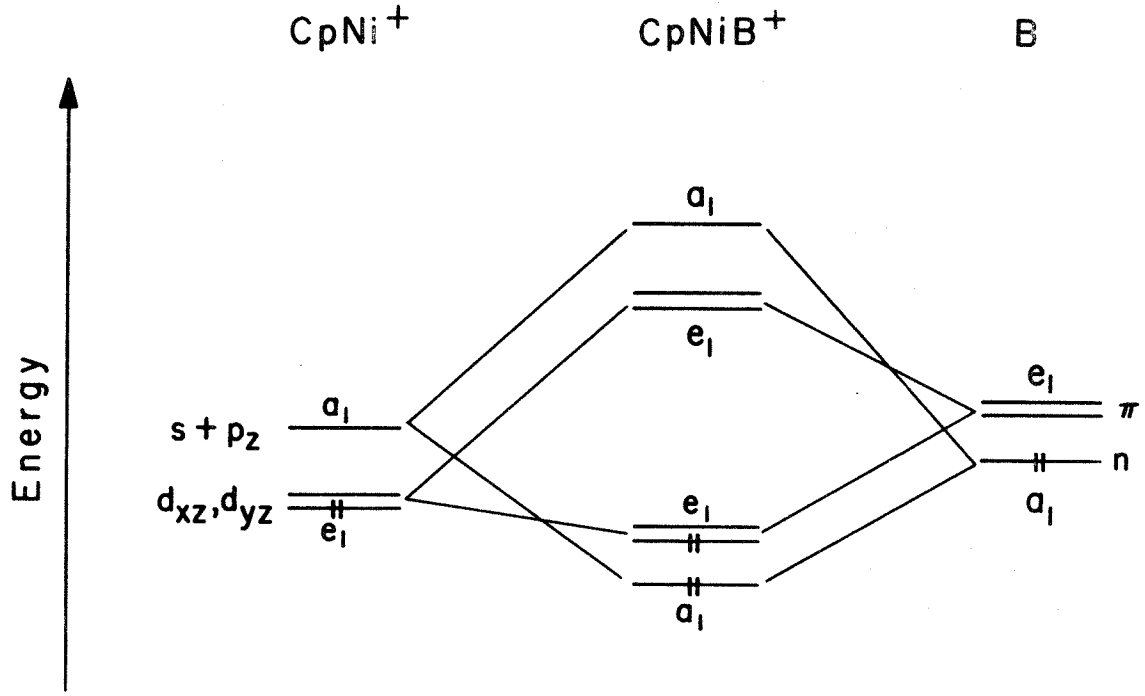
CpNi+
CpNiB+
B
Energy
a1
e1
a1
s + pz
dxz,dyz
e1
e1
e1
a1
e1
π
n
a1

Calculations of the electronic structure of NiCO,[60] $NiCO^+$,[61] and CpNi·[18] employing the ab initio generalized valence bond method,[62] in which the dominant electron correlation effects are solved for self-consistently, lead to a similar description of the bonding in $CpNi^+$ and $CpNiB^+$ species. These calculations suggest that bonding in $CpNi^+$ occurs by singlet coupling the 4s orbital of nickel ions in the $4s^13d^8$ configuration to the delocalized, five-fold degenerate radical orbital of $C_5H_5\cdot$.[18] Upon bringing $CpNi^+$ and an n-donor base B together, the base lone pair orbital delocalizes just slightly onto Ni^+ forming a metal-ligand dative bond[18, 60, 61] using the half-filled 4s orbital. As in the previous semiempirical bonding description, delocalization of ligand π electrons into the empty Ni^+ $\pi\pi$ holes (d_{xz} and d_{yz} orbitals) may occur. Ab initio calculations are in progress to further characterize the relative importance of metal-ligand vs. ligand-metal electron donation.[63]

A comparison of base strengths towards $CpNi^+$ and Li^+ from a graph of $D(B-CpNi^+)$[5] vs. $D(B-Li^+)$[35, 36] is consistent with the expectation that while bonding to Li^+ is largely electrostatic (non-covalent) in nature,[35, 36, 64] as Li^+ has a closed-shell $1s^2$ configuration, bonding to $CpNi^+$ involves covalent interactions, similar to H^+ although not as strong.[53] This is in part reflected in the ionization potentials of these two species; IP(CpNi·) = 7.8 ± 0.3 eV,[27] while IP(Li) = 5.39 eV.[28] The smaller difference between IP(B) and IP(CpNi·) leads to the expectation of more covalent bonding in $(CpNi-B)^+$ than is the case for Li. The contrast for alkenes is particularly striking; the interaction of alkenes with Li^+ is particularly weak relative to $CpNi^+$, for which covalent interactions may occur (structure 1).[52]

Several factors may influence the mechanism of processes such as the dehydrohalogenation of alkyl halides, the dehydration of alcohols, and the dehydrogenation of hydrocarbons. Müller has noted that the mass spectral decomposition patterns of organotransition metal complexes are characterized by the tendency of the central metal to keep its electron deficiency as low as possible, usually through the formation of π-bonds between the metal ion and newly formed centers of unsaturation.[65] The observation that Li^+[3, 8, 42] and Al^+[66] readily dehydrohalogenate alkyl halides and dehydrate alcohols suggests a more general reaction mechanism, however. Scheme II outlines three paths for the reaction of Lewis acids with organic molecules. The initial interaction of the metal ion with the organic substrate leads to the formation of a chemically activated species, 3, with an internal excitation energy approximately equal to $D(B-M^+)$. Intermediate 4 is produced by X^- (X = H, Cl, Br, I, OH) transfer to M^+, forming a species in which MX interacts with an alkyl carbonium ion. This process may be either exothermic, e.g., for the reaction of Ni^+ with C_2H_5Cl in which $D(Cl^--Ni^+)$ = 208 kcal/mol while $D(Cl^--C_2H_5^+)$ = 190 kcal/mol, or slightly endothermic, as for $CpNi^+$ [$D(Cl^--CpNi^+) \approx 175$ kcal/mol[67]], in which case the internal excitation energy of species 3 is reduced. Decomposition of 4 may occur along three possible reaction channels. In path A, hydrogen atom transfer to X forms intermediate 5, which rearranges to 6, from which either XH or an alkene is eliminated. Path A is expected for those Lewis acids which are not easily oxidized, e.g., Li^+ and Al^+.

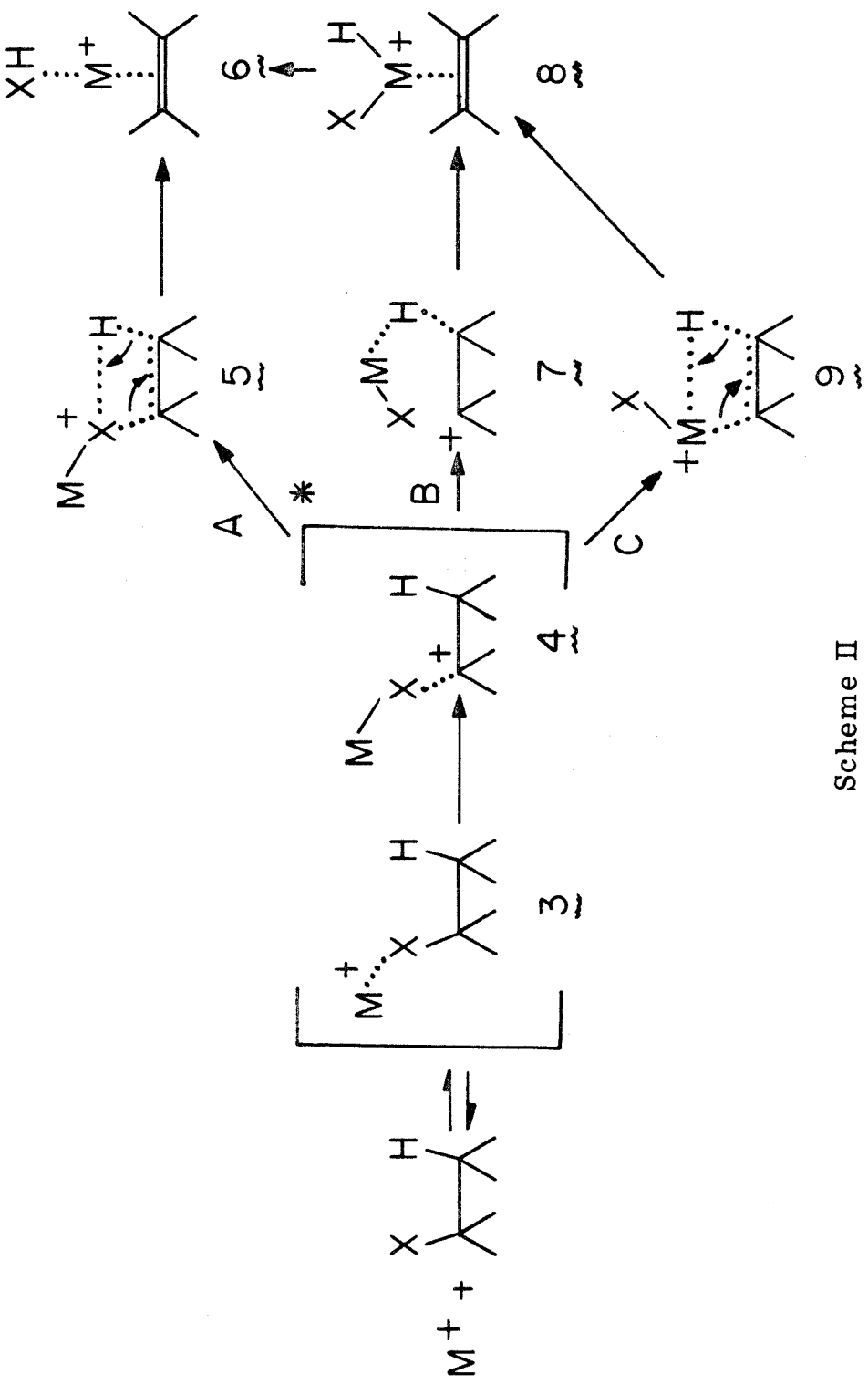

Scheme II

Route B involves a β-hydrogen migration from the alkyl carbonium complex $\underset{\sim}{4}$ to the metal, $\underset{\sim}{7}$, producing $\underset{\sim}{8}$, in which H and X are dissociated on the metal-alkene complex. X and H may recombine on the metal center to form species $\underset{\sim}{6}$. Alternatively, the metal may insert directly into the R-X bond in Pact C, producing a σ-bonded $X\text{-}\overset{+}{M}\text{-}R$ complex, $\underset{\sim}{9}$. As in channel B, β-hydrogen migration occurs to produce $\underset{\sim}{8}$. Paths B and C are expected for Lewis acids with variable oxidation states which are energetically accessible, e.g., $CpNi^+$, Ni^+, and Fe^+. Ridge has shown that for organic substrates which have β-hydrogens available, H-atom migration to metal is fast compared to the lifetime of the activated complex,[8] which accounts for the facility of elimination processes in $CpNi^+$–RX systems (R $\geq$ Et).

For the oxidative addition processes illustrated in Scheme II to be exothermic requires that for reaction 51, $D(A\text{–}CpNi^+) + D(B\text{–}CpNi^+)$

$$CpNi^+ + A\text{–}B \rightarrow \overset{+}{CpNi}\begin{matrix}\diagup A \\ \diagdown B\end{matrix} \qquad (51)$$

$\geq D(A\text{–}B)$, with the extent of inequality determining the internal excitation available to effect further rearrangement. Also, the oxidative addition (eq 51) is energetically attractive if there are $\leq$ 18 electrons in the valence shell of the metal. With D(M–H) typically 55-65 kcal/mol,[68] D(M–C) $\approx$ 30-40 kcal/mol,[69] and D(C–H) $\approx$ 90-100 kcal/mol,[40] the oxidative addition process will be moderately exothermic, in general, by approximately 5 kcal/mol for C–H substrates.

Similarly, with D(M–X) ≈ 70-90 kcal/mol (X = F, Cl, Br, I)[68] and D(C–X) ≈ 50-100 kcal/mol,[40] reaction 51 will be approximately 40 kcal/mol exothermic for C–X substrates. Oxidative addition of $CpNi^+$ into C–C bonds will not be a facile process, however, and is endothermic by ≈ 12 kcal/mol, assuming D(C–C) is typically between 77-88 kcal/mol.[40]

The energy profile diagram presented in Figure 14 summarizes the salient thermochemical features for the dehydrogenation of cyclopentane by $CpNi^+$.[70] The initial interaction results in the formation of a weakly bound CpNi (cyclopentane)$^+$ complex, I. The internal excitation of intermediate I is estimated to be approximately E* ≈ 30 kcal/mol, assuming no release of energy to translation of internal excitation of H_2. Intermediate II results from hydride transfer and subsequent oxidative insertion of nickel into the C–H bond. Hydrogen elimination involving hydrogen on the metal and cyclopentyl hydrogen endo to nickel produces CpNi (cyclopentene)$^+$, III. Formation of CpNi(c$-C_5H_8$)$^+$ produces a species with an internal excitation of approximately 23 kcal/mol [assuming D(c$-C_5H_8$–$CpNi^+$) ≈ 49 ± 5 kcal/mol as for isobutylene], and dehydrogenates further to CpNi (cyclopentadiene)$^+$, or protonated nickelocene.[13] The dashed curve would result from the loss of H_2 in the v = 1 level (4395 cm^{-1} = 12.6 kcal/mol[71]); in this case loss of a second H_2 molecule is not energetically possible. Loss of energy to translation (product repulsion) would give similar results. From the observed product distribution (Table VI), in 49% of the reactions the loss of the first H_2 molecule removes sufficient internal excitation to inhibit loss of a second.

FIGURE 14

Proposed energy profile diagram for the energetic changes associated with the dehydrogenation of cyclopentane by $CpNi^+$. The dashed curve results from the loss of H_2 in the v = 1 level from intermediate II.

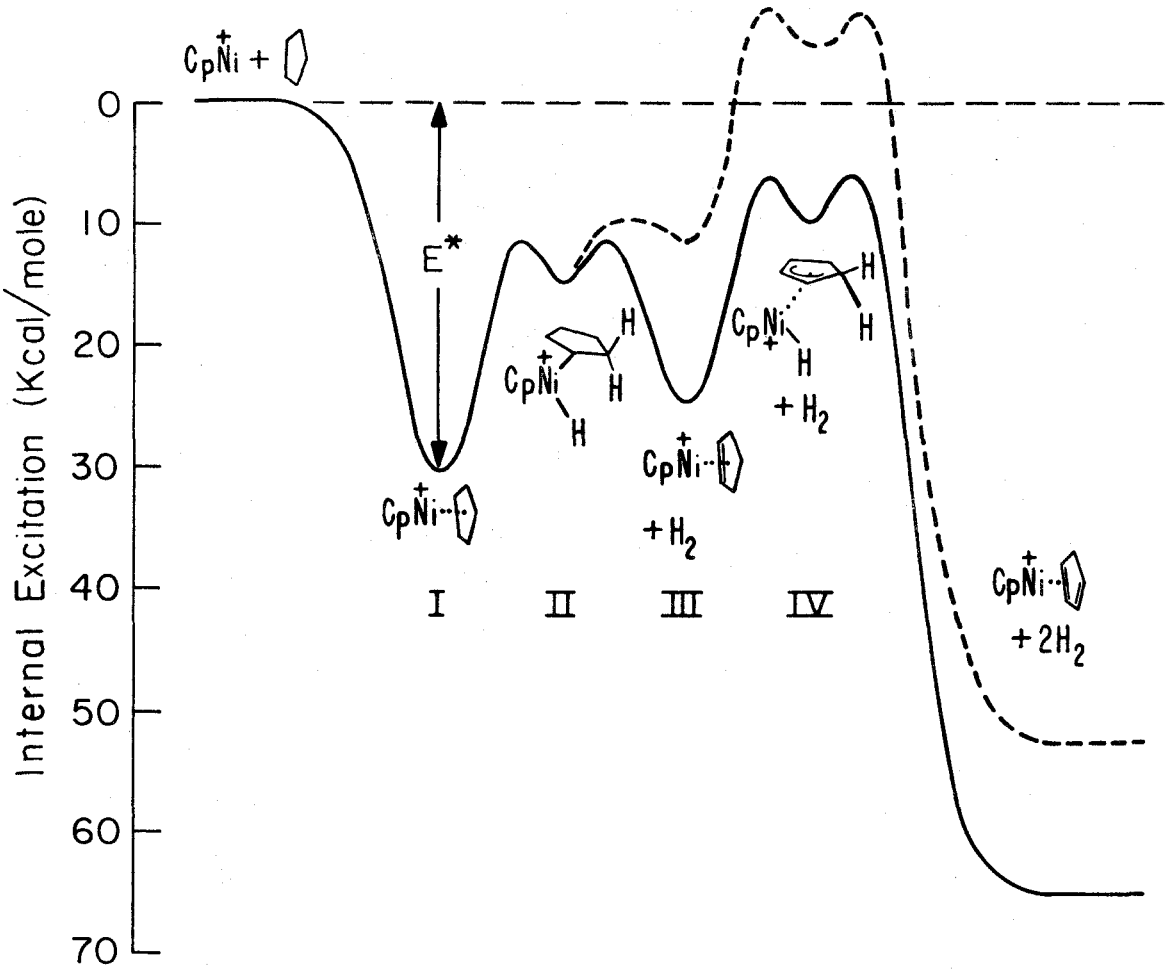
Internal Excitation (Kcal/mole)
0
10
20
30
40
50
60
70
CpNi + ⬡
E*
CpNi⋯⬡
I
CpNi
H
H
H
II
CpNi⋯⬡
+ H2
III
CpNi
H
H
H
+ H2
IV
CpNi⋯⬡
+ 2H2

Additional evidence for a stepwise dehydrogenation mechanism is provided by the observation that $CpNi^+$ dehydrogenates both 1, 3- and 1, 4-cyclohexadiene to benzene with equal rates (Table VI), in contrast to the gas phase homogeneous dehydrogenation reactions of these species.[72, 73] For both olefins, hydride transfer and oxidative insertion of nickel produces identical cyclohexyl species bound to nickel, which subsequently eliminates H_2. $CpNi(benzene)^+$ is not observed in the reaction of $CpNi^+$ with n-hexane, indicating that dehydrocyclization processes do not occur. Mass spectral studies of the fragmentation of $(c-C_6H_8)FeCp$ and $(c-C_6H_8)Fe(CO)_3$ complexes indicate that stereoselective migration of hydrogen endo to metal occurs,[74] and that dehydrogenation processes are particularly facile for organotransition metal complexes with olefinic ligands containing two adjacent sp^3 hydridized carbon atoms.[75]

The experimental data lead to several conclusions concerning decarbonylation reactions effected by $CpNi^+$. The reaction mechanism is specific for aldehydes, as none of the molecules CH_3COX (X = Cl, Br, CH_3, OCH_3) are decarbonylated. This suggests that hydrogen on the acyl carbon is important, since product ions which result from facile X^- transfer to nickel are observed only for X = H, and not for X = Cl, Br, CH_3, OCH_3. A measure of acyl carbon-hydrogen bond strengths is given by the hydride affinity, $D(RCO^+-H^-)$, of these cations. Using available thermochemical data,[28, 39-41] Table VIII lists values of $D(RCO^+-H^-)$ for several of the relevant molecules. When $D(RCO^+-H^-)$ becomes greater than $\sim$ 250 kcal/mol, decarbonylation is not observed, presumably because hydride transfer to

Table VIII. Hydride Affinities of R^+ and RCO^+ Cations[a]

R^+	$\Delta H_f(R^+)$	$D(R^+-H^-)$
$C_2H_5^+$	219	272
i-$C_3H_7^+$	190	248
s-$C_4H_9^+$	192	256
t-$C_4H_9^+$	176	242
c-$C_5H_9^+$	196.7[b]	248
c-$C_6H_{11}^+$	185	248
HCO^+	195.9[c]	257
CH_3CO^+	160[d]	233
$C_2H_5CO^+$	143	225
i-$C_3H_7CO^+$	133	222
t-$C_4H_9CO^+$	125	219
$C_6H_5CO^+$	190[e]	234
$CH_3COCH_2^+$	258[f]	343
c-$C_4H_7^+$	213	239
$CpNi^+$	310.7[g]	226[g]

[a]All values in kcal/mol, thermochemical quantities from reference 28 unless otherwise noted; $\Delta H_f(H^-) = 33.2$ kcal/mol (reference 41). [b]F. P. Lossing and J. L. Traeger, J. Am. Chem. Soc., 97, 1579 (1975). [c]N. Jonathan, A. Morris, M. Okuda, and D. J. Smith, J. Chem. Phys., 55, 3046 (1971). [d]R. Kräsig, D. Reinke, and H. Baumgärtel, Ber. Bunsenges Phys. Chem., 78, 425 (1974). [e]B. S. Freiser and J. L. Beauchamp, J. Am. Chem. Soc., 98, 3136 (1976). [f]E. Murad and M. G. Inghram, J. Chem. Phys., 41, 404 (1964). [g]See Appendix.

$CpNi^+$ does not occur. Finally, the decarbonylation must involve a final reaction intermediate from which competitive elimination of RH or CO can occur. The weaker of the two bonds $CpNi(RH)^+$–CO or $CpNi(CO)^+$–RH will be preferentially broken in the dissociation of this species. Reaction 29 is thus expected with $D(C_6H_6–CpNi^+) > D(CO–CpNi^+) \cong 40$ kcal/mol (see Appendix).

A generalized energy profile diagram and proposed intermediates for the decarbonylation of aldehydes by $CpNi^+$ is shown in Figure 15. Choice of reaction intermediates is based in part on studies of the mechanism of this process in solution.[76-79] The initial interaction of $CpNi^+$ with RCHO produces the chemically activated species I with an internal energy approximately equal to $D(RCHO–CpNi^+)$.[5] This is followed by hydride migration to nickel, producing intermediate II. While formation of RH may be preceeded by migration of R onto nickel, giving intermediate III,[80] it seems more likely that RH results from a four center process starting with II. The intermediate species IV results from the interaction of RH and CO with $CpNi^+$. The stabilities of intermediates II and III and the height of the barriers connecting these species to I and IV remain unknown.

The combination of ICR double resonance techniques[19, 20] and the use of deuterium-labelled methyl bromide provide considerable information about the mechanism of the sequential alkylation reaction 32. Scheme III illustrates a proposed mechanism for the first step in the sequential alkylation of $CpNi^+$ by CD_3Br. Initially, the $CpNi^+$ cation interacts with CD_3Br to form the activated complex 10, which has an

FIGURE 15

Proposed generalized energy profile diagram and reaction intermediates for the decarbonylation of aldehydes by $CpNi^{+}$. The stabilities of the intermediates II and III are uncertain, as are the barriers connecting these species with other proposed intermediates.

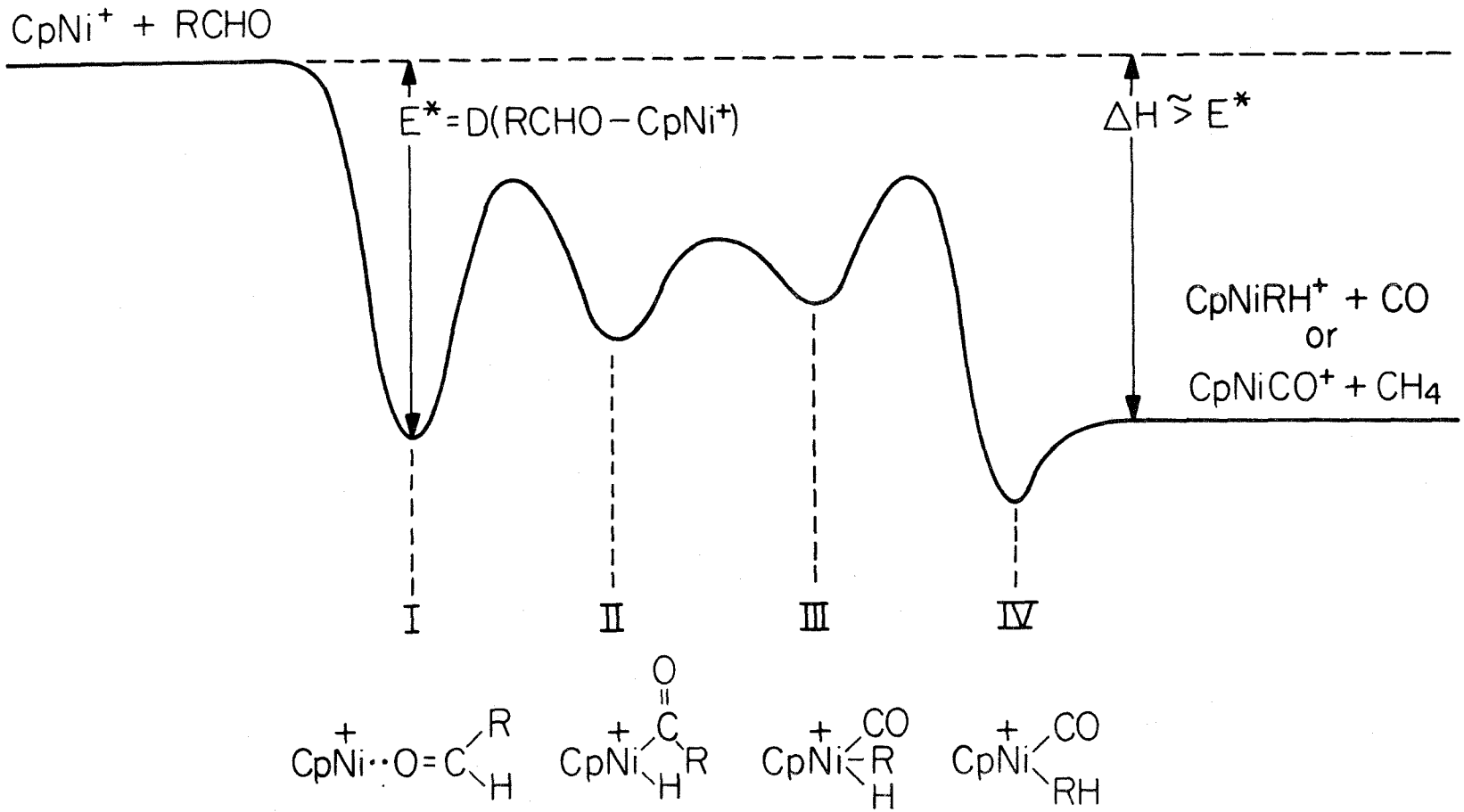
CpNi+ + RCHO
E* = D(RCHO – CpNi+)
ΔH ≳ E*
CpNiRH+ + CO
or
CpNiCO+ + CH4
I
II
III
IV
CpNi··O=C
R
H
O
C
CpNi
R
H
CO
CpNi
R
H
CO
CpNi
RH

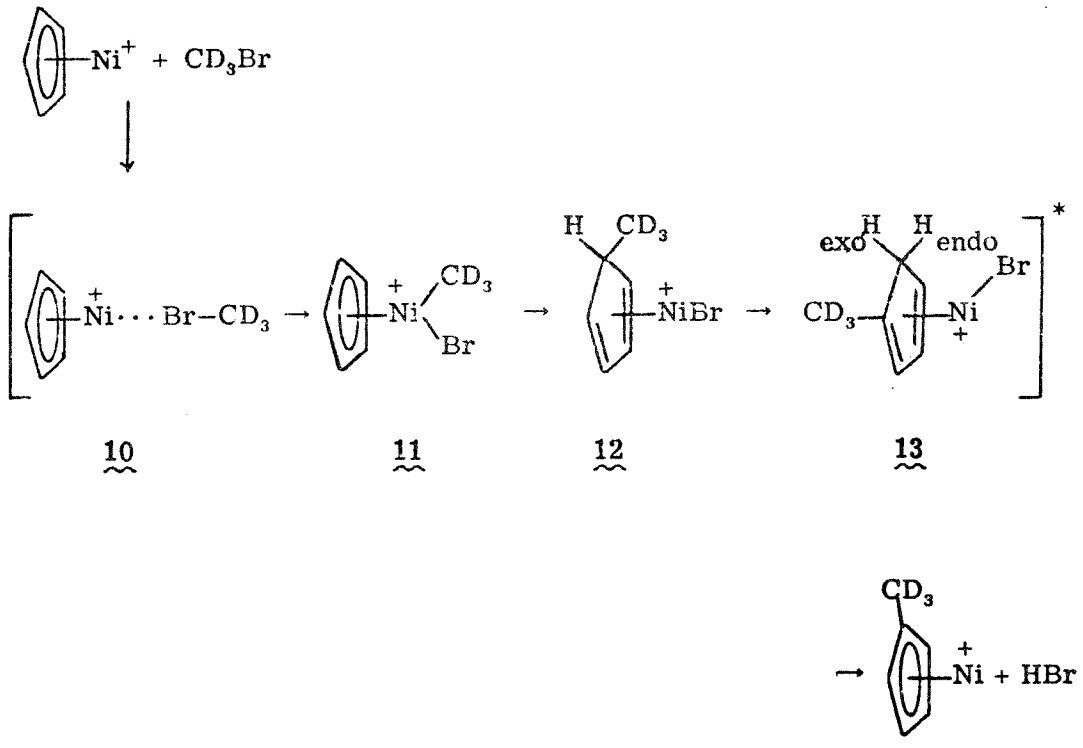

Scheme III

internal energy equal to $D(CD_3Br-CpNi^+) \approx 40$ kcal/mol.[81] The internal energy of 10 is sufficient to allow for oxidative addition of nickel to the carbon-bromine bond, yielding 11. CD_3 migrates to the cyclopentadienyl ring, giving 12, methyl-d_3 cyclopentadiene nickel bromide cation. Species 12 rapidly rearranges to 13 via a [1, 5] sigmatropic shift (thermally allowed in the ground state[82]), which is known to occur rapidly at room temperature in methyl cyclopentadiene.[83] Finally, HBr elimination from 13 involving the endo hydrogen yields the product ion, $(CD_3)C_5H_4Ni^+$. The sequence of Scheme III is repeated four times, and is facilitated by the increasing activation of the cyclopentadienyl ring towards electrophilic substitution with each successive alkylation.[84]

The appealing feature of the proposed mechanism is that it allows for only four alkylations since the fifth step would require HBr elimination to involve the exo hydrogen from 14 (Scheme IV). Apparently in

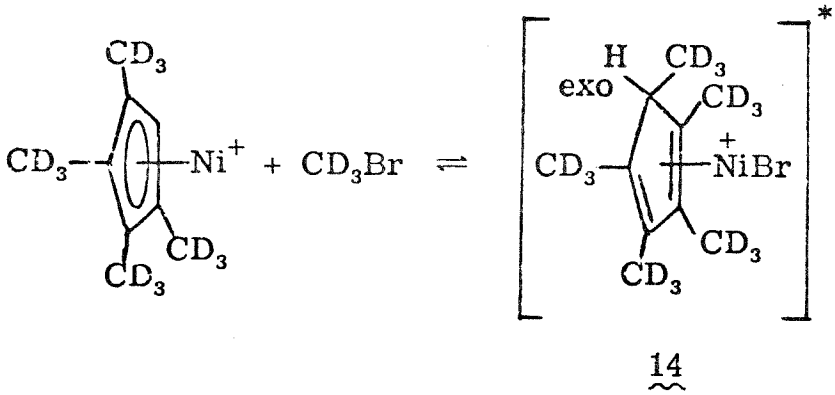

14

Scheme IV

this case the reaction intermediate reverts to reactants, if it is formed at all.

Experiments to determine the site of protonation of CpNiNO give results which do not clearly distinguish between the four possible locations in this molecule (ring, Ni, N, and O). Observation of $(B)NiNO^+$ (eq 36 and 37) strongly suggests that in most instances the cyclopentadienyl ring is protonated. Proton transfer to the ring produces $(\eta^4-C_5H_6)NiNO^+$, formally oxidizing the nickel atom and resulting in a coordinately unsaturated species which can bind an n-donor base, B. Upon interaction of $(\eta^4-C_5H_6)NiNO^+$ with B, an 18-electron intermediate, $(\eta^1-C_5H_6)NiNO(B)^+$, is produced, which decomposes to $(B)NiNO^+$ by loss of C_5H_6.

We note briefly that the linear correlation of $D(B-CpNi^+)$ vs. $D(B-H^+)$ (eq 50) and the value of PA(CpNiNO) = 198 ± 4 kcal/mol measured in this study may be used to calculate $D(CpNiNO-CpNi^+)$ = 51 ± 4 kcal/mol. This value is in good agreement with the result that $D(CpNiNO-CpNi^+)$ is slightly less than $D(NH_3-CpNi^+)$ (c.f. reaction 14), and suggests that CpNiNO may bond to $CpNi^+$ through oxygen. Studies of the site of protonation in strongly acidic media (98% H_2SO_4, $BF_3 \cdot H_2O$, and 100% CF_3CO_2H) are inconclusive as CpNiNO decomposes rapidly in these media.[85]

Conclusions

Most significantly, the present results provide the first direct measurements of the relative contributions of σ- and π-bonding interactions to the strengths of transition metal-ligand bonds. π-Bonding effects, where important (HCN, MeCN, MeNC, and Me_3As), account for approximately 10% of the total bond dissociation energy, which is substantial compared to the full range of metal-ligand bond dissociation energies measured in this study (45.3 to 57.6 kcal/mol). The observation that phosphorus ligands fit the correlation of $D(B-CpNi^+)$ vs. $D(B-H^+)$ (Figure 12) reasonably well may be the fortuitous result of a stronger π-bond approximately cancelling the effects of a weaker σ-bond to $CpNi^+$.[56-58] Future studies of ligand exchange processes will include the investigation of organometallic complexes with two or more exchangeable ligands (e.g., $CpFeB_1B_2^+$) in which synergistic effects of different pairs of ligands can be examined. Also of interest are ligand exchange processes involving anionic transition metal

complexes, in which the bonding may be quite different compared to cationic metal species.[86]

The present results also suggest a specific mechanism for elimination and decarbonylation reactions effected by coordinatively unsaturated $CpNi^+$. Following the initial interaction between electrophilic $CpNi^+$ and a heteroatomic center, X^- transfer (X = Cl, Br, I, OH, H) to nickel produces a species in which oxidative addition of $CpNi^+$ to the carbon-heteroatom bond has formally occurred. Elimination of an alkene or HX occurs with preferential bond cleavage of the more weakly bonded species to $CpNi^+$. Further study of metal ion chemistry is needed to distinguish Lewis acid reactivity from processes which require accessible variable oxidation states. The activation energies for homogeneous dehydrogenation and dehydrohalogenation are often quite high ($\sim$ 40-60 kcal/mol[40, 72, 73, 87]) and hence the $CpNi^+$ ion provides a single reactive center on which facile bond breaking and bond formation can occur without requiring a high energy transition state. Of particular interest is the observation that the stoichiometry and mechanism of the $CpNi^+$-induced dehydrogenation reaction (Figure 14) is exactly analogous to the first step in the catalytic hydrogenolysis of alkanes by heterogeneous catalysts.[88] Thus, the dehydrogenation of hydrocarbons, dehydrohalogenation of alkyl halides, and decarbonylation of aldehydes represent only three examples where gas phase studies can provide insights into the energetics and mechanisms of reactions which may be important in further understanding processes that involve homogeneous and heterogeneous catalysis.[88]

Acknowledgments. This research was supported in part by the Energy Research and Development Administration under Grant No. E(04-3)767-8. The Caltech-JPL facility for photoionization mass spectrometry was made possible by a grant from the President's Fund of the California Institute of Technology.

Appendix - Sources of Thermochemical Data

The enthalpies of formation of several key ions and neutrals considered in this study are presented in Table IX. The enthalpy of formation of CpNi· was computed from the appearance potential of $CpNi^+$ in the mass spectrum of Cp_2Ni [$AP(CpNi^+) = 12.63 \pm 0.05$ eV],[89] and the ionization potential of CpNi· .[27] These results combine to give $\Delta H_f(CpNiNO^+)$, and from IP(CpNiNO) = 8.21 ± 0.03 eV measured in this study, $\Delta H_f(CpNiNO) = 97.1 \pm 2.2$ kcal/mol is computed. $\Delta H_f(CpNiH)$ is calculated from $\Delta H_f(CpNi\cdot)$ and D(CpNi–H) = 65 ± 5 kcal/mol.[18] $D(CO–CpNi^+)$ is calculated from PA(CO) = 143 kcal/mol[90] and the linear relation between $D(B–H^+)$ and $D(B–CpNi^+)$ (eq 50). An additional 5 kcal/mol was added to account for expected π-bonding interactions. $D(NO–Ni^+)$ was chosen to be 59 ± 10 kcal/mol by noting that $D(CO–Ni^+) = 48.6 \pm 1.4$ kcal/mol[91] and adding 10 kcal/mol to account for π-bonding effects.

Table IX. Thermochemical Data Used in this Study

Species, M	$\Delta H_f(M)$[a]	IP(M)[b]	$\Delta H_f(M^+)$[a]
CpNiNO	97.1 ± 2.2[c]	8.21 ± 0.03[d]	286.4 ± 2.1[c]
CpNi·	130.8 ± 1.8[c]	7.8 ± 0.3[e]	310.7 ± 1.8[c]
Cp·	60.9 ± 1.2[f]	8.41 ± 0.10[f]	254.8 ± 1.2[f]
Ni	102.7 ± 1.0[g]	7.635[g]	278.8 ± 1.0
Cp_2Ni	80.3 ± 0.7[h]	6.2 ± 0.1[i]	223.3 ± 0.7
CpNiH	117.9 ± 5.3	- -	- -
$(CpNiNO)H^+$	- -	- -	266.3 ± 4.6[c]
$(Cp_2Ni)H^+$	- -	- -	227.3 ± 1.0[j]
$CpNiCO^+$	- -	- -	244.3 ± 5.3[c]
$NiNO^+$	- -	- -	241 ± 10[c]

[a]All values in kcal/mol at 298°K. [b]All values in eV. [c]Calculated (see Appendix). [d]This work. [e]Reference 27. [f]F. P. Lossing and J. L. Traeger, J. Am. Chem. Soc., 97, 1579 (1975). [g]Reference 28. [h]Reference 39. [i]Reference 29. [j]Reference 13.

References and Notes

(1) M. S. Foster and J. L. Beauchamp, J. Am. Chem. Soc., 93, 4924 (1971).

(2) M. S. Foster and J. L. Beauchamp, J. Am. Chem. Soc., 97, 4808 (1975).

(3) J. Allison and D. P. Ridge, J. Organomet. Chem., 99, C11 (1975).

(4) G. H. Weddle, J. Allison, and D. P. Ridge, J. Am. Chem. Soc., 99, 105 (1977).

(5) R. R. Corderman and J. L. Beauchamp, J. Am. Chem. Soc., 98, 3998 (1976).

(6) R. R. Corderman and J. L. Beauchamp, J. Am. Chem. Soc., 98, 5700 (1976).

(7) J. Allison and D. P. Ridge, J. Am. Chem. Soc., 99, 35 (1977).

(8) J. Allison and D. P. Ridge, presented in part at the 24th Annual Conference on Mass Spectrometry and Allied Topics, San Diego, California, May 1976; J. Am. Chem. Soc., 98, 7445 (1976).

(9) R. D. Bach, A. T. Weibel, J. Patane, and L. Kevan, J. Am. Chem. Soc., 98, 6237 (1976); R. D. Bach, J. Gauglhofer, and L. Kevan, J. Am. Chem. Soc., 94, 6860 (1972); R. D. Bach, J. Pantane, and L. Kevan, J. Org. Chem., 40, 257 (1975).

(10) R. C. Dunbar, J. F. Ennever, and J. P. Fackler, Jr., Inorg. Chem., 12, 2734 (1973).

(11) Müller has studied the ion chemistry of a variety of n- and π-donor organic bases with several different transition metal complexes using high pressure mass spectrometry; see, for example,

J. Müller, Adv. in Mass Spectrom., 6, 823 (1974) and references contained therein.

(12) M. S. Foster and J. L. Beauchamp, J. Am. Chem. Soc., 97, 4814 (1975).

(13) R. R. Corderman and J. L. Beauchamp, Inorg. Chem., 15, 665 (1976).

(14) J. Müller and W. Goll, Chem. Ber., 106, 1129 (1973).

(15) For reviews of oxidative addition reactions in solution, see J. P. Collman and W. R. Roper, Adv. Organomet. Chem., 7, 53 (1968); J. Halpern, Acc. Chem. Res., 3, 386 (1970).

(16) S. Evans, M. F. Guest, I. H. Hillier, and A. F. Orchard, J. Chem. Soc., Faraday Trans. II, 70, 417 (1974).

(17) I. H. Hillier and V. R. Saunders, Molec. Phys., 23, 449 (1972).

(18) A. K. Rappé and W. A. Goddard III, unpublished results.

(19) For reviews, see J. L. Beauchamp, Ann. Rev. Phys. Chem., 22, 527 (1971); G. A. Gray, Adv. Chem. Phys., 19, 141 (1971); J. D. Baldeschwieler and S. S. Woodgate, Acc. Chem. Res., 4, 114 (1971); T. A. Lehman and M. M. Bursey, "Ion Cyclotron Resonance Spectrometry", Wiley, New York, N.Y., 1976.

(20) B. S. Freiser, T. B. McMahon, and J. L. Beauchamp, Int. J. Mass Spectrom. Ion Phys., 12, 249 (1973).

(21) T. B. McMahon and J. L. Beauchamp, Rev. Sci. Instrum., 43, 509 (1972).

(22) E. O. Fischer, O. Beckert, W. Hafner, and H. O. Stahl, Z. Naturforsch., 10B, 598 (1955).

(23) R. J. Blint, T. B. McMahon, and J. L. Beauchamp, J. Am. Chem. Soc., 96, 1269 (1974).

(24) R. R. Corderman, P. R. LeBreton, S. E. Buttrill, Jr., A. D. Williamson, and J. L. Beauchamp, J. Chem. Phys., 65, 4929 (1976); A. D. Williamson, Ph.D. Thesis, California Institute of Technology, Pasadena, California, 1976.

(25) R. C. Weast, Ed., "Handbook of Chemistry and Physics", 51st ed., Chemical Rubber Co., Cleveland, Ohio, 1970, p. B-264.

(26) The neutral products are inferred, e.g., in reaction 4 the products may be either NiNO or Ni + NO.

(27) P. Schissel, D. J. McAdoo, E. Hedaya, and D. W. McNeil, J. Chem. Phys., 49, 5061 (1968).

(28) J. L. Franklin, J. G. Dillard, H. M. Rosenstock, J. T. Herron, K. Draxl, and F. H. Field, Natl. Stand. Ref. Data Ser., Natl. Bur. Stand., No. 26 (1969).

(29) J. W. Rabalais, L. O. Werme, T. Bergmath, L. Karlsson, M. Hussain, and K. Siegbahn, J. Chem. Phys., 57, 1185 (1972).

(30) Product yields reported in reference 14 are different than those reported here, presumably due to the higher kinetic energy of the reactant ions in the high-pressure mass spectrometer.

(31) Reactant and product ions from MeCHO alone [A. S. Blair and A. G. Harrison, Can. J. Chem., 51, 703 (1973)] are not included in the normalization of data for Figure 4.

(32) J. L. Beauchamp and J. Y. Park, J. Phys. Chem., 80, 575 (1976); R. J. Blint, T. B. McMahon, and J. L. Beauchamp,

J. Am. Chem. Soc., 96, 1269 (1974); R. H. Staley and J. L. Beauchamp, J. Chem. Phys., 62, 1998 (1975).

(33) S. W. Benson, J. Am. Chem. Soc., 80, 5151 (1958).

(34) J. F. Wolf, R. H. Staley, I. Koppel, M. Taagepera, R. T. McIver, Jr., J. L. Beauchamp, and R. W. Taft, submitted for publication in J. Am. Chem. Soc.; P. Kebarle, R. Yamdagni, K. Hiraoka, and T. B. McMahon, Int. J. Mass Spectrom. Ion Phys., 19, 71 (1976).

(35) R. H. Staley and J. L. Beauchamp, J. Am. Chem. Soc., 97, 5920 (1975).

(36) R. L. Woodin and J. L. Beauchamp, submitted for publication in J. Am. Chem. Soc.,

(37) $D(NH_3-CpNi^+)$ = 52.3 ± 2.0 kcal/mol is obtained from $D(NO-CpNi^+)$ = 45.9 ± 1.0 kcal/mol and the measured value of $\delta D(NO-CpNi^+)$ = -6.4 kcal/mol (reference 5).

(38) J. L. Beauchamp and S. E. Buttrill, J. Chem. Phys., 48, 1783 (1968).

(39) J. D. Cox and G. Pilcher, "Thermochemistry of Organic and Organometallic Compounds", Academic Press, New York, N.Y., 1970.

(40) S. W. Benson, "Thermochemical Kinetics", Wiley, New York, N.Y., 1968.

(41) D. R. Stull and H. Prophet, "JANAF Thermochemical Tables", 2nd ed., Natl. Stand. Ref. Data Ser., Natl. Bur. Stand., No. 37 (1971).

(42) R. D. Wieting, R. H. Staley, and J. L. Beauchamp, J. Am. Chem. Soc., 97, 924 (1975).

(43) J. F. Vogt and J. L. Beauchamp, unpublished results.

(44) The abundance of ions from both CpNiNO alone (Figures 2 and 3) and cyclopentane are not included in the normalization of data given in Figure 8.

(45) R. H. Wyatt, D. Holtz, T. B. McMahon, and J. L. Beauchamp, Inorg. Chem., 13, 1511 (1974); S. R. Gunn, Inorg. Chem., 11, 796 (1972).

(46) R. R. Corderman and J. L. Beauchamp, submitted for publication in Inorg. Chem.

(47) J. L. Beauchamp, D. Holtz, S. D. Woodgate, and S. L. Patt, J. Am. Chem. Soc., 94, 2798 (1972).

(48) B. S. Freiser, R. L. Woodin, and J. L. Beauchamp, J. Am. Chem. Soc., 97, 6893 (1975); D. P. Martinsen and S. E. Buttrill, Jr., Org. Mass Spec., 11, 762 (1976).

(49) S. Furuyama, D. M. Golden, and S. W. Benson, Int. J. Chem. Kinet., 3, 237 (1971).

(50) E. O. Fischer and R. Jira, Z. Naturforsch., 10b, 355 (1955).

(51) R. D. Bach and H. F. Henneike, J. Am. Chem. Soc., 92, 5589 (1970).

(52) S. D. Ittel and J. A. Ibers, Adv. Organomet. Chem., 14, 33 (1976).

(53) R. G. Denning and R. A. D. Wentworth, J. Am. Chem. Soc., 88, 4619 (1966).

(54) S. K. Searles and P. Kebarle, Can. J. Chem., 47, 2619 (1969). See also, T. L. Hill, "An Introduction to Statistical Thermodynamics", Addison-Wesley, Reading, MA., 1960.

(55) P. R. Bevington, "Data Reduction and Error Analysis for the Physical Sciences", McGraw-Hill, New York, N.Y., 1973.

(56) F. Basolo and R. Pearson, "Mechanisms of Inorganic Reactions", 2nd ed., Wiley, New York, N.Y., 1967, Chapter 7, and references cited therein.

(57) F. A. Cotton and G. Wilkinson, "Advanced Inorganic Chemistry", 3rd ed., Interscience, New York, N.Y., 1972, Chapter 22; F. A. Cotton, Inorg, Chem., 3, 702 (1964).

(58) For a recent discussion of π-bonding to phosphorus ligands, see J. Emsley and D. Hall, "The Chemistry of Phosphorus", Harper and Row, London, 1976, Chapter 5.

(59) M. Elian, M. M. L. Chen. D. M. P. Mingos, and R. Hoffmann, Inorg. Chem., 15, 1148 (1976).

(60) S. P. Walch and W. A. Goddard III, J. Am. Chem. Soc., 98, 7908 (1976).

(61) S. P. Walch and W. A. Goddard III, submitted for publication in J. Am. Chem. Soc.,

(62) W. A. Goddard III, T. H. Dunning, Jr., W. J. Hunt, and P. J. Hay, Acc. Chem. Res., 6, 368 (1973).

(63) R. R. Corderman, A. K. Rappé, and W. A. Goddard III, unpublished results.

(64) R. L. Woodin, F. A. Houle, and W. A. Goddard III, Chem. Phys., 14, 461 (1976).

(65) J. Müller, Angew. Chem. Int. Ed., 11, 653 (1972); J. Müller in "Mass Spectrometry of Metal Compounds", J. Charalambous, ed., Butterworths, London, 1975, Chapter 8.

(66) R. V. Hodges and J. L. Beauchamp, unpublished results.

(67) $D(CpNi^{+}-Cl^{-})$ = 175 kcal/mol is calculated from the data in the Appendix and reference 28, and assuming that D(CpNi–Cl) ≈ 80 kcal/mol.

(68) B. deB. Darwent, "Bond Dissociation Energies of Simple Molecules", Nat. Stand. Ref. Data Ser., Natl. Bur. Stand., 31, (1971).

(69) H. A. Skinner, Adv. Organomet. Chem., 2, 49 (1964).

(70) For a review of transition metal catalyzed dehydrogenation reactions in solution, see J. Kwiatek in "Transition Metals in Homogeneous Catalysis", G. N. Schrauzer, ed., Marcel Dekker Inc., New York, N.Y., 1971, Chapter 2.

(71) G. Herzberg, "Spectra of Diatomic Molecules", 2nd ed., D. van Nostrand Co., Princeton, N.J., 1950, p. 532.

(72) Z. B. Alfassi, S. W. Benson, and D. M. Golden, J. Am. Chem. Soc., 95, 4784 (1973); S. W. Benson and R. Shaw, Trans. Faraday Soc., 63, 985 (1967); S. W. Benson and R. Shaw, J. Am. Chem. Soc., 89, 5351 (1967).

(73) S. W. Orchard and B. A. Thrush, J. Chem. Soc. Chem. Commun., 14 (1973).

(74) C. O. Lee, R. G. Sutterland, and B. J. Tomson, Tetrahedron Lett., 2625 (1972); A. N. Nesmeyanov, Yu. S. Nekrasov, N. I.

Vasyukova, L. S. Kotova, and N. A. Vol'kenau, J. Organomet. Chem., 96, 265 (1975); T. H. Whitesides and R. W. Arhart, Tetrahedron Lett., 297 (1972).

(75) R. B. King, Fortschr. Chem. Forsch., 14, 92 (1970).

(76) J. Halpern in "Organotransition Chemistry", Y. Ishii and M. Tsutsui, eds., Plenum Press, New York, N.Y., 1975, p. 109.

(77) C. W. Bird, "Transition Metal Intermediates in Organic Synthesis", Academic Press, New York, N.Y., 1967, p. 239.

(78) M. C. Baird, C. J. Nyman, and G. Wilkinson, J. Chem. Soc. A 348 (1968).

(79) R. F. Heck, "Organotransition Metal Chemistry", Academic Press, New York, N.Y., 1974.

(80) The proposed $CpNi(CH_3)(CO)(H)^+$ intermediate III is analogous to intermediates such as $Cp_2Zr(R)(CO)(Cl)$ proposed in the hydrozirconation reaction of alkenes with carbon monoxide to produce aldehydes [C. A. Bertolo and J. Schwartz, J. Am. Chem. Soc., 97, 230 (1975); J. W. Lauher and R. Hoffmann, ibid., 98, 1729 (1976)].

(81) $D(CD_3Br-CpNi^+) \cong 40 \pm 5$ kcal/mol $\cong E^*$ is calculated by taking $PA(CD_3Br) \cong PA(CH_3Br) = 163$ kcal/mol[47] and using the linear correlation (eq 50).

(82) C. W. Spangler, Chem. Rev., 76, 187 (1976).

(83) S. McLean, C. J. Webster, and R. J. D. Rutherford, Can. J. Chem., 47, 1555 (1969).

(84) K. Hafner and K. L. Moritz, in "Friedel-Crafts and Related Reactions", G. A. Olah, ed., Wiley-Interscience, New York, N.Y., 1965, Chapter 49; V. N. Setkina and D. N. Kursanov, Russ.Chem. Rev., 37, 737 (1968).

(85) A. Davison, W. McFarlane, L. Pratt, and G. Wilkinson, J. Chem. Soc., 3653 (1962).

(86) R. R. Corderman and J. L. Beauchamp, submitted for publication in J. Am. Chem. Soc.,

(87) P. J. Robinson and K. A. Holbrook, "Unimolecular Reactions", Wiley, New York, N.Y., 1972, Chapter 7.

(88) J. H. Sinfelt, Science, 195, 641 (1977); J. H. Sinfelt, Acc. Chem. Res., 10, 15 (1977).

(89) G. D. Flesch, G. A. Junk, and H. J. Svec, J. Chem. Soc., Dalton Trans., 1102 (1972).

(90) A. E. Roche, M. M. Sutton, D. K. Bohme, and H. I. Schiff, J. Chem. Phys., 55, 5480 (1971).

(91) G. Distefano, J. Res. Natl. Bur. Stand., A74, 233 (1970).

CHAPTER III

Ion Cyclotron Resonance Investigations of Alkylation of $(\eta^5-C_5H_5)Ni^+$ and $(\eta^5-C_5H_5)Fe^+$ by Methyl Halides in the Gas Phase

Reed R. Corderman and J. L. Beauchamp

Contribution No. 5516 from the Arthur Amos Noyes Laboratory of Chemical Physics, California Institute of Technology, Pasadena, California 91125

ABSTRACT

A detailed study of the sequential alkylation of $(\eta^5\text{–}C_5H_5)Ni^+$ and $(\eta^5\text{–}C_5H_5)Fe^+$ by methyl bromide in the gas using the techniques of ion cyclotron resonance (ICR) spectroscopy is reported. A reaction mechanism for the alkylation process is proposed through the use of both ICR double resonance techniques and deuterium labelled methyl bromide. The reactions of $CpNi^+$ and C_2H_4Br and of $CpNi^+$ and $CpFe^+$ with CH_3X (X = F, Cl, I) are briefly discussed.

Introduction

Ion cyclotron resonance spectroscopy (ICR) is proving to be a valuable tool for investigating the reactions,[1-3] thermochemistry,[3] and photochemistry[4] of metal ions in the gas phase. In the condensed phase, solvation effects may obscure the intrinsic reactivity of chemical species[5] and complicating rapid equilibria between different reaction intermediates are common.[6] ICR methods, however, facilitate the study of single bimolecular ion-molecule encounters; reaction intermediates which may be similar to those hypothesized to occur in solution can be observed, and reaction mechanisms proposed. The present work describes an ICR study of the sequential alkylation of the $CpNi^+$ and $CpFe^+$ cations[7] by repeated ion-molecule reaction with CD_3Br. The results are discussed in terms of a proposed mechanism for the alkylation process.

Experimental

The theory and instrumentation of ICR mass spectrometry have been previously described.[8-10] This work employed an instrument constructed at Caltech equipped with a 15-inch electromagnet capable of a maximum field strength of 23.4 kG.

Both cyclopentadienyl nickel nitrosyl (Strem Chemicals, Inc., Danvers, Mass.) and methyl-d_3 bromide (EM Laboratories Inc., Elmsford, N.Y.) were obtained commercially and used without further purification; no impurities were observed in their ICR mass spectra. Because of the high vapor pressure of CpNiNO at 25°C (mp = -41°C, bp_{15} = 47-48°C), the sample was kept in an ice water bath during use to

prevent it from condensing in the ICR spectrometer inlet. Cyclopentadiene was prepared immediately before use by thermally cracking dicyclopentadiene[11] and was kept in a dry ice-acetone bath (-78 °C) during use to inhibit the rapid dimerization which occurs at room temperature.[11] All other chemicals used in this study were readily available from commercial sources. Before use, each sample was degassed by repeated freeze-pump-thaw cycles.

Pressures were measured with a Schulz-Phelps type ion gauge calibrated against a MKS Baratron Model 90H1-E capacitance manometer in a manner previously described.[12] The estimated uncertainty in absolute pressures, and thus in all rate constants reported, is ± 10%. All experiments were performed at ambient temperature (20-25 °C).

Results

When a mixture of CpNiNO and CD_3Br is examined using trapped ion ICR techniques,[9] the series of reactions 1-4 are initiated by $CpNi^+$.

$$C_5H_5Ni^+ + CD_3Br \rightarrow (CD_3)C_5H_4Ni^+ + HBr \quad (1)$$

$$(CD_3)C_5H_4Ni^+ + CD_3Br \rightarrow (CD_3)_2C_5H_3Ni^+ + HBr \quad (2)$$

$$(CD_3)_2C_5H_3Ni^+ + CD_3Br \rightarrow (CD_3)_3C_5H_2Ni^+ + HBr \quad (3)$$

$$(CD_3)_3C_5H_2Ni^+ + CD_3Br \rightarrow (CD_3)_4C_5HNi^+ + HBr \quad (4)$$

The temporal variation of relative ion abundance in a 1:3 mixture of CpNiNO and CD_3Br following a 20-eV, 10-ms electron beam pulse is illustrated in Figure 1 (exclusive of ions from CpNiNO[13] or CD_3Br[14] alone)[15]; rates for these processes are given in Table I. Reactions 1-4 suggest the sequential alkylation of the cyclopentadienyl ring of $CpNi^+$

FIGURE 1

Temporal abundances of the variously alkylated $CpNi^+$ ions observed in a mixture of CpNiNO (3.2×10^{-7} Torr) and CD_3Br (1.0×10^{-6} Torr) following a 20 eV, 10 ms electron beam pulse. Other ions present, not included in the normalization, are CD_3Br^+ and $CpNiNO^+$ and their various product and fragment ions.

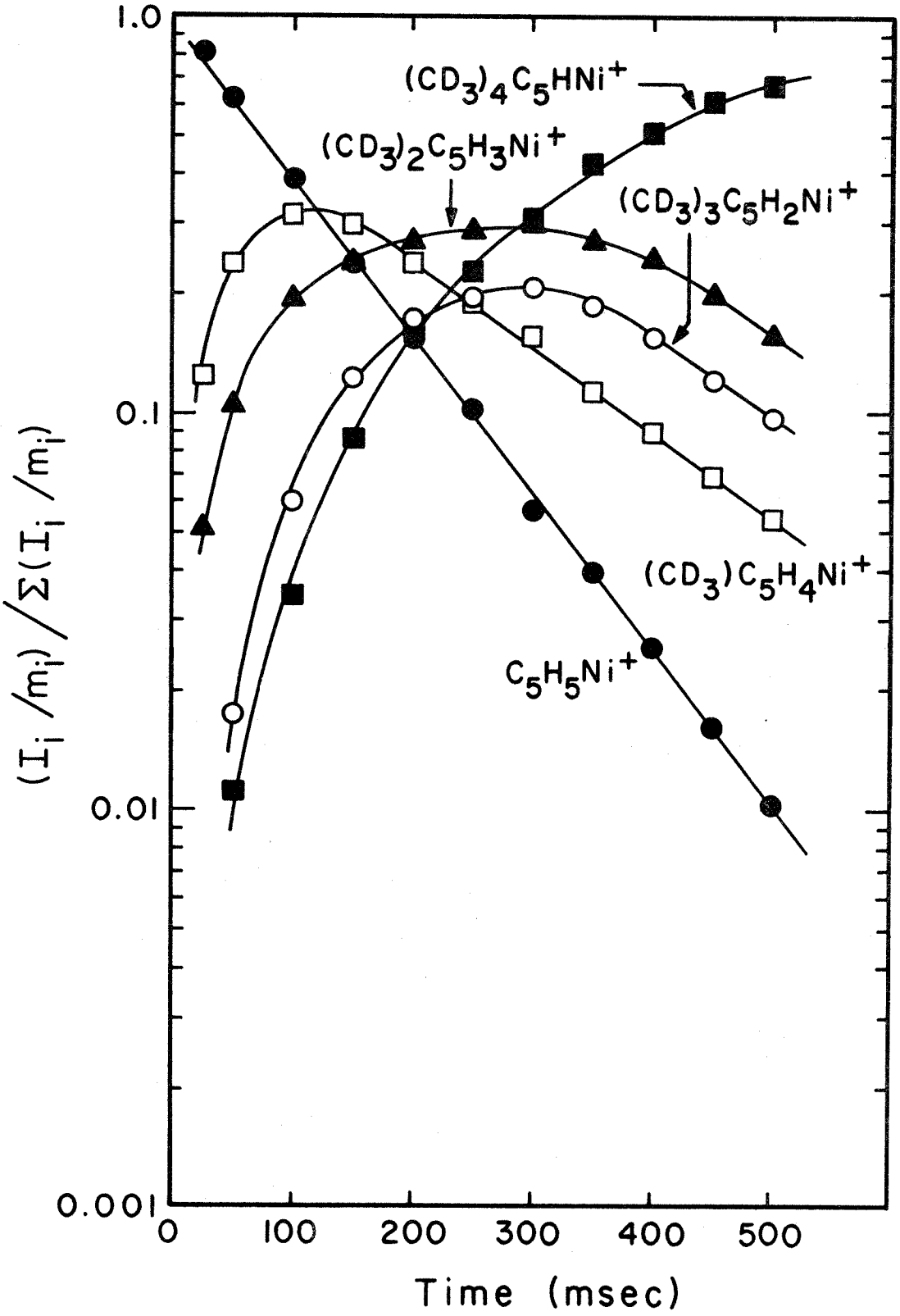
1.0
0.1
0.01
0.001
0
100
200
300
400
500
Time (msec)
$(I_i/m_i)/\Sigma(I_i/m_i)$
$(CD_3)_4C_5HNi^+$
$(CD_3)_2C_5H_3Ni^+$
$(CD_3)_3C_5H_2Ni^+$
$(CD_3)C_5H_4Ni^+$
$C_5H_5Ni^+$

Table I. Ion Molecule Reactions and Rate Constants for the Reactions of $CpNi^+$ with CD_3Br and C_2H_5Br.

Reaction	k^a
$CpNi^+ + CD_3Br \rightarrow (CD_3)C_5H_4Ni^+ + HBr$	2.8
$(CD_3)C_5H_4Ni^+ + CD_3Br \rightarrow (CD_3)_2C_5H_3Ni^+ + HBr$	1.5
$(CD_3)_2C_5H_3Ni^+ + CD_3Br \rightarrow (CD_3)_3C_5H_2Ni^+ + HBr$	1.5
$(CD_3)_3C_5H_2Ni^+ + CD_3Br \rightarrow (CD_3)_4C_5HNi^+ + HBr$	1.5
$CpNi^+ + C_2H_5Br \rightarrow CpNi(HBr)^+ + C_2H_4$	5.0
$CpNi^+ + C_2H_5Br \rightarrow CpNi(C_2H_4)^+ + HBr$	

[a]Total rate constants in units of 10^{-10} $cm^3 molecule^{-1} s^{-1}$ measured for the disappearance of the reactant ion.

by CD_3Br. The four alkylation steps (eqs 1-4) proceed rapidly in accordance with the generalized scheme of reaction 5, with each step

$$(CD_3)_nC_5H_{5-n}Ni^+ + CD_3Br \rightarrow (CD_3)_{n+1}C_5H_{4-n}Ni^+ + HBr \quad (n = 0\text{-}3) \tag{5}$$

involving CD_3 addition to the ring and subsequent loss of H in the form of HBr. Double resonance experiments[8, 10] clearly demonstrate the sequential nature of process 5, with each product ion exhibiting double resonance signals[8] from each of its precursor ions. The rate of addition of a fifth CD_3 group (eq 6) is so slow that the process, if it occurs at all, is not observed in these experiments.

$$(CD_3)_4C_5HNi^+ + CD_3Br \rightarrow (CD_3)_5C_5Ni^+ + HBR \tag{6}$$

For reasons which are not understood, the sequential alkylation of $CpNi^+$ by CH_3Br is somewhat unique. Under otherwise identical conditions, the yields of alkylation products with CH_3F, CH_3Cl, and CH_3I are less than 2% of those observed with CD_3Br, making the process difficult to fully characterize for these species.

In contrast to CD_3Br, $CpNi^+$ reacts with C_2H_5Br to give only two products, $CpNi(HBr)^+$ and $CpNi(C_2H_4)^+$ (eq 7 and 8). Reactions 7 and 8

$$CpNi^+ + C_2H_5Br \xrightarrow{87\%} CpNi(HBr)^+ + C_2H_4 \tag{7}$$

$$CpNi^+ + C_2H_5Br \xrightarrow{13\%} CpNi(C_2H_4)^+ + HBr \tag{8}$$

represent two different product channels for the $CpNi^+$ induced

dehydrohalogenation of ethyl bromide.[13] Both HBr in $CpNi(HBr)^+$ and C_2H_4 in $CpNi(C_2H_4)^+$ are weakly bound labile species which are rapidly displaced by C_2H_5Br in the ligand transfer reactions 9 and 10.

$$CpNi(HBr)^+ + C_2H_5Br \rightarrow CpNi(C_2H_5Br)^+ + HBr \quad (9)$$

$$CpNi(C_2H_4)^+ + C_2H_5Br \rightarrow CpNi(C_2H_5Br)^+ + C_2H_4 \quad (10)$$

Reaction of $CpFe^+$[7] with CH_3X (X = F, Cl, Br, I) leads to the four alkylations of the Cp ring (eq 11). The abundance of any product

$$(CH_3)_nC_5H_{5-n}Fe^+ + CH_3X \rightarrow (CH_3)_{n+1}C_5H_{4-n}Fe^+ + HX \quad (11)$$

(X = F, Cl, Br, I; n = 0-3)

ions formed as the result of a fifth alkylation step was so low as to be undetectable in these experiments. As with $CpNi^+$, significant product yields are obtained only in the case of CH_3Br.

Sequential alkylation reactions are not observed for the $C_5H_5^+$, $C_5H_6^+$, and $C_5H_5^-$ ions from cyclopentadiene, nor for the $C_6H_6^+$ and $C_6H_7^+$ ions from benzene.

Discussion

The combination of ion cyclotron double resonance techniques[8, 10] and the use of deuterium-labelled methyl bromide provide considerable information about the mechanism of the sequential alkylation reactions 1-4. Scheme I illustrates a proposed mechanism for the first step in the sequential alkylation of $CpNi^+$ by CD_3Br (reaction 1). Initially, the coordinatively unsaturated $CpNi^+$ cation interacts with CD_3Br to form the activated complex 1, which has an internal energy

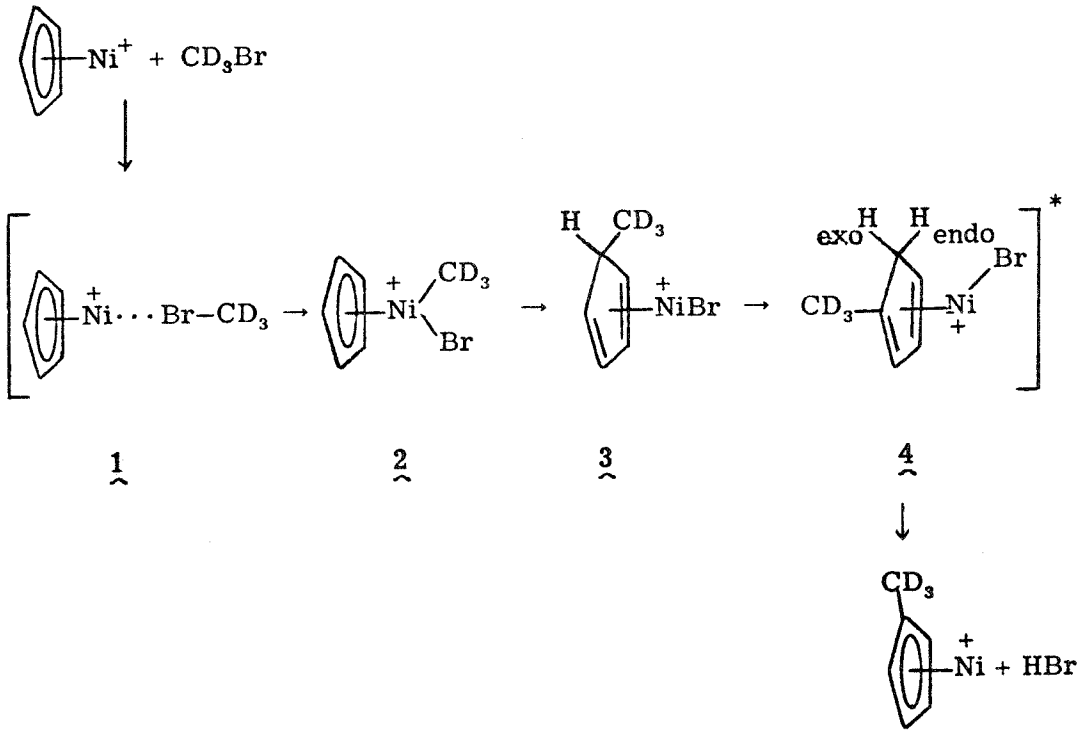

Scheme I

equal to $D(CD_3Br–CpNi^+) \simeq 40$ kcal/mole.[16] The internal energy of 1 is sufficient to allow for oxidative addition of nickel to the carbon-bromine bond, yielding 2.[17, 18] CD_3 migrates to the cyclopentadienyl ring, giving 3, the methyl-d_3 cyclopentadiene nickel bromide cation. Species 3 rapidly rearranges to 4 via a [1, 5] sigmatropic shift (thermally allowed in the ground state[19]), which is known to occur rapidly at room temperature in methyl cyclopentadiene.[20] Finally, HBr elimination from 4 involving the endo hydrogen yields the product ion, $(CD_3)C_5H_4Ni^+$. The sequence of Scheme I is repeated four times, and is facilitated by the increasing activation of the cyclopentadienyl ring towards electrophilic substitution with each successive

alkylation.[21] The appealing feature of the proposed mechanism is that it allows for only four alkylations since the fifth step would require HBr elimination to involve the exo hydrogen from 5. Apparently in this case

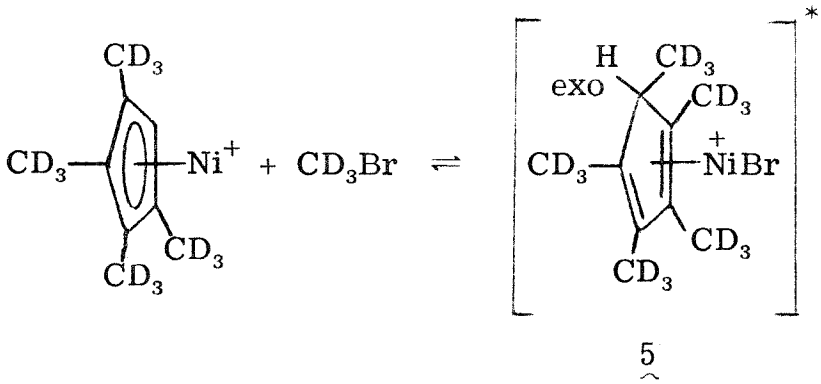

5

Scheme II

the reaction intermediate reverts to reactants, if it is formed at all.

The proposed mechanism does not require expansion of the valence shell of nickel beyond 18 electrons;[22] the situation with $CpFe^+$ is even less restrictive and consequently the similar reactivity is not surprising. The differential reactivity of the methyl halides is puzzling, since CH_3F, CH_3Cl, and CH_3I sequentially alkylate $CpNi^+$ in very small yield compared to CD_3Br. The thermochemistry of the alkylation reactions 5 and 11 may be compared for the different methyl halides by examining the enthalpy of reaction 12 for the series (Table II).

$$CH_3X \xrightarrow{\Delta H_r} CH_2 + HX \qquad (12)$$

While the reaction with CH_3F will be somewhat more exothermic than with the remaining methyl halides, there is no indication of unusual behavior to be expected for CH_3Br. The internal excitation of 1

Table II. Enthalpy of Reaction for the Process $CH_3X \rightarrow CH_2 + HX$[a]

X	$\Delta H_f(CH_3X)$[b]	$\Delta H_f(HX)$[c]	ΔH_r
F	-55.9	-64.8	83.2
Cl	-20.6	-22.0	90.7
Br	- 9.1	- 8.7	92.5
I	3.4	6.3	95.0

[a]Reaction (12) in the text; all values in kcal/mol; $\Delta H_f(CH_2)$ = 92.1 ± 1.0 (D. R. Stull and H. Prophet, Natl. Stand. Res. Data Ser. Natl. Bur. Stand., 37 (1971)). [b]J. D. Cox and G. Pilcher, "Thermochemistry of Organic and Organometallic Compounds", Academic Press, London, 1970. [c]J. L. Franklin, J. G. Dillard, N. M. Rosenstock, J. T. Herron, K. Draxl, and F. H. Field, Natl. Stand. Res. Data Ser. Natl. Bur. Stand., 26 (1969).

depends on the metal ligand bond dissociation energy. Also for the oxidative addition to be exothermic (formation of 2) it is required that $D(Ni-CH_3) + D(Ni-Br) \geq D(CH_3-Br)$, with the extent of inequality determining the internal excitation available to effect further rearrangement of 2. It is perhaps in these two steps that CH_3Br is distinguished from the remaining methyl halides, being favored by a synergistic metal -Br interaction.

C_2H_5Br reacts with $CpNi^+$ in a somewhat different manner than CD_3Br. This is attributed to the rapid β-hydrogen atom shift onto Ni^+ (eqs 13 and 14), which is a facile process both in the gas phase[17] and in

$$CpNi^+ + C_2H_5Br \rightarrow$$

$$\left[CpNi^+(C_2H_5)(Br) \rightleftharpoons CpNi^+(CH_2{=}CH_2)(H)(Br) \right]^* \begin{cases} \rightarrow CpNi(C_2H_4)^+ + HBr & (13) \\ \rightarrow CpNi(HBr)^+ + C_2H_4 & (14) \end{cases}$$

solution.[18] It is noted, however, that Lewis acids such as Li^+ also effect dehydrohalogenation reactions of alkyl halides analogous to processes 6 and 7.[23] Consequently an oxidative addition step is not required.

That the metal ion plays a decisive role in the alkylation reactions 5 and 11 is confirmed by the observation that ions produced from both cyclopentadiene and benzene are not alkylated by CH_3Br.

Acknowledgments. This research was supported in part by the Energy Research and Development Administration under Grant No. E(04-3)767-8.

References and Notes

(1) J. Allison and D. P. Ridge, J. Organomet. Chem., 99, C11 (1975); J. Allison and D. P. Ridge, J. Am. Chem. Soc., 99, 35 (1977); R. D. Bach, A. T. Weibel, J. Patane, and L. Kevan, J. Am. Chem. Soc., 98, 6237 (1976) and reference contained therein.

(2) M. S. Foster and J. L. Beauchamp, J. Am. Chem. Soc., 93, 4924 (1971); ibid., 97, 4808, 4814 (1975); R. R. Corderman and J. L. Beauchamp, Inorg. Chem., 15, 665 (1976).

(3) R. R. Corderman and J. L. Beauchamp, J. Am. Chem. Soc., 98, 3998, 5700 (1976); R. H. Staley and J. L. Beauchamp, J. Am. Chem. Soc., 97, 5920 (1975).

(4) R. C. Dunbar and B. B. Hutchinson, J. Am. Chem. Soc., 96, 3816 (1974); J. H. Richardson, L. M. Stephenson, and J. I. Brauman, J. Am. Chem. Soc., 96, 3671 (1974).

(5) E. M. Arnett, F. M. Jones III, M. Taagepera, W. G. Henderson, J. L. Beauchamp, D. Holtz, and R. W. Taft, J. Am. Chem. Soc., 94, 4724 (1972); S. Ahrland, Helv. Chim. Acta, 50, 306 (1967); G. Klopman, J. Am. Chem. Soc., 90, 223 (1968).

(6) J. Halpern in "Organotransition Chemistry", Y. Ishii and M. Tsutsui, Eds., Plenum Press, New York, N.Y., 1975, p. 109; C. W. Bird, "Transition Metal Intermediates in Organic Synthesis", Academic Press, New York, N.Y., 1967.

(7) $CpNi^+$ and $CpFe^+$ cations are produced by the electron impact dissociative ionization of CpNiNO and Cp_2Fe, respectively.

(8) For reviews, see J. L. Beauchamp, Annu. Rev. Phys. Chem., 22, 527 (1971); G. A. Gray, Adv. Chem. Phys., 19, 141 (1971).

(9) T. B. McMahon and J. L. Beauchamp, Rev. Sci. Instrum., 43, 509 (1972).

(10) B. S. Freiser, T. B. McMahon, and J. L. Beauchamp, Int. J. Mass Spectrom. Ion Phys., 12, 249 (1973).

(11) "Organic Syntheses, Collective Volume 4", N. Rabjohn, Ed., Wiley, New York, N.Y., 1963, p. 238.

(12) R. J. Blint, T. B. McMahon, and J. L. Beauchamp, J. Am. Chem. Soc., 96, 1269 (1974).

(13) R. R. Corderman and J. L. Beauchamp, unpublished observations.

(14) J. L. Beauchamp, D. Holtz, S. D. Woodgate, and S. L. Patt, J. Am. Chem. Soc., 94, 2798 (1972).

(15) The product of the alkylation reaction 1 reacts further with CpNiNO in accordance with the process $(CD_3)C_5H_4Ni^+ + CpNiNO \rightarrow (CD_3)C_5H_4NiCp^+ + NiNO$.

(16) $D(CD_3Br-CpNi^+) \approx 40 \pm 5$ kcal/mol $\approx E^*$ is calculated by taking $PA(CD_3Br) \approx PA(CH_3Br) = 163$ kcal/mol and using the data of Ref. 3.

(17) Intermediates analogous to 2 have been observed in the reaction of Fe^+ with CH_3I; J. Allison and D. Ridge, J. Am. Chem. Soc., 98, 7445 (1976).

(18) R. F. Heck, "Organotransition Metal Chemistry - A Mechanistic Approach", Academic Press, New York, N.Y., 1974; J. P. Collman and W. R. Roper, Advan. Organometal. Chem., 7, 53 (1968); J. Halpern, Accts. Chem. Res., 3, 386 (1970).

(19) C. W. Spangler, Chem. Rev., 76, 187 (1976).

(20) S. McLean, C. J. Webster, and R. J. D. Rutherford, Can J. Chem., 47, 1555 (1969).

(21) K. Hafner and K. L. Moritz in "Friedel-Crafts and Related Reactions", G. A. Olah, Ed., Wiley-Interscience, New York, N.Y., 1965, Chapter 49; V. N. Setkina and D. N. Kursanov, Russ. Chem. Rev., 37, 737 (1968).

(22) Using $CpNi^+$, species 1, 2, and 3 are 16, 16, and 14 electron intermediates, respectively.

(23) R. D. Wieting, R. H. Staley, and J. L. Beauchamp, J. Am. Chem. Soc., 97, 924 (1975).

CHAPTER IV

Negative Ion Chemistry of $(\eta^5-C_5H_5)Co(CO)_2$ in the Gas Phase by Ion Cyclotron Resonance Spectroscopy. The π-Acceptor Ability of PF_3 Compared to CO.

Reed R. Corderman and J. L. Beauchamp

Contribution No. 5557 from the Arthur Amos Noyes Laboratory of Chemical Physics, California Institute of Technology, Pasadena, California 91125

ABSTRACT

The gas-phase negative ion chemistry of $(\eta^5-C_5H_5)Co(CO)_2$ is studied using the techniques of ion cyclotron resonance spectroscopy. Attachment of trapped electrons leads to the formation of $CpCo(CO)_2^-$ and $CpCo(CO)^-$. While the molecular anion is unreactive, $CpCo(CO)^-$ reacts with the neutral precursor to yield $[CpCo(CO)]_2^-$, which has been previously characterized in solution. The first observed example of a ligand displacement reaction involving an anionic transition metal complex, in which PF_3 displaces CO from $CpCo(CO)^-$, is reported, and leads directly to the conclusion that PF_3 is a stronger π-acceptor ligand than CO towards $CpCo^-$ in the gas phase. Nitric oxide reacts with both $CpCo(CO)^-$ and $CpCo(CO)_2^-$ to yield the very stable anion, $CpCo(NO)^-$, which is isoelectronic with CpNiNO. π-Acids weaker than CO (C_2F_4, NCH, ethylene oxide, MeCN, NH_3, NMe_3, and PMe_3) were not observed to react with $CpCo(CO)^-$. The relative contribution of σ- and π-bonding in the metal-ligand bonds of $CpCoB^-$ and $CpNiB^+$ is discussed. Reactions of the anions F^- and CD_3O^- with $CpCo(CO)_2$ are briefly considered.

Introduction

While the study of transition metal complexes using the techniques of ion cyclotron resonance spectroscopy (ICR) is a rapidly expanding field of endeavor,[1-7] the results reported to date deal predominately with the thermochemical properties and reactions of cationic species.[1-5] Only a very few reports have appeared concerning the negative ion chemistry of transition metal complexes, and these deal almost exclusively with the photodecomposition spectra[6] and condensation reactions of metal carbonyls.[3-7] Negative ion-molecule reactions have also been observed in the high-pressure ($> 5 \times 10^{-6}$ Torr) mass spectra of chromium oxyhalides[8] and perchloroalkyl mercury compounds.[9] Neither ligand displacement nor condensation reactions have been observed for the nickelocene anion, Cp_2Ni^-[2], or $Fe(CO)_4^-$[3] with a variety of simple molecules. Reactions of several anionic species (F^-, $C_2H_5O^-$) with $Fe(CO)_5$, which result in the formation of tetra-coordinate 16-electron products, have been investigated.[3]

The present work describes an ICR study of the negative ion chemistry of $(\eta^5-C_5H_5)Co(CO)_2$, both alone and in mixtures with other molecules. Processes which are of particular interest include the formation of binuclear cobalt complexes which have been observed and characterized in solution.[10-12] The reactions of a series of π-acids with cobalt-containing anions and of anions with neutral $CpCo(CO)_2$ are presented. Processes observed in the former instance include the first examples of ligand displacement reactions involving transition metal anionic complexes. These studies permit an assessment of the

relative π-acceptor abilities of ligands in the gas phase. A previous investigation of the mass spectrometry[13] of $CpCo(CO)_2$ provides information useful in the interpretation of the present results.

Experimental

The theory and instrumentation of ICR mass spectrometry have been previously described.[14-16] This work employed an instrument constructed at Caltech equipped with a 15-inch electromagnet capable of a maximum field strength of 23.4 kG.

Cyclopentadienyl cobalt dicarbonyl was obtained commercially (Alfa Products, Ventron Corporation) and used without further purification; no impurities were observed in the positive-ion ICR mass spectrum at 70 eV, which is in excellent agreement with the reported mass spectrum.[13] Because of the high vapor pressure of $CpCo(CO)_2$ at 25 °C (mp = -22 °C[17]) the sample was kept in an ice water bath during use to prevent condensation in the spectrometer inlet. All other chemicals used in this study were readily available from commercial sources. Before use, each sample was degassed by repeated freeze-pump-thaw cycles.

Pressures were measured with a Schulz-Phelps type ion gauge calibrated against a MKS Baratron Model 90H1-E capacitance manometer in a manner previously described.[18] The estimated uncertainty in absolute pressures, and thus in all rate constants reported, is ± 20%. All experiments were performed at ambient temperature (20-25 °C). $CpCo(CO)_2$ is well-behaved in the ICR spectrometer and no experimental difficulties were encountered.

Results

Negative Ions. The negative-ion ICR mass spectrum of $CpCo(CO)_2$ at 1.7×10^{-6} Torr and an electron beam energy of 70 eV agrees qualitatively with that reported by Winters and Kiser.[13] The ions observed and their relative abundances are $CpCo(CO)_2^-$ (84%) and $CpCo(CO)^-$ (16%). The molecular anion, $CpCo(CO)_2^-$, is formed by capture of low-energy electrons scattered and trapped in the ICR cell, and appears to have an essentially infinite lifetime against autodetachment; the observed behavior is quite analogous to that exhibited by Cp_2Ni[2] and SF_6.[19] A low-energy dissociative electron attachment process[20] generates $CpCo(CO)^-$ from $CpCo(CO)_2$. Ions of the formulae $(C_5H_4)Co(CO)_n^-$ and $(C_5H_3)Co(CO)_n^-$ (n = 1, 2) are not detected in the present experiments, although they were proposed in an earlier low-resolution study.[13]

The relative abundances of $CpCo(CO)_2^-$ and $CpCo(CO)^-$ are strongly dependent on the electron energy distribution. This is demonstrated in an experiment in which a non-resonant radiofrequency electric field is used to excite electrons scattered and trapped in the ICR cell.[21] With $CpCo(CO)_2$ at 5.0×10^{-7} Torr and an electron beam energy of 70 eV, the abundance of $CpCo(CO)^-$ increases at the expense of $CpCo(CO)_2^-$ as the RF amplitude is increased (Figure 1). The total production of anions, as given by the sum of the $CpCo(CO)_2^-$ and $CpCo(CO)^-$ signal intensities, remains constant. The coupling between the RF field (≈ 7.1 MHz) and the electron motion is very weak, as strong coupling leads to electron ejection,[14, 15, 21] in which case the total yield of anions decreases. These results are consistent with the

FIGURE 1

Change in the negative ion mass spectrum of $CpCo(CO)_2$ at 70 eV and 5.0×10^{-7} Torr upon radiofrequency heating of the electrons scattered and trapped in the ICR cell.

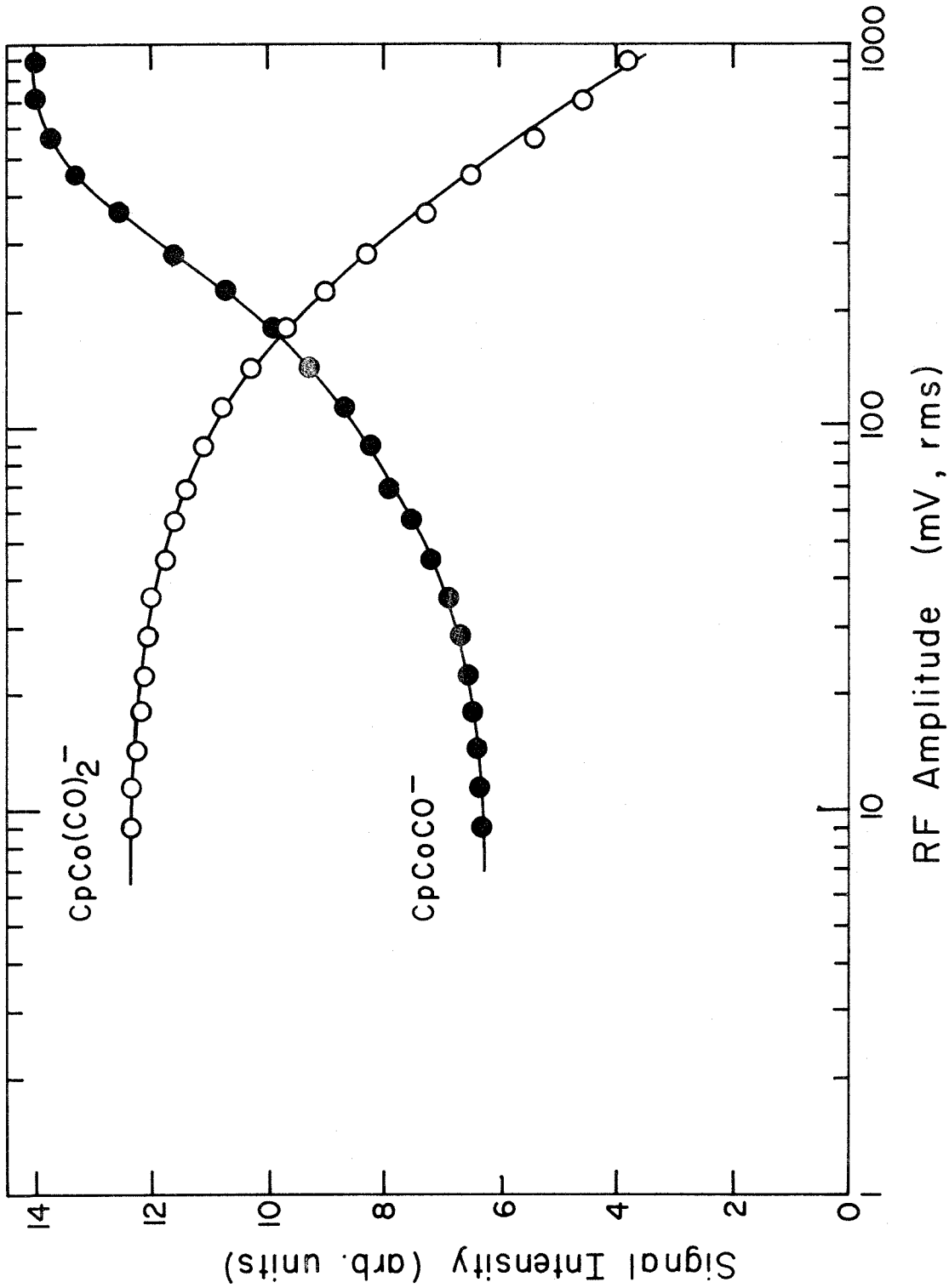
Signal Intensity (arb. units)
0
2
4
6
8
10
12
14
RF Amplitude (mV, rms)
1
10
100
1000
$CpCo(CO)_2^-$
$CpCoCO^-$

dissociative electron attachment process (eq 1) being slightly

$$CpCo(CO)_2 + e^- \rightarrow CpCo(CO)^- + CO \qquad (1)$$

endothermic.[22] The possibility that the reverse of eq 1 occurs (associative detachment) was briefly investigated. Addition of excess CO did not lead to an increase in $CpCo(CO)_2^-$ at the expense of $CpCoCO^-$ (i.e., the reverse of eq 1 and subsequent electron capture).

Negative-Ion Chemistry of $CpCo(CO)_2$. Figure 2 presents the temporal variation of relative ion abundance for $CpCo(CO)_2$ at 4.4×10^{-7} Torr following a 70 eV, 10 ms electron beam pulse. Double-resonance experiments[14, 15] unambiguously identify the condensation reaction 2 as occurring in this system. From the slope

$$CpCo(CO)^- + CpCo(CO)_2 \rightarrow [CpCo(CO)]_2^- + CO \qquad (2)$$

for the disappearance of $CpCo(CO)^-$ with time, the rate constant of reaction 2 is calculated to be $k = 3.2 \times 10^{-10}$ $cm^3 molecule^{-1} s^{-1}$. The molecular anion, $CpCo(CO)_2^-$, is unreactive.

The dimer ion $[CpCo(CO)]_2^-$ (1) has been prepared in solution by the sodium amalgam reduction of $CpCo(CO)_2$.[10] The structure of 1

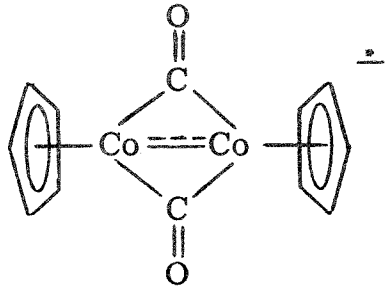

1

FIGURE 2

Temporal variation of ion abundance in CpCo(CO) at 4.4×10^{-7} Torr following ionization by a 70 eV, 10 ms electron beam pulse.

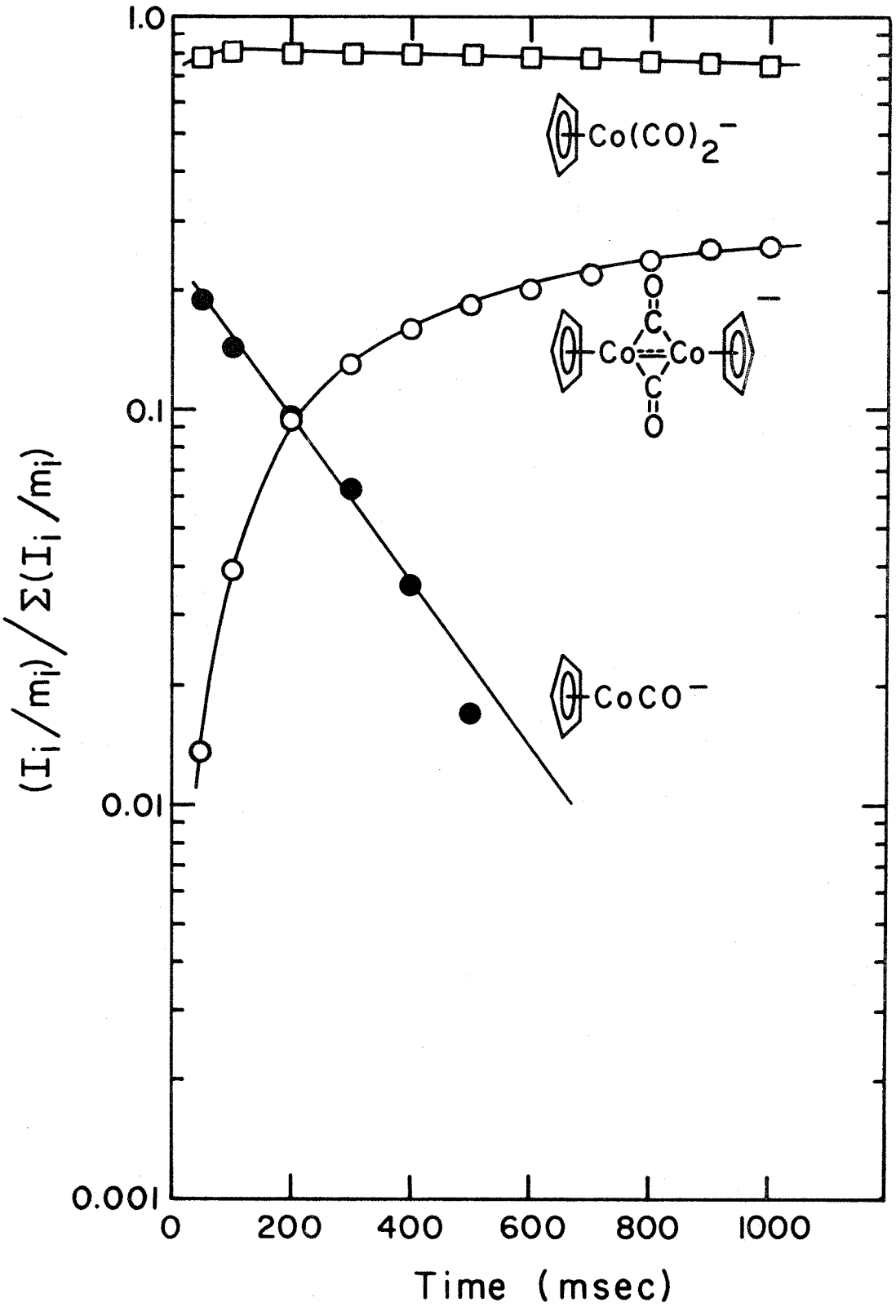
1.0
0.1
0.01
0.001
0
200
400
600
800
1000
Time (msec)
$(I_i/m_i)/\Sigma(I_i/m_i)$
$Co(CO)_2^-$
$CoCO^-$
Co
Co
C
O
C
O
−

has been determined by x-ray crystallography of the PPN^+ salt, $[P(C_6H_5)_3]_2N^+[CpCo(CO)]_2^-$, and an unusually short Co–Co bond is found,[23] consistent with molecular orbital predictions of partial double bond character.[12] The ESR spectrum of PPN^+ $[CpCo(CO)]_2^-$ indicates that the unpaired electron is shared equally by both cobalt nuclei and suggests that $[CpCo(CO)]_2^-$ may be considered as a mixed-valence complex.[11, 12, 24]

Reactions of Cobalt Anions with Strong π-Acceptor Ligands. Mixtures of $CpCo(CO)_2$ with the two π-acceptor ligands NO and PF_3 were studied, principally to elucidate ligand exchange reactions occurring in these systems.

Figure 3 presents the temporal variation of relative ion abundance in a 8.2:1 mixture of NO and $CpCo(CO)_2$ following a 70 eV, 10 ms electron beam pulse at a total pressure of 4.2×10^{-6} Torr. The only reaction observed in this mixture is the NO displacement of both CO molecules from the molecular anion (eq 3), with a rate constant of

$$CpCo(CO)_2^- + NO \rightarrow CpCo(NO)^- + 2CO \qquad (3)$$

$k = 2.2 \times 10^{-11}$ $cm^3 molecule^{-1} s^{-1}$. At lower NO pressures (ca., $5\text{-}10 \times 10^{-7}$ Torr), both $CpCo(CO)^-$ and consequently $[CpCo(CO)]_2^-$ (eq 2) are observed. Double-resonance experiments verify that $CpCo(CO)^-$ reacts with NO to produce $CpCo(NO)^-$ (eq 4), while $[CpCo(CO)]_2^-$ is

$$CpCo(CO)^- + NO \rightarrow CpCo(NO)^- + CO \qquad (4)$$

unreactive towards ligand substitution by NO. The species $CpCo(NO)^-$

FIGURE 3

Temporal variation of ion abundance in a 8:1 mixture of NO and $CpCo(CO)_2$ following a 70 eV, 10 ms electron beam pulse at a total pressure of 4.3×10^{-6} Torr.

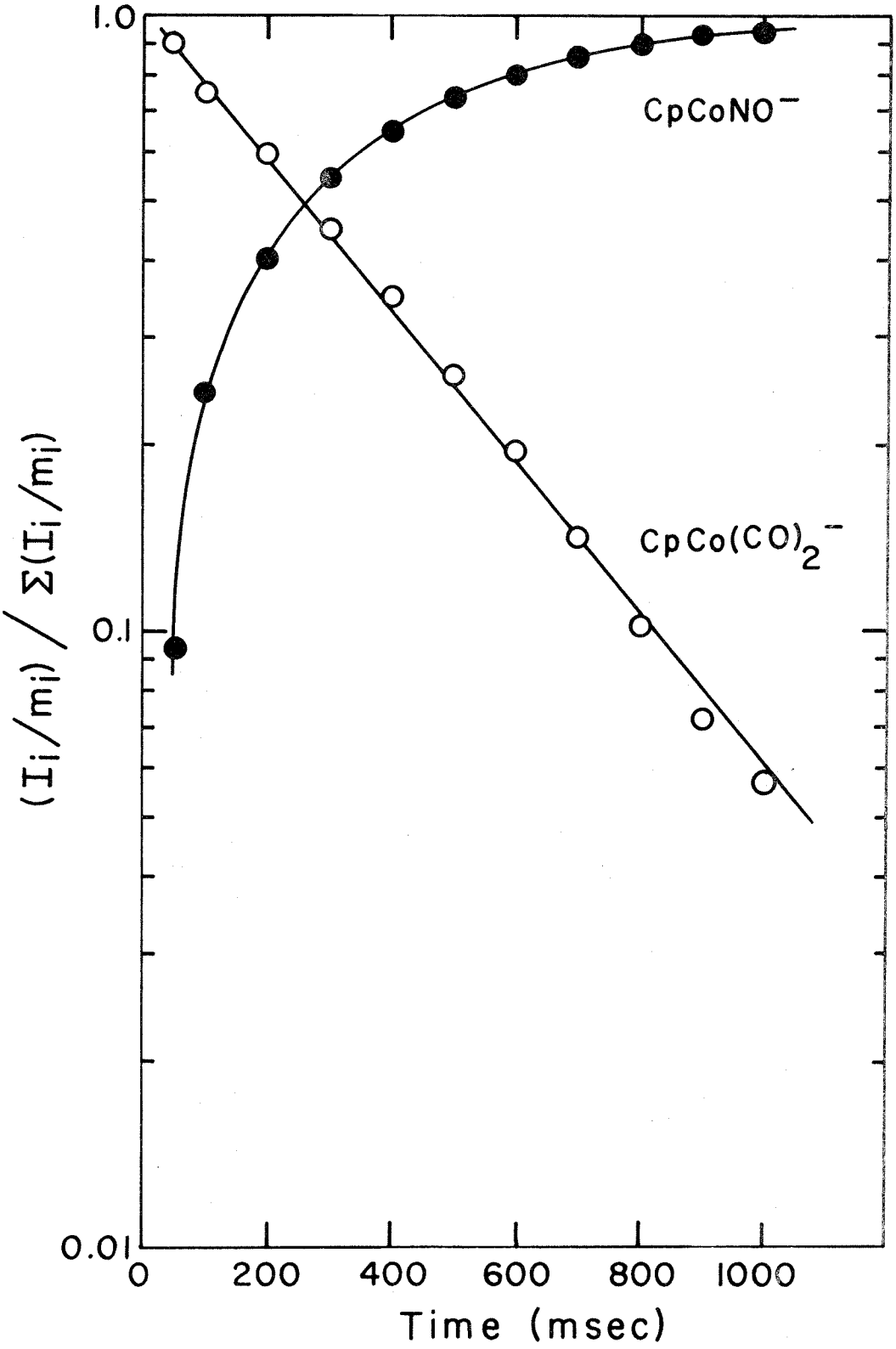
1.0
0.1
0.01
$(I_i/m_i) / \Sigma(I_i/m_i)$
$CpCoNO^-$
$CpCo(CO)_2^-$
0
200
400
600
800
1000
Time (msec)

is isoelectronic with CpNiNO,[1] and as such is expected to be a very stable 18-electron diamagnetic anion. The neutral dimer of $CpCo(NO)^-$, $[CpCo(NO)]_2$ has been synthesized in solution and characterized by mass spectrometry.[25] $CpCo(NO)^-$ has been prepared by introducing sodium amalgam to a solution of $[CpCo(NO)]_2$.[26]

Perhaps the most interesting reactions of $CpCo(CO)^-$ are observed in mixtures of $CpCo(CO)_2$ and PF_3. Figure 4 presents the temporal variation of relative ion abundance in a 4.8:1 mixture of PF_3 with $CpCo(CO)_2$ following a 70 eV, 10 ms electron beam pulse at a total pressure of 5.8×10^{-6} Torr. Double resonance experiments[14, 15] conclusively indicate that the sequence of reactions 2, 5, and 6 occurs in this system. The addition of PF_3 to $CpCo(CO)_2$ causes two new ions,

$$CpCo(CO)^- + PF_3 \rightarrow CpCo(PF_3)^- + CO \qquad (5)$$

$$CpCo(PF_3)^- + PF_3 \rightarrow CpCo(PF_3)_2^- \qquad (6)$$

$CpCo(PF_3)^-$ and $CpCo(PF_3)_2^-$, to appear in addition to $[CpCO(CO)]_2^-$ which is present in $CpCo(CO)_2$ alone (reaction 2). Although many examples of cationic ligand displacement reactions are known,[1, 3, 4, 27] reaction 5, in which PF_3 displaces CO from $CpCoCO^-$ ($k = 5.3 \times 10^{-11}$ $cm^3 molecule^{-1} s^{-1}$), is the first observed example of an anionic ligand displacement reaction. The species $CpCo(PF_3)^-$ further reacts with PF_3 (eq. 6, $k = 4.0 \times 10^{-11}$ $cm^3 molecule^{-1} s^{-1}$) to produce $CpCo(PF_3)_2^-$ which is analogous to the molecular anion $CpCo(CO)_2^-$ where both carbonyls have been replaced by PF_3. The neutral species

FIGURE 4

Temporal variation of ion abundance in a 4.8:1 mixture of PF_3 and $CpCo(CO)_2$ following a 70 eV, 10 ms electron beam pulse at a total pressure of 5.8×10^{-6} Torr.

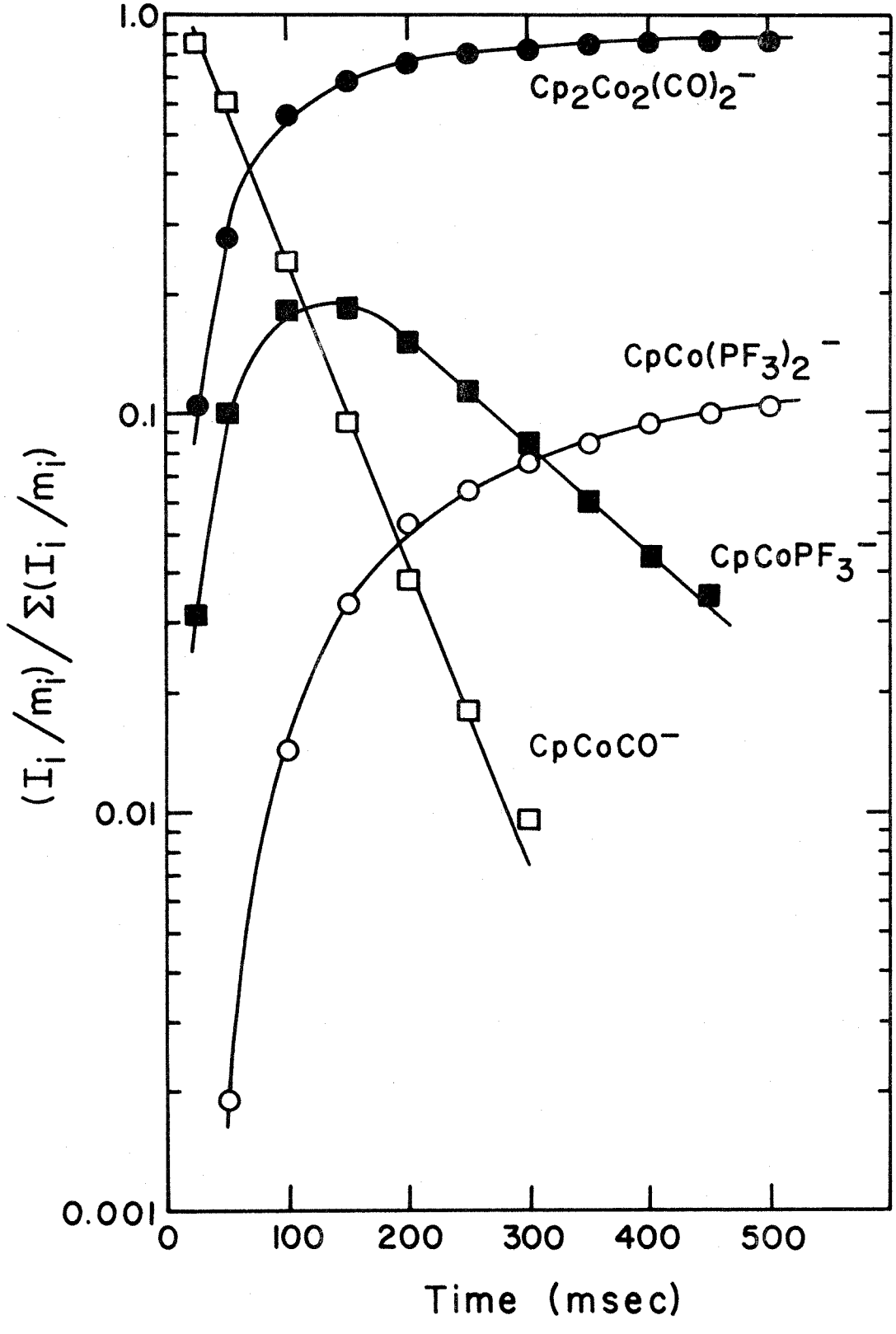
1.0
0.1
0.01
0.001
0
100
200
300
400
500
Time (msec)
$(I_i/m_i)/\Sigma(I_i/m_i)$
$Cp_2Co_2(CO)_2^-$
$CpCo(PF_3)_2^-$
$CpCoPF_3^-$
$CpCoCO^-$

$CpCo(PF_3)_2$ has been synthesized in solution by the reaction of cobaltocene with PF_3,[28] and considerable π-bonding contribution to the Co–P bond was found from interpretation of the IR spectrum, consistent with the similar conclusion reached from these results. The molecular anion $CpCo(CO)_2^-$ accounts for ~85% of the total ionization in the $CpCo(CO)_2$-PF_3 mixture. A small fraction of the parent anion, possibly with excess internal energy, reacts to produce $CpCo(CO)PF_3^-$ (eq 7) in

$$CpCo(CO)_2^- + PF_3 \rightarrow CpCo(CO)PF_3^- + CO \qquad (7)$$

< 1% yield. Neither $CpCo(CO)_2^-$ nor $CpCo(CO)PF_3^-$ are included in the normalization of data presented in Figure 4.

A mixture of $CpCo(CO)_2$, PF_3, and NO was examined with the purpose of determining the preferred direction of ligand displacement (reaction 8). While both the $CpCo(PF_3)^-$ and $CpCo(NO)^-$ anions are

$$CpCo(PF_3)^- + NO \rightleftharpoons CpCo(NO)^- + PF_3 \qquad (8)$$

observed in this mixture, double resonance experiments[14, 15] indicate that neither the forward nor reverse reactions (eq 8) occur. The failure to observe either of these reactions is not particularly well understood, especially for the forward reaction since NO is a stronger π-acid than PF_3,[29] but is possibly because the reactions are too slow to observe ($k < 10^{-11}$ $cm^3 molecule^{-1} s^{-1}$) using ICR techniques.[14]

Reactions of Cobalt Anions with Weak π-Acceptor Ligands. Mixtures of $CpCo(CO)_2$ with a wide variety of weak π-acceptor ligands were investigated. The ligands included C_2F_4, HCN, ethylene oxide, MeCN, NH_3, NMe_3, and PMe_3, all of which are much weaker π-acids

than NO, PF_3, and CO.[29, 30] In no instance are ligand displacement reactions analogous to eq 5 observed. In fact, the yield of any product ions from the reactions of $CpCo(CO)_2^-$ and $CpCo(CO)^-$ with the weak π-acceptor ligands was so small as to be undetectable in these experiments.

Reactions of Anions with $CpCo(CO)_2$. The ion chemistry of a variety of anions of differing proton affinity[31] (kcal/mol), including CD_3O^- (376.8), F^- (371.3), CN^- (348.9), NO_2^- (340.0), Cl^- (333.3), and I^- (314.4) with $CpCo(CO)_2$ was studied. Only F^- and CD_3O^- were reactive with $CpCo(CO)_2$; the remaining anions were unreactive and no product ions were detected. Figure 5 shows the temporal variation of ion abundance in a 9:1 mixture of NF_3 and $CpCo(CO)_2$ following a 70 eV, 10 ms electron beam pulse at a total pressure of 5.0×10^{-6} Torr. F^- produced by the dissociative attachment of electrons to NF_3[32] is the reactive anion in this mixture, producing the $CpCo(CO)F^-$ (eq 9; $k = 2.1 \times 10^{-9}$ $cm^3 molecule^{-1} s^{-1}$) and $CpCo(F)^-$ (eq 10; $k = 9.9 \times 10^{-10}$ cm^3 $molecule^{-1} s^{-1}$) ions. Neither $CpCo(CO)^-$ nor $[CpCo(CO)]_2^-$ are

$$F^- + CpCo(CO)_2 \xrightarrow{68\%} CpCo(CO)F^- + CO \qquad (9)$$

$$F^- + CpCo(CO)_2 \xrightarrow{32\%} CpCo(F)^- - 2CO \qquad (10)$$

observed in this system. This indicates that excess NF_3 efficiently scavenges epithermal electrons necessary for the formation of $CpCo(CO)^-$.[32]

Processes analogous to reactions 9 and 10 produce $CpCo(CO)OCD_3^-$ and $CpCo(OCD_3)^-$ in a mixture of $CpCo(CO)_2$ and CD_3ONO (eqs 11 and 12).[33] The $CpCo(CO)_2OCD_3^-$ ion formed in the

FIGURE 5

Temporal variation of ion abundance in a 9:1 mixture of NF_3 and $CpCo(CO)_2$ following a 70 eV, 10 ms electron beam pulse at a total pressure of 5.0×10^{-6} Torr.

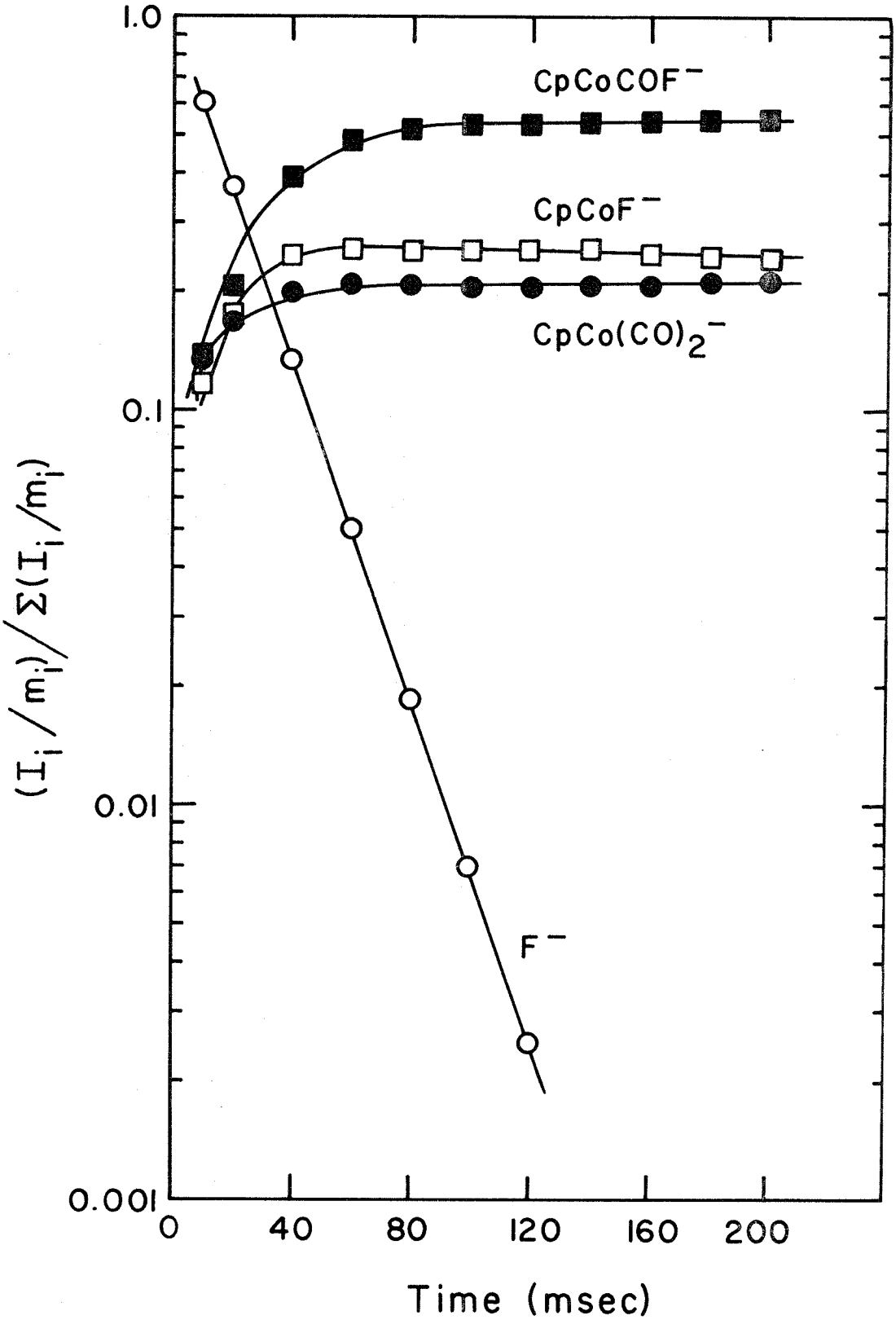
1.0
0.1
0.01
0.001
0
40
80
120
160
200
Time (msec)
$(I_i/m_i)/\Sigma(I_i/m_i)$
$CpCoCOF^-$
$CpCoF^-$
$CpCo(CO)_2^-$
F^-

bimolecular condensation of CD_3O^- with $CpCo(CO)_2$ is also observed (eq 13).

$$CD_3O^- + CpCo(CO)_2 \xrightarrow{84\%} CpCo(CO)OCD_3^- + CO \quad (11)$$

$$\xrightarrow{8\%} CpCo(OCD_3)^- + 2CO \quad (12)$$

$$\xrightarrow{8\%} CpCo(CO)_2OCD_3^- \quad (13)$$

Discussion

The present result that both PF_3 and NO displace CO from $CpCo(CO)^-$ (eqs 4, 5) demonstrates the feasibility of employing ICR techniques to investigate ligand displacement reactions involving anionic transition metal complexes. While photoelectron spectroscopy of $Ni(PF_3)_4$[29, 34] and a series of chromium, maganese, and iron trifluorophosphine metal complexes[35] indicates that PF_3 is as strong or a stronger π-acid than CO, [30] these results unambiguously show that PF_3 is a better π-acceptor than CO towards $CpCo^-$, or $D(PF_3-CpCo^-) > D(CO-CpCo^-)$. The result that π-acids such as C_2F_4, MeCN, and PMe_3 do not displace CO from $CpCo(CO)^-$ indicates that $D(CO-CpCo^-) > D(B-CpCo^-)$ or that these ligands, B, are weaker π-acids than CO. This conclusion has been previously verified by measurement of carbonyl stretching frequencies in π-acceptor substituted metal complexes.[29] Conversely, these results indicate that $D(B-CpCo^-)$ is predominately dependent upon the π-acceptor ability of B and that the σ-donor ability of B plays a much less important role in $D(B-CpCo^-)$.

Precisely the opposite effects are present in the bonding of n-donor ligands to $CpNi^+$.[1, 4] In this system the dissociative bond

energy $D(B-CpNi^+)$ is largely determined by the σ-donor ability of B, while π-bonding effects, where they occur, are much less important, and account for only $\approx 10\%$ of $D(B-CpNi^+)$.[14] PF_3 and CO are very poor σ-donors,[37] so that both $D(PF_3-CpNi^+) \approx 42 \pm 5$ kcal/mol,[36] and $D(CO-CpNi^+) \approx 40 \pm 5$ kcal/mol,[5] are much less than $D(NH_3-CpNi^+) = 52.3 \pm 2.0$ kcal/mol[1,4] and $D(Me_3P-CpNi^+) = 57.6 \pm 2.0$ kcal/mol.[1,4] A qualitative picture of these two different metal-ligand bonding schemes for $CpCo^-$ and $CpNi^+$ is presented in Figure 6. These results suggest that by starting with a cyclopentadienyl cobalt complex with weakly bound π-acceptor ligands [e.g., $CpCo(PMe_3)_2$ or $CpCo(P(C_6H_5)_3)_2$],[37] a quantitative scale of π-acceptor ability can be measured using ICR techniques, as such scales for H^+,[38] Li^+,[27] and $CpNi^+$[1,4] have been constructed.

The results concerning formation of the cobalt dimer anion $[CpCo(CO)]_2^-$ are of particular interest because the scheme of reaction 2, verified by double resonance methods,[14,15] is exactly the same as the mechanism proposed to occur in solution.[10] This demonstrates the utility of ICR techniques in elucidating anionic reaction mechanisms which have solution analogues.

Reactions of the strong bases F^- and CD_3O^-[31] lead to formation of substituted anionic even-electron cyclopentadienyl cobalt species, $CpCo(CO)_nX^-$ (n = 0-2). The anions CN^-, NO_2^-, Cl^-, and I^- are not observed to react with $CpCo(CO)_2$. This result may reflect the much weaker gas phase basicity of these species as compared to F^- and CD_3O^-.[31]

FIGURE 6

Qualitative description of metal-ligand bonding in $CpCo^{-}$ and $CpNi^{+}$.

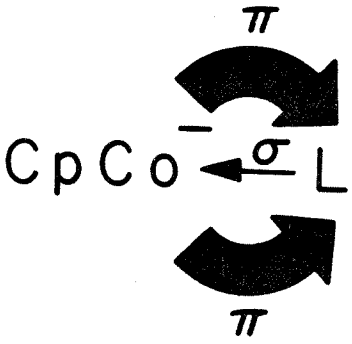
π
CpCo
σ
L
π

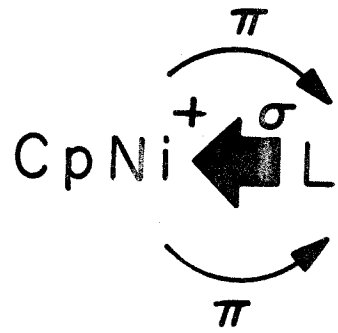
π
CpNi
σ
L
π

Acknowledgments. This research was supported in part by the Energy Research and Development Administration under Grant No. E(04-3)767-8.

References and Notes

(1) R. R. Corderman and J. L. Beauchamp, unpublished results.

(2) R. R. Corderman and J. L. Beauchamp, Inorg. Chem., 15, 665 (1976).

(3) M. S. Foster and J. L. Beauchamp, J. Am. Chem. Soc., 93, 4924 (1971); ibid., 97, 4808 (1975).

(4) R. R. Corderman and J. L. Beauchamp, J. Am. Chem. Soc., 98, 3998 (1976).

(5) R. R. Corderman and J. L. Beauchamp, J. Am. Chem. Soc., 98, 5700 (1976).

(6) R. C. Dunbar and B. B. Hutchinson, J. Am. Chem. Soc., 96, 3816 (1974); J. H. Richardson, I. M. Stephenson, and J. I. Brauman, ibid., 96, 3671 (1974).

(7) R. C. Dunbar, J. F. Ennever, and J. P. Fackler, Jr., Inorg. Chem., 12, 2734 (1973).

(8) G. D. Flesch, R. M. White, and H. J. Svec, Int. J. Mass Spectrom. and Ion Phys., 3, 339 (1969).

(9) S. C. Cohen, Inorg. Nucl. Chem. Lett., 6, 757 (1970).

(10) C. S. Ilenda, N. E. Schore, and R. G. Bergman, J. Am. Chem. Soc., 98, 255 (1976).

(11) N. E. Schore, C. S. Ilenda, and R. G. Bergman, J. Am. Chem. Soc., 98, 256 (1976).

(12) N. E. Schore, C. S. Ilenda, and R. G. Bergman, J. Am. Chem. Soc., J. Am. Chem. Soc., 99, 1781 (1977).

(13) R. E. Winters and R. W. Kiser, J. Organomet. Chem., 4, 190 (1965).

(14) For reviews see, J. L. Beauchamp, Annu. Rev. Phys. Chem., 22, 527 (1971); G. A. Gray, Adv. Chem. Phys., 19, 141 (1971); T. A. Lehman and M. M. Bursey, "Ion Cyclotron Resonance Spectrometry", Wiley, New York, N.Y., 1976.

(15) B. S. Freiser, T. B. McMahon, and J. L. Beauchamp, Int. J. Mass Spectrom. Ion Phys., 12, 249 (1973).

(16) T. B. McMahon and J. L. Beauchamp, Rev. Sci. Instrum., 43, 509 (1972).

(17) G. E. Coates, M. L. H. Green, and K. Wade, "Organometallic Compounds", Vol. II, 3rd ed, Chapman and Hall, London, 1968.

(18) R. J. Blint, T. B. McMahon, and J. L. Beauchamp, J. Am. Chem. Soc., 96, 1269 (1974).

(19) M. S. Foster and J. L. Beauchamp, Chem. Phys. Lett., 31, 482 (1975).

(20) For reviews of dissociative electron attachment processes see, J. G. Dillard, Chem. Rev., 73, 590 (1973); J. L. Franklin and P. W. Harland, Annu. Rev. Phys. Chem., 25, 485 (1974); G. E. Caledonia, Chem. Rev., 75, 333 (1975).

(21) The non-resonant RF field used to excite the electron energy distribution is applied to the lower source plate of the ICR cell in these experiments. Application of RF across the trapping plates can also be used to excite oscillatory electron motion (J. L. Beauchamp and J. T. Armstrong, Rev. Sci. Instrum., 40, 123 (1969)). With the latter technique, resonance electron ejection occurs with very low RF fields.

(22) The dissociative electron attachment process (eq 1) is not required to be endothermic, however.

(23) The Co–Co bond length in $[CpCo(CO)]_2^-$ is 2.36 Å[11] compared to 2.52 Å for $Co_2(CO)_8$ (H. Lorenz, Chem. Ber., 108, 973 (1975)).

(24) For reviews of mixed-valence complexes see, M. B. Robin and P. Day, Adv. Inorg. Chem. Radiochem., 10, 247 (1967); G. C. Allen and N. S. Hush, Prog. Inorg. Chem., 8, 357 (1967); D. O. Cowan, C. Le Vanda, J. Park, and F. Kaufman, Acc. Chem. Res., 6, 1 (1973); A. F. Garito and A. J. Heeger, ibid., 7, 232 (1974).

(25) H. Brunner, J. Organomet. Chem., 12, 517 (1968).

(26) M. A. White and R. G. Bergman, private communication.

(27) R. H. Staley and J. L. Beauchamp, J. Am. Chem. Soc., 97, 5920 (1975).

(28) T. Kruck, W. Hieber, and W. Lang, Angew Chem. Int. Edit. Engl., 5, 1247 (1966).

(29) F. A. Cotton and G. Wilkinson, "Advanced Inorganic Chemistry", 3rd ed, Wiley, New York, N.Y., 1972, p. 720.

(30) R. B. King, Acc. Chem. Res., 3, 417 (1970).

(31) S. A. Sullivan and J. L. Beauchamp, J. Am. Chem. Soc., 98, 1160 (1976); unpublished observations.

(32) J. C. J. Thynne, J. Phys. Chem., 73, 1586 (1969).

(33) CD_3O^- is readily produced by dissociative electron capture from CD_3ONO.[20]

(34) J. C. Green, D. I. King, and J. H. D. Eland, Chem. Comm., 1121 (1970).

(35) J. Müller, K. Fenderl, and B. Mertschenk, Chem. Ber., 104, 700 (1971).

(36) $D(PF_3-CpNi^+)$ is estimated from $PA(PF_3)$ = 170 kcal/mol (D. H. McDaniel, Abstracts, 169th National Meeting of the American Chemical Society, Philadelphia, Pa., April 1975, No. INOR-50) and the data given in references 1 and 4.

(37) R. W. Rudolph and R. W. Parry, J. Am. Chem. Soc., 89, 1621 (1967), reference 26; Th. Kruck, Angew Chem. Int. Edit. Engl., 6, 53 (1967).

(38) J. F. Wolf, R. H. Staley, I. Koppel, M. Taagepera, R. T. McIver, Jr., J. L. Beauchamp, and R. W. Taft, J. Am. Chem. Soc., submitted for publication.

CHAPTER V

Properties and Reactions of Phosphorus Trifluoride in the Gas Phase by Ion Cyclotron Resonance Spectroscopy. Energetics of Formation of PF_2^+, PF_4^+, HPF_3^+, and $CH_3PF_3^+$.

Reed R. Corderman and J. L. Beauchamp

Contribution No. 5581 from the Arthur Amos Noyes Laboratory of Chemical Physics, California Institute of Technology, Pasadena, California 91125

ABSTRACT

The techniques of ion cyclotron resonance spectroscopy are used to examine the gas phase ion chemistry of PF_3. The gas phase basicity, or proton affinity, of PF_3 is determined to be 160 ± 5 kcal/mol, which leads directly to a homolytic bond dissociation energy $D(PF_3^+-H)$ = 113.2 kcal/mol. The proton affinities and homolytic bond dissociation energies for NH_3, NF_3, PH_3, and PF_3 and bond strengths D(B–H) for isoelectronic neutral congeners to BH^+ are compared and discussed in terms of contributions from inductive and hyperconjugative interactions involving p_π-d_π bonding in HPF_3^+. Ion-molecule reactions of PF_3 in mixtures with SiF_4, BF_3, SF_6, NF_3, CH_3F, and $(CH_3)_2CO$ are briefly considered. The $CH_3PF_3^+$ ion is produced in a mixture of PF_3 and CH_3F; various thermochemical considerations give $\Delta H(CH_3PF_3^+)$ = -8.5 ± 5 kcal/mol. Fluorine atom transfer reactions lead to the formation of PF_4^+ and yield an estimated enthalpy of formation of 69 ± 9 kcal/mol for this species. When a trace of acetone is added to a mixture of PF_3 and NF_3, the $(CH_3)_2CF^+$ ion is produced in a four-center reaction in which the carbonyl oxygen exchanges with F^+ in PF_3^+ and PF_4^+. Fluoride transfer reactions observed in mixtures of PF_3 with SiF_4, BF_3, SF_6, and NF_3 lead directly to the energetics of formation of PF_2^+.

Introduction

The techniques of ion cyclotron resonance spectroscopy[1-3] (ICR) are especially suited for the quantitative determination of gas-phase thermochemical quantities such as the proton basicity[4-15] and acidity[16, 17] of molecules. Our recent studies extending these techniques to the measurement of metal-ligand bond dissociation energies of the transition metal ions $(\eta^5-C_5H_5)Ni^+$[18] and $(\eta^5-C_5H_5)Co^-$[19] to various ligands have prompted, in part, our interest in trifluorophosphine, PF_3. While PF_3 is known to be an excellent π-acceptor ligand,[20, 21] little quantitative information which relates to its σ-donor ability towards different acids is available.[22, 23]

Also of interest are the effects of alkyl and fluoroalkyl substitution on the heterolytic and homolytic bond dissociation energies of protonated phosphorus bases,[8] as much less is known about such effects for phosphorus than for nitrogen bases.[15] In addition to an examination of the ion chemistry of PF_3 alone and in several mixtures, the present work reports the quantitative determination of the gas phase proton affinity (basicity) and homolytic bond dissociation energy, $D(B^+-H)$, of PF_3 using ICR techniques.[24] Studies of the He(I) photoelectron spectrum of PF_3,[25-28] ab initio calculations of the electronic structure of PF_3,[28, 29] and appearance potential measurements of ions derived from PF_3[30-32] are useful in interpreting the present results.

Experimental

The theory and instrumentation of ICR mass spectrometry have been previously described.[1-3, 33] This work employed an instrument

constructed at Caltech equipped with a 15-inch electromagnet capable of a maximum field strength of 23.4 kG. All chemicals used in this study were obtained commercially and used without further purification. Before use, each sample was degassed by repeated freeze-pump-thaw cycles. All experiments were performed at ambient temperature (~ 25°C).

Results and Discussion

Mass Spectrum and Positive Ion Chemistry of PF_3. The 70 eV ICR single-resonance spectrum of PF_3 at 4.8×10^{-7} Torr is in good agreement with previously reported mass spectra.[30-32] The ions observed and their relative abundances are PF_3^+ (35%), PF_2^+ (60%), and PF^+ (5%). At electron energies ≤ 15 eV, only the molecular ion is observed, consistent with a previous measurement of the appearance potential of PF_2^+, $AP(PF_2^+) = 15.5 \pm 0.2$ eV.[30] The temporal variation of relative ion abundance for PF_3 at 1.0×10^{-6} Torr following a 70 eV, 10 ms electron beam pulse is shown in Figure 1. The single ion molecule process observed in PF_3 is reaction 1, producing PF_2^+

$$PF^+ + PF_3 \rightarrow PF_2^+ + PF_2 \qquad (1)$$

($k = 3.2 \times 10^{-10}$ $cm^3 molecule^{-1} s^{-1}$; $\Delta H = -15 \pm 13$ kcal/mol[34, 35]). Reaction 1 may involve either fluoride ion or fluorine atom transfer as the two processes are indistinguishable. The slight decrease of PF_3^+ ion abundance with a concomitant increase in PF_2^+ abundance suggests that some fraction of the PF_3 formed by electron impact is vibrationally

FIGURE 1

Temporal variation of relative ion abundance in PF_3 at 1.0×10^{-6} Torr following a 70 eV, 10 ms electron beam pulse.

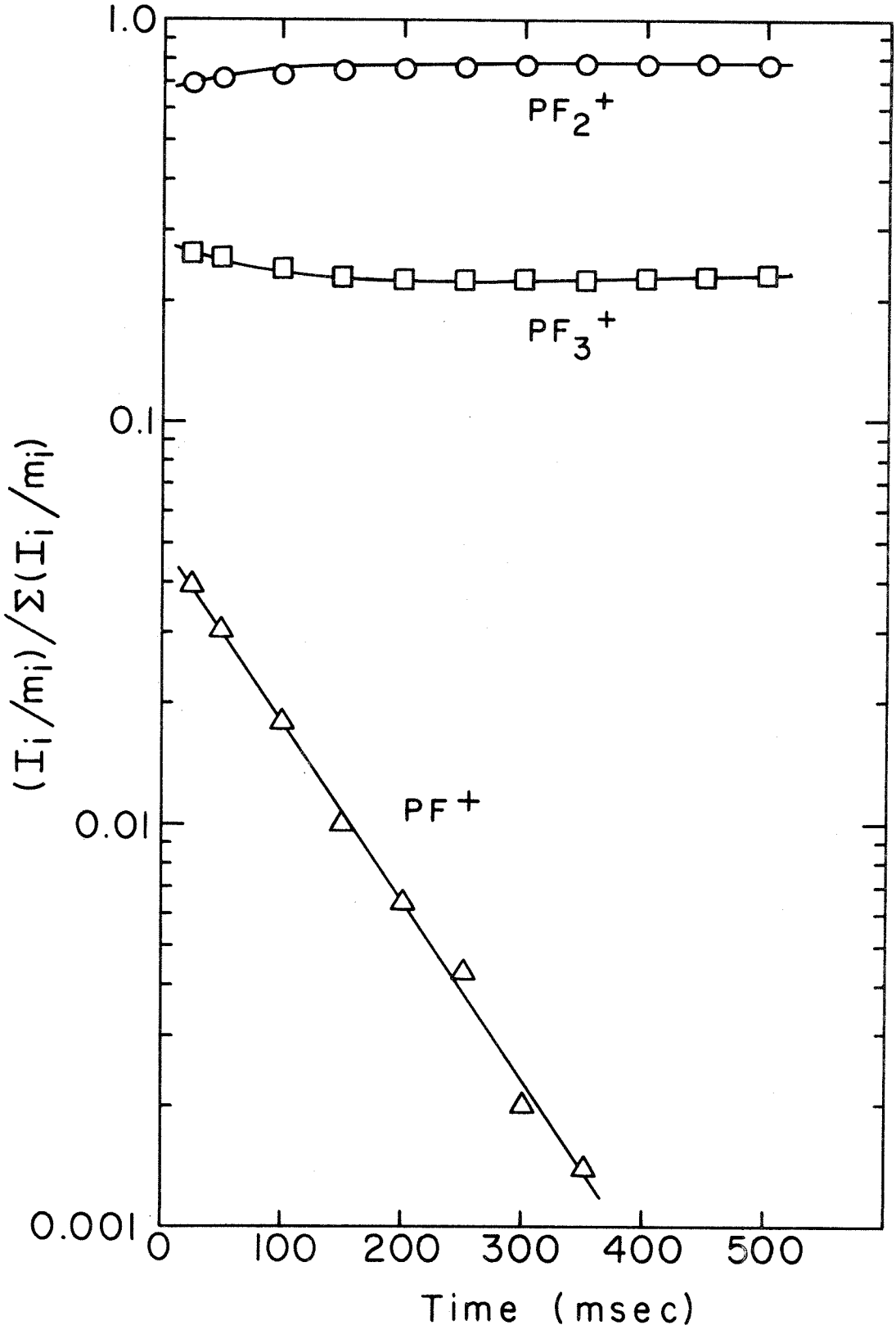
1.0
0.1
0.01
0.001
$(I_i/m_i)/\Sigma(I_i/m_i)$
PF_2^+
PF_3^+
PF^+
0
100
200
300
400
500
Time (msec)

excited and collisionally dissociates to PF_2^+. Both PF_3^+ and PF_2^+ are unreactive towards PF_3.

Gas Phase Basicity of PF_3. Mixtures of PF_3 with molecules having a range of base strengths were examined to determine the preferred direction of proton transfer. Proton transfer reactions from CH_5^+, HCO^+, CH_3FH^+, and HNF_3^+ were confirmed by double resonance techniques[1, 2] to produce HPF_3^+. With CH_3Cl, reversible proton transfer (eq 2) was observed and verified by double resonance.[1, 2] For

$$CH_3ClH^+ + PF_3 \rightleftharpoons HPF_3^+ + CH_3Cl \qquad (2)$$

B = $(CF_3)_2CO$, CF_3CHO, CF_3CN, CF_3CH_2OH, and H_2S, no evidence for the formation of HPF_3^+ from BH^+ is observed, and is taken to indicate that proton transfer from BH^+ to PF_3 is endothermic for these molecules. For each mixture examined, proton transfer reactions involving PF_3 are observed to be slow ($k < 10^{-10}$ $cm^3 molecule^{-1} s^{-1}$), which precludes accurate measurement of an equilibrium constant for reaction 2 [which is also complicated by the formation of $(CH_3)_2Cl^+$ by reaction of CH_3ClH^+ with methyl chloride[36]], and necessitates the use of double resonance techniques[1, 2] to bracket the proton affinity between upper and lower bounds.[37] Thermochemical data relevant to the present results are given in Table I, from which the proton affinity of PF_3 is established as 160 ± 5 kcal/mol, corresponding to $\Delta H_f(HPF_3^+)$ = -18 ± 5 kcal/mol.[34]

The homolytic bond dissociation energy, $D(M^+-H)$, is defined as the enthalpy change for the reaction $MH^+ \rightarrow M^+ + H$ and is related

Table I. Proton Transfer Reactions Involving PF_3

Reaction Observed	$PA(PF_3)$[a]
$CH_5^+ + PF_3 \rightarrow HPF_3^+ + CH_4$	> 128[b]
$HCO^+ + PF_3 \rightarrow HPF_3^+ + CO$	> 143[b]
$CH_3FH^+ + PF_3 \rightarrow HPF_3^+ + CH_3F$	> 151[b]
$HNF_3^+ + PF_3 \rightarrow HPF_3^+ + NF_3$	> 151[c]
$CH_3ClH^+ + PF_3 \rightleftharpoons HPF_3^+ + CH_3Cl$	≈ 160[b]
$HPF_3^+ + (CF_3)_2CO \rightarrow (CF_3)_2COH^+ + PF_3$	< 164.7[d]
$HPF_3^+ + CF_3CHO \rightarrow CF_3CHOH^+ + PF_3$	< 165.7[d]
$HPF_3^+ + CF_3CN \rightarrow CF_3CNH^+ + PF_3$	< 166.7[d]
$HPF_3^+ + CF_3CH_2OH \rightarrow CF_3CH_2OH_2^+ + PF_3$	< 172.2[d]
$HPF_3^+ + H_2S \rightarrow H_3S^+ + PF_3$	< 173.9[e]

[a]All values in kcal/mol. [b]J. L. Beauchamp in "Interactions Between Ions and Molecules", P. Ausloos, Ed., Plenum, New York, N.Y., 1975, pp. 413-444. [c]Reference 14. [d]I. Koppel and R. W. Taft, unpublished results. [e]Reference 11.

to the proton affinity of M by eq 3, where the indicated ionization

$$PA(M) - D(M^+-H) = IP(H) - IP(M) \quad (3)$$

potentials refer to the adiabatic values. Homolytic bond energies are useful for correlating gas-phase basicities because they generally remain constant for a homologous series, yielding a linear relationship between PA(M) and IP(M).[1, 6, 8, 15] The He(I) photoelectron spectrum of PF_3 reveals the first adiabatic IP at 11.57 ± 0.01 eV.[25] Combining this value with $PA(PF_3)$ = 160 ± 5 kcal/mol measured in this study gives $D(PF_3^+-H)$ = 113.2 ± 5 kcal/mol.

Table II presents the proton affinities, adiabatic ionization potentials, and homolytic bond dissociation energies, $D(B^+-H)$ for several Group V hydrides and fluorides. Included for comparison are the bond strengths D(R–H) for the Group IV molecules isoelectronic to the protonated nitrogen and phosphorus bases, BH^+. Fluorine substituted directly on nitrogen or phosphorus causes a significant decrease in PA(B), and a somewhat smaller increase in $D(B^+-H)$. The greater decreases in proton affinity are attributed to the electron-withdrawing effects of fluorine relative to hydrogen, whereby fluorine destablizes positive charge development at nitrogen or phosphorus.[15] The smaller effect of fluorine substitution on PF_3 [$PA(PH_3)$ - $PA(PF_3)$ = 27.3 kcal/mol while $PA(NH_3)$ - $PA(NF_3)$ = 51.3 kcal/mol] may be due to the increased importance of structures of type 1 which involve donation from filled p_π orbitals of fluorine into empty phosphorous d_π orbitals.[24] Since these structures stabilize the conjugate acid of

Table II. Thermochemical Data Related to Base Strengths of Group V Hydrides and Fluorides

Molecule (B)	PA(B)[a, b]	IP(B)[a]	$D(B^+-H)$[a]	Isoelectronic Neutral (RH)	D(R-H)[a, c]
NH_3	202.3	234.5 (10.17)	123.1	CH_4	104.0
NF_3	151[d]	300.0 (13.00)[a]	137	CF_3H	106.2
PH_3	187.3	229.7 (9.96)[f]	103.4	SiH_4	89.5
PF_3	160[g]	266.8 (11.57)[f]	113.2	SiF_3H	85.1

[a]All data in kcal/mol except values quoted in parentheses for ionization potentials are in electron volts. [b]Proton affinities relative to $PA(NH_3)$ = 202.3 kcal/mol, Reference 11. [c]M. K. Murphy and J. L. Beauchamp, J. Am. Chem. Soc., submitted for publication. [d]Reference 14. [e]V. H. Dibeler and J. A. Walker, Inorg Chem., 8, 1728 (1969). [f]Reference 25. [g]Present work.

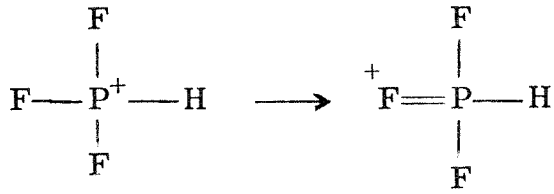

1

PF_3, they lead to smaller fluorine substituent effects on PA(B) and $D(B^+-H)$ for PF_3 relative to NF_3, for which structures of type 1 are not expected to be important. Additionally, the ion of structure 1 is isoelectronic with HF_2PO, for which ab initio calculations show appreciable charge transfer from the filled fluorine p_π orbitals into the empty phosphorous d_π orbitals.[38] As expected, the homolytic B–H bond strengths (Table II) increase upon proceeding to the isoelectronic ion; an increase of 20-30 kcal/mol has been previously noted for other systems.[1, 13, 14]

In previous studies of the ion chemistry of mixtures of $(\eta^5-C_5H_5)NiNO$ and PF_3,[18, 39] it has been observed that PF_3 is incapable of displacing NO from $CpNiNO^+$ (reaction 4). Using the value for

$$CpNiNO^+ + PF_3 \longrightarrow CpNiPF_3^+ + NO \qquad (4)$$

$PA(PF_3)$ = 160 kcal/mol measured in this study and the previously determined linear relationship between $D(B-H^+)$ and $D(B-CpNi^+)$,[18] the value of $D(PF_3-CpNi^+)$ = 39.3 ± 5 kcal/mol is calculated. This value is substantially less than the dissociative bond energy of NO to $CpNi^+$, $D(NO-CpNi^+)$ = 45.9 ± 1.0 kcal/mol[18] and corroborates the observation that PF_3 does not displace NO from $CpNiNO^+$ (eq 4).

Formation of $CH_3PF_3^+$. A mixture of CH_3F and PF_3 exhibits several interesting reactions in addition to those observed in CH_3F[36] and PF_3 (Figure 1) alone. Figure 2 presents the temporal variation of relative ion abundance in a 1:1 mixture of PF_3 and CH_3F at 1.6×10^{-6} Torr total pressure following a 20 eV, 10 ms electron beam pulse. Lower limits to $D(PF_3^+-H)$ and $PA(PF_3)$ are established by observation of reaction 5, a hydrogen-atom transfer from CH_3F to PF_3^+. For

$$PF_3^+ + CH_3F \rightarrow HPF_3^+ + CH_2F \qquad (5)$$

process 5 to be exothermic requires that $D(PF_3^+-H) > D(CH_2F-H) = 101$ kcal/mol,[40] from which $PA(PF_3) > 148$ kcal/mol is directly inferred (eq 3). HPF_3^+ reacts further with CH_3F in reaction 6 to

$$HPF_3^+ + CH_3F \rightarrow CH_3PF_3^+ + HF \qquad (6)$$

produce $CH_3PF_3^+$ and eliminate HF. Reactions 7 and 8 present tentative schemes for the formation of $CH_3PF_3^+$, both of which involve a four

$$HPF_3^+ + CH_3F \rightarrow \left[\begin{array}{c} F\cdots H \\ \vdots \quad + \quad \vdots \\ H_3C\cdots PF_3 \end{array}\right]^* \rightarrow H_3CPF_3^+ + HF \qquad (7)$$

$$HPF_3^+ + CH_3F \rightarrow \left[\begin{array}{c} H\cdots F \\ \vdots \quad + \quad \vdots \\ H_2FC\cdots PF_2H \end{array}\right]^* \rightarrow H_2FCPF_2H^+ + HF \qquad (8)$$

center elimination of HF from the activated complex. The protonated methyene phosphorane product,[41] $CH_3PF_3^+$ (eq 7), is expected to be more abundant than $H_2FCPF_2H^+$ (eq 8) since $D(PHF_2^+-F) \approx 143$ kcal/mol

FIGURE 2

Temporal variation of relative ion abundance in a 1:1 mixture of PF_3 and CH_3F at 1.6×10^{-6} Torr total pressure following a 20 eV, 10 ms electron beam pulse.

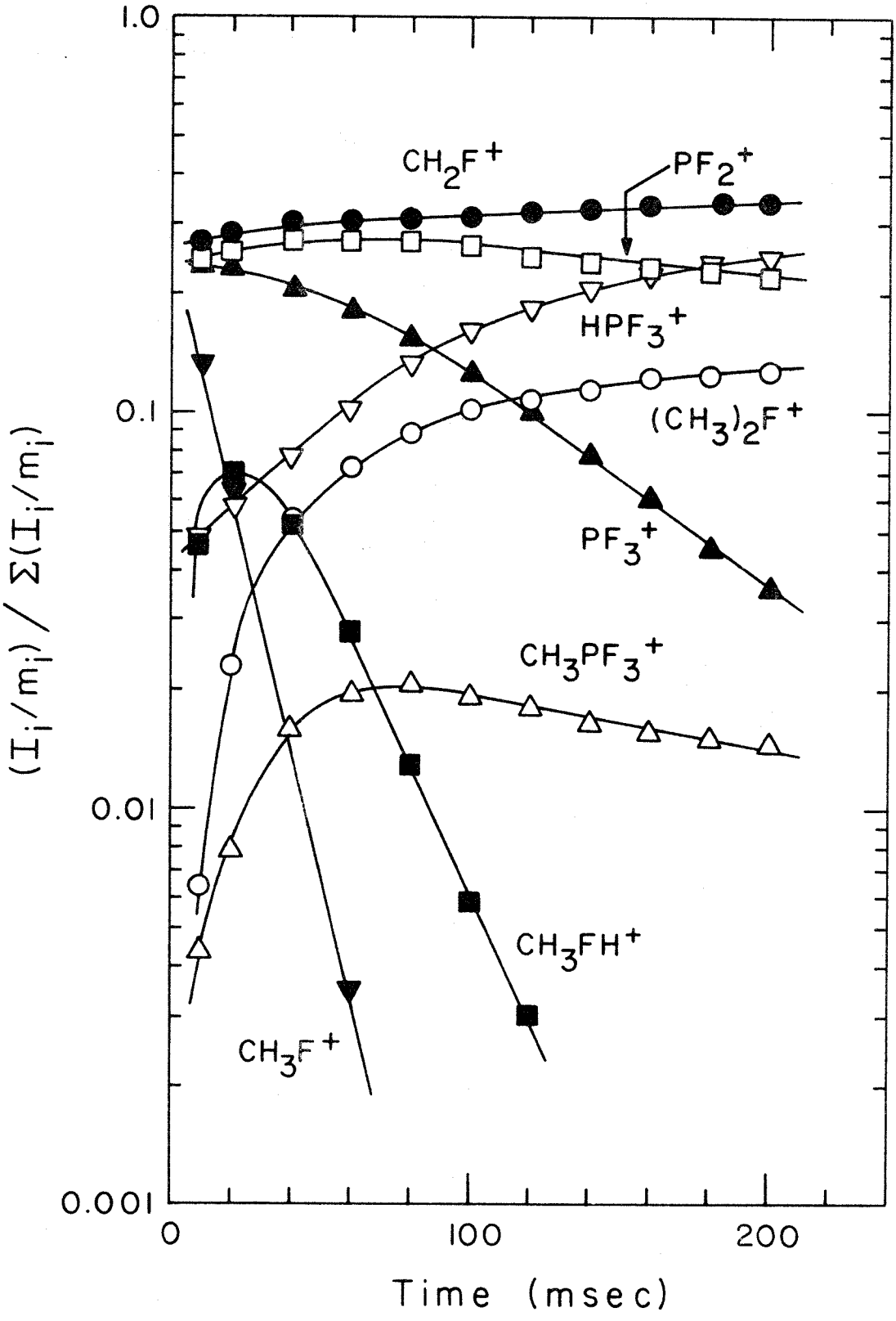
1.0
0.1
0.01
0.001
0
100
200
Time (msec)
$(I_i/m_i) / \Sigma(I_i/m_i)$
CH_2F^+
PF_2^+
HPF_3^+
$(CH_3)_2F^+$
PF_3^+
$CH_3PF_3^+$
CH_3FH^+
CH_3F^+

(estimated) is much larger than $D(PF_3^+-H) = 113.2$ kcal/mol (this work), while $D(CH_3-F) \approx D(CH_2F-H) \approx 105$ kcal/mol.[40] Studies using deuterium labelled methyl fluoride would distinguish between reactions 7 and 8. An alternative mechanism involving nucleophilic attack by CH_3F on the phosphonium center is also possible (eq 9).

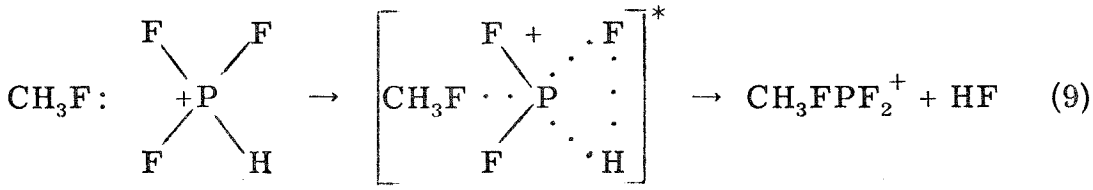

$$CH_3F: \quad +PF_2H \rightarrow [CH_3F \cdots PF_2H]^* \rightarrow CH_3FPF_2^+ + HF \qquad (9)$$

In this case, the difluorophosphine methyl fluoronium ion may result, which appears unusual at first, but is isoelectronic with CH_3OPF_2.[42] At long ion trapping times ($t > 100$ msec), $CH_3PF_3^+$ slowly reacts with the neutral CH_3F present to produce the dimethylfluoronium ion (eq 10; $k = 1.2 \times 10^{-10}$ $cm^3 molecules^{-1} s^{-1}$). By assuming that both

$$CH_3PF_3^+ + CH_3F \rightarrow (CH_3)_2F^+ + PF_3 \qquad (10)$$

reactions 6 and 10 are exothermic or thermoneutral, upper and lower limits, respectively, of $\Delta H_f(CH_3PF_3^+)$ may be calculated, and give an average value of $\Delta H_f(CH_3PF_3^+) = -8.5 \pm 5$ kcal/mol, which leads directly to $D(CH_3^+-PF_3) = 44 \pm 5$ kcal/mol.

Fluorine Atom Transfer Reactions Leading to PF_4^+. In a mixture of PF_3 and NF_3, fluorine atom transfer from neutral NF_3 to PF_3^+ is observed (eq 11), and indicates that $D(PF_3^+-F) > D(NF_2-F) = 60.2$

$$PF_3^+ + NF_3 \rightarrow PF_4^+ + NF_2 \qquad (11)$$

kcal/mol (Table III). Failure to observe this process with SF_6 suggests

Table III. Thermochemical Data for Inorganic Fluorides[a]

M	$\Delta H_f(M)$	$\Delta H_f(M^+)$	$\Delta H_f(MF)$	D(M-F)	$D(M^+-F^-)$
BF_2	-141.0	77.1	-271.7	149.4	287.4
CF_3	-112.2[b]	100.6	-223.0	129.5	262.6
SiF_3	-250.0[c]	- 22.7[c]	-386.0	154.7	347.6
NF_2	+ 10.1	278.1[d]	- 31.4	60.2	248.5
PF_2	-105.0	117.6[e]	-224.9	138.6	281.4
SF_5	-232.0[f]	41.8[g]	-291.8	78.5	272.5
UF_5	-455.0[h]	-209.0[h]	-511.0[h]	74.7	241.0
WF_5	-309.1[i]	- 78.8[i]	-411.5	121.0	271.7

[a]All values in kcal/mol, from Reference 34 and M. W. Chase, J. L. Curnott, A. T. Hu, H. Prophet, A. N. Syverud, and L. C. Walker, J. Phys. Chem. Ref. Data, 3, 311 (1974) unless otherwise noted. [b]F. P. Lossing and G. P. Semeluk, Can. J. Chem., 48, 955 (1970). [c]M. K. Murphy and J. L. Beauchamp, J. Am. Chem. Soc., 99, 2085 (1977). [d]A. B. Cornford, D. C. Frost, F. G. Herring, and C. A. McDowell, J. Chem. Phys., 54, 1872 (1971). [e]Reference 30. [f]M. S. Foster, S. A. Sullivan, and J. L. Beauchamp, unpublished results. [g]V. H. Dibeler and J. A. Walker, J. Chem. Phys., 44, 4405 (1966). [h]J. L. Beauchamp, J. Chem. Phys., 64, 718 (1976). [i]D. L. Hildenbrand, J. Chem. Phys., 62, 3074 (1975).

that $D(PF_3^+-F) < 78.5$ kcal/mol. Choosing the value $D(PF_3^+-F) = 69 \pm 9$ kcal/mol midway between the values for $D(NF_2-F)$ and $D(SF_5-F)$ gives $\Delta H_f(PF_4^+) = -8.4 \pm 9$ kcal/mol. As discussed above, homolytic bond energies to hydrogen are usually higher in an ion than in the corresponding isoelectronic neutral. It is thus interesting to note that bonds to fluorine are substantially weaker, $D(PF_3^+-F) = 69$ kcal/mol being less than half of $D(SiF_3-F) = 154.7$ kcal/mol (Table III).

When a trace of acetone (3×10^{-8} Torr) is added to a mixture of NF_3 and PF_3, several new ionic species result. Figure 3 presents the temporal variation of relative ion abundance for a 53:20:1 mixture of NF_3, PF_3, and $(CH_3)_2CO$ at a total pressure of 2.7×10^{-6} Torr [excluding ions observed in $(CH_3)_2CO$ alone[43]], following a 20 eV, 10 msec electron beam pulse. The sequence of reactions 11-15

$$PF_2^+ + NF_3 \rightarrow NF_2^+ + PF_3 \quad (12)$$

$$NF_2^+ + PF_3 \rightarrow PF_3^+ + NF_2 \quad (13)$$

$$PF_3^+ + (CH_3)_2CO \rightarrow (CH_3)_2CF^+ + F_2PO \quad (14)$$

$$PF_4^+ + (CH_3)_2CO \rightarrow (CH_3)_2CF^+ + F_3PO \quad (15)$$

describe the ion-molecule processes which occur in this system. Reaction 12 (discussed in greater detail below) is a fluoride transfer from NF_3 to PF_2^+ ($k = 3.1 \times 10^{-10}$ $cm^3 molecule^{-1} s^{-1}$), and indicates that $D(PF_2^+-F^-) > D(NF_2^+-F^-) = 248.5$ kcal/mol (Table III). The NF_2^+ formed in eq 12 reacts further to produce PF_3^+ by charge exchange (reaction 13; $k = 5.8 \times 10^{-10}$ $cm^3 molecule^{-1} s^{-1}$). Particularly

FIGURE 3

Temporal variation of relative ion abundance in a 53:20:1 mixture of NF_3, PF_3, and $(CH_3)_2CO$ at 2.7×10^{-6} Torr total pressure following a 20 eV, 10 ms electron beam pulse.

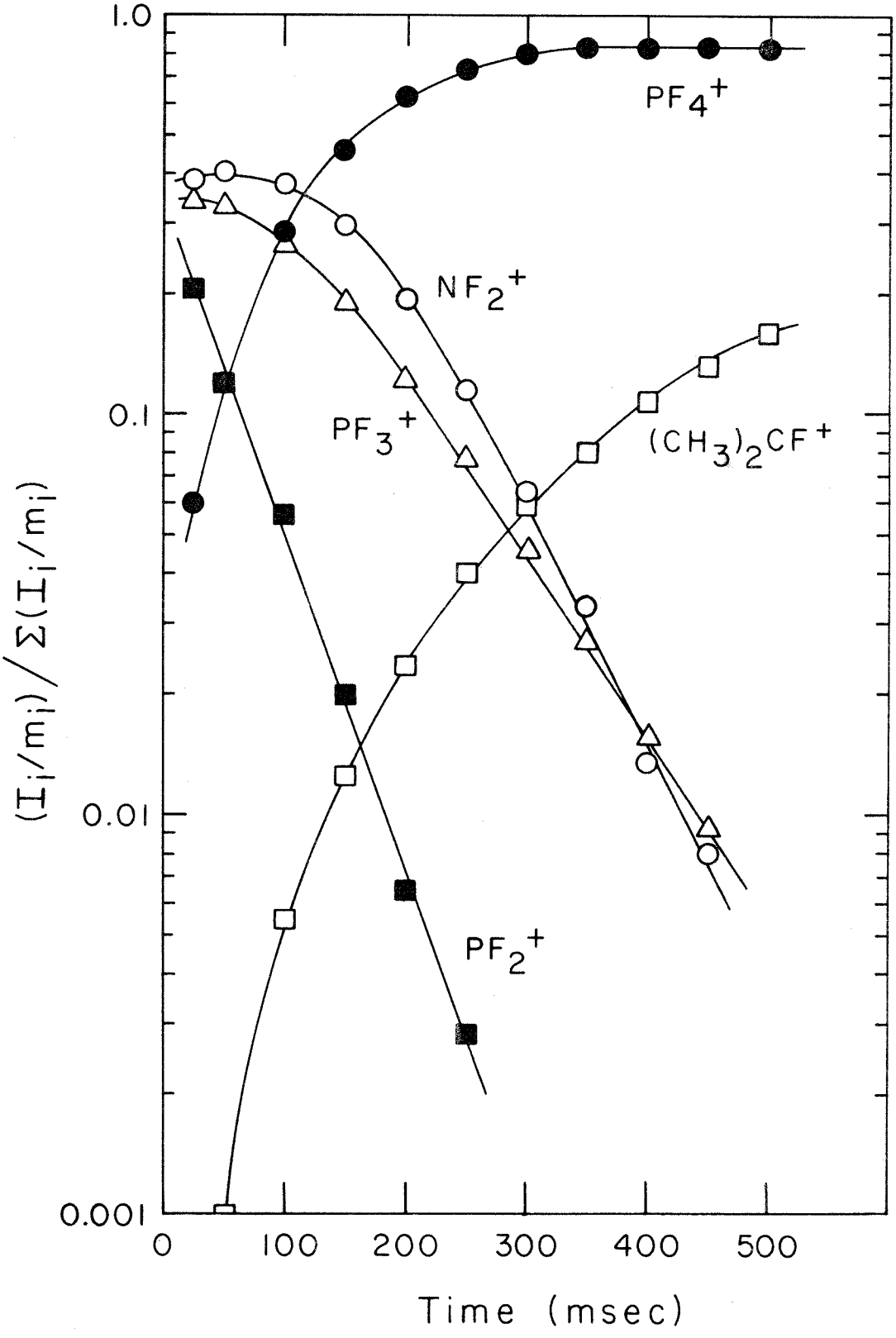
1.0
0.1
0.01
0.001
0
100
200
300
400
500
Time (msec)
$(I_i/m_i)/\Sigma(I_i/m_i)$
PF_4^+
NF_2^+
PF_3^+
$(CH_3)_2CF^+$
PF_2^+

interesting, however, are reactions 14 and 15, in which the carbonyl oxygen exchanges with F^+ in PF_3^+ and PF_4^+. Analogous reactions have been observed by Ausloos et al. in mixtures of aldehydes, ketones, esters, acids, and acetic anhydride with CX_3^+ ions (X = F or Cl).[44] Their results demonstrate that a four-center reaction mechanism resulting in the formation of a monohalogenated carbonium ion predominates.[44] This mechanism is described for this system by equation 16. The

$$PF_n^+ + (CH_3)_2CO \rightarrow \left[\begin{array}{c} O \cdots PF_{n-1} \\ \vdots \quad + \quad \vdots \\ CH_3{-}C \cdots F \\ | \\ CH_3 \end{array} \right]^* \rightarrow (CH_3)_2CF^+ + OPF_{n-1} \qquad (16)$$

$$(n = 3, 4)$$

$(CH_3)_2CF^+$ product ion dissociated by loss of HF (eq 17),

$$[(CH_3)_2CF^+]^* \rightarrow C_3H_5^+ + HF \qquad (17)$$

which reflects the exothermicity of reactions 14 ($\Delta H = -49 \pm 10$ kcal/mol) and 15 ($\Delta H = -97 \pm 10$ kcal/mol).[44]

Fluoride Transfer Reactions Involving PF_2^+. The ion chemistry of mixtures of PF_3 with a variety of inorganic fluorides including SiF_4, BF_3, SF_6, CF_4, and NF_3 was examined. The SiF_3^+ and BF_2^+ ions produced by electron impact ionization of SiF_4 and BF_3, respectively, abstract F^- from neutral PF_3 (eq 18 and 19). Figure 4 presents the

$$SiF_3^+ + PF_3 \rightarrow PF_2^+ + SiF_4 \qquad (18)$$

$$BF_2^+ + PF_3 \rightarrow PF_2^+ + BF_3 \qquad (19)$$

FIGURE 4

Temporal variation of relative ion abundance in a 9.6:1 mixture of SiF_4 and PF_3 at a total pressure of 2.2×10^{-6} Torr following an 18 eV, 10 ms electron beam pulse.

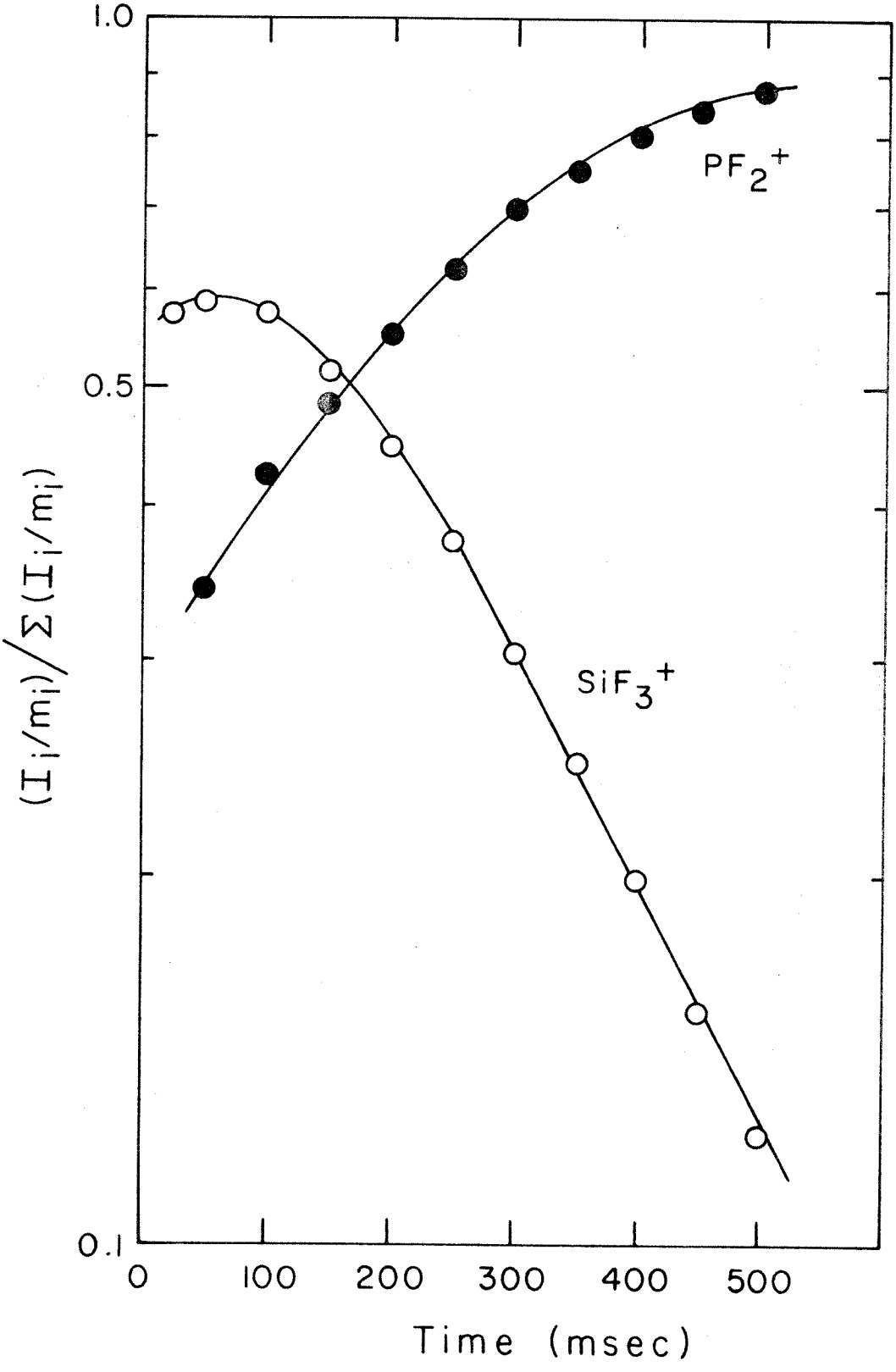
1.0
0.5
0.1
0
100
200
300
400
500
Time (msec)
$(I_i/m_i)/\Sigma(I_i/m_i)$
PF_2^+
SiF_3^+

temporal variation of relative ion abundance in a 9.6:1 mixture of SiF_4 and PF_3 at a total pressure of 2.2×10^{-6} Torr following an 18 eV, 10 ms electron beam pulse. Reaction 18 is the only ion-molecule reaction observed in this system under these conditions. From the linear portion of the decrease in SiF_3^+ relative abundance ($t > 200$ ms), $k = 6.7 \times 10^{-10}$ $cm^3 molecule^{-1} s^{-1}$ is calculated. PF_2^+ reacts with SF_6 and NF_3, on the other hand, to produce SF_5^+ (eq 20) and NF_2^+

$$PF_2^+ + SF_6 \rightarrow SF_5^+ + PF_3 \qquad (20)$$

(eq 12; Figure 3). Fluoride ion transfer reactions cannot be observed in mixtures of PF_3 and CF_4 since the reactant and product ions, PF_2^+ and CF_3^+, have the same mass. From these results, the heterolytic bond dissociation energy $D(PF_2^+-F^-)$ is less than $D(SiF_3^+-F^-)$ and $D(BF_2^+-F^-)$ and greater than $D(SF_5^+-F^-)$ and $D(NF_2^+-F^-)$. The thermochemical changes associated with these reactions can be inferred from the data presented in Table III, which are entirely consistent with the derived order. These experiments thus confirm available data which yield $D(PF_2^+-F^-) = 281.4 \pm 6.1$ kcal/mol (Table III). With a larger number of fluorides, it would be possible to accurately establish relative heterolytic bond dissociation energies for species such as those listed in Table III. In most cases there are no competing reactions which would interfere with the examination of halide transfer equilibria.[45]

Acknowledgment. This research was supported in part by the U.S. Army Research Office under Grant No. DAAG29-76-G-0274.

References and Notes

(1) For reviews, see J. L. Beauchamp, Annu. Rev. Phys. Chem., 22, 527 (1971); G. A. Gray, Adv. Chem. Phys., 19, 141 (1971); T. A. Lehman and M. M. Bursey, "Ion Cyclotron Resonance Spectrometry", Wiley, New York, N.Y., 1976.

(2) B. S. Freiser, T. B. McMahon, and J. L. Beauchamp, Int. J. Mass Spectrom. Ion Phys., 12, 249 (1973).

(3) T. B. McMahon and J. L. Beauchamp, Rev. Sci. Instrum., 43, 509 (1972).

(4) M. T. Bowers, D. H. Aue, H. M. Webb, and R. T. McIver, Jr., J. Am. Chem. Soc., 93, 4314 (1971).

(5) D. H. Aue, H. M. Webb, and M. T. Bowers, J. Am. Chem. Soc., 94, 4726 (1972); ibid., 95, 2699 (1973); ibid., 97, 4136, 4137 (1975); ibid., 98, 311, 318 (1976).

(6) W. G. Henderson, M. Taagepera, D. Holtz, R. T. McIver, Jr., J. L. Beauchamp, and R. W. Taft, J. Am. Chem. Soc., 94, 4728 (1972).

(7) M. Taagepera, W. G. Henderson, R. T. C. Brownlee, J. L. Beauchamp, D. Holtz, and R. W. Taft, J. Am. Chem. Soc., 94, 1369 (1972).

(8) R. H. Staley and J. L. Beauchamp, J. Am. Chem. Soc., 96, 6252 (1974).

(9) R. H. Staley and J. L. Beauchamp, J. Am. Chem. Soc., 96, 1604 (1974).

(10) R. W. Taft in "Proton Transfer Reactions", E. F. Caldin and V. Gold, eds., Chapman and Hall, London, 1975.

(11) J. F. Wolf, R. H. Staley, I. Koppel, J. L. Beauchamp, and R. W. Taft, J. Am. Chem. Soc., submitted for publication.

(12) R. H. Staley, J. E. Kleckner, and J. L. Beauchamp, J. Am. Chem. Soc., 98, 2081 (1976).

(13) D. Holtz and J. L. Beauchamp, J. Am. Chem. Soc., 91, 5913 (1969).

(14) D. Holtz, J. L. Beauchamp, W. G. Henderson, and R. W. Taft, Inorg. Chem., 10, 201 (1971).

(15) R. H. Staley, M. Taagepera, W. G. Henderson, I. Koppel, J. L. Beauchamp, and R. W. Taft, J. Am. Chem. Soc., 99, 326 (1977).

(16) S. A. Sullivan and J. L. Beauchamp, J. Am. Chem. Soc., 98, 1160 (1976).

(17) R. T. McIver and J. S. Miller, J. Am. Chem. Soc., 96, 4325 (1974).

(18) R. R. Corderman and J. L. Beauchamp, J. Am. Chem. Soc., 98, 3998 (1976); ibid., submitted for publication.

(19) R. R. Corderman and J. L. Beauchamp, J. Am. Chem. Soc., submitted for publication.

(20) F. A. Cotton and G. Wilkinson, "Advanced Inorganic Chemistry", 3rd ed., Wiley, New York, N.Y., 1972, p. 720.

(21) J. F. Nixon, Adv. Inorg. Chem. Radiochem., 13, 363 (1970); Th. Kruck, Angew Chem. Int. Edit. Engl., 6, 53 (1967); O. Stelzer, Topics Phosphorus Chem., 9, 1 (1977).

(22) G. A. Olah and C. W. McFarland, Inorg. Chem., 11, 845 (1972).

(23) R. W. Rudolph and R. W. Parry, J. Am. Chem. Soc., 89, 1621 (1967).

(24) A preliminary report giving the value of $PA(PF_3)$ = 170 kcal/mol has been published (S. V. Lucas and D. H. McDaniel, Abstracts, 169th National Meeting of the American Chemical Society, Philadelphia, Pa., April 1975, No. INOR-50).

(25) J. P. Maier and D. W. Turner, J. Chem. Soc. Faraday Trans. II, 68, 711 (1972).

(26) J. C. Green, D. I. King, and J. H. D. Eland, Chem. Commun., 1121 (1970).

(27) J. Müller, K. Fenderl, and B. Mertschenk, Chem. Ber., 104, 700 (1971).

(28) P. J. Bassett, D. R. Lloyd, I. H. Hillier, and V. R. Saunders, Chem. Phys. Lett., 6, 253 (1970).

(29) C. J. Aarons, M. F. Guest, M. B. Hall, and I. H. Hillier, J. Chem. Soc. Faraday Trans. II, 69, 643 (1973).

(30) D. F. Torgerson and J. B. Westmore, Can. J. Chem., 53, 933 (1975).

(31) P. W. Harland, D. W. H. Rankin, and J. C. J. Thynne, Int. J. Mass Spectrom. Ion Phys., 13, 395 (1974).

(32) C. R. S. Dean, A. Finch, P. J. Gardner, and D. W. Payling, J. Chem. Soc. Faraday Trans. I, 70, 1921 (1974).

(33) Gas pressures in the spectrometer were measured as described in R. J. Blint, T. B. McMahon, and J. L. Beauchamp, J. Am. Chem. Soc., 96, 1269 (1974).

(34) $\Delta H_f(PF_3)$ = -224.9 ± 0.9 kcal/mol (D. R. Stull and H. Prophet, "JANAF Thermochemical Tables", 2nd ed., Natl. Stand. Ref. Data Ser. Natl. Bur. Stand., No. 37 (1971)).

(35) $\Delta H_f(PF^+)$ = 247.8 ± 5.0 kcal/mol is calculated from the data given in References 30 and 34.

(36) J. L. Beauchamp, D. Holtz, S. D. Woodgate, and S. L. Patt, J. Am. Chem. Soc., 94, 2798 (1972).

(37) J. L. Beauchamp and S. E. Buttrill, J. Chem. Phys., 48, 1783 (1968).

(38) I. Absar and J. R. Van Wazer, J. Am. Chem. Soc., 94, 6294 (1972).

(39) J. Müller, Adv. Mass Spectrom., 6, 823 (1974).

(40) F. P. Lossing, Bull Soc. Chim. Belges, 81, 125 (1972).

(41) H. Lischka, J. Am. Chem. Soc., 99, 353 (1977).

(42) D. R. Martin and P. J. Pizzolato, J. Am. Chem. Soc., 72, 4584 (1950).

(43) K. A. G. MacNeil and J. H. Futrell, J. Phys. Chem., 76, 409 (1972); A. S. Blair and A. G. Harrison, Can. J. Chem., 51, 703 (1973).

(44) J. R. Eyler, P. Ausloos, and S. G. Lias, J. Am. Chem. Soc., 96, 3675 (1974); P. Ausloos, S. G. Lias, and J. R. Eyler, Int. J. Mass Spectrom. Ion Phys., 18, 261 (1975).

(45) For a recent study of bromide transfer reactions, see R. H. Staley, R. D. Wieting, and J. L. Beauchamp, J. Am. Chem. Soc., accepted for publication.

CHAPTER VI

Ion Cyclotron Resonance Studies of Chain Reactions Involving Ionic Intermediates. Interchange of Fluorine and Hydrogen Between Carbon and Silicon Centers In Mixtures of Fluorocarbons and Silanes

Reed R. Corderman, M. K. Murphy,[1] and J. L. Beauchamp

Contribution No. 5584 from the Arthur Amos Noyes Laboratory of Chemical Physics, California Institute of Technology, Pasadena, California 91125

ABSTRACT

Chain reactions initiated by ions derived from fluoroalkanes and silanes are studied using the techniques of ion cyclotron resonance mass spectroscopy in the gas phase. Chain propagation reactions involve hydride and fluoride transfer between pairs of siliconium ions R_1^+ and carbonium ions R_2^+, for which $D(R_1^+-F^-) \geq D(R_2^+-F^-)$ and and $D(R_1^+-H^-) \leq D(R_2^+-H^-)$. The reversal in heterolytic bond dissociation energies primarily reflects the relative R–H and R–F homolytic bond dissociation energies in neutral fluorocarbons and methylsilanes. A general discussion of possible chemical applications of chain reactions which proceed through ionic intermediates is presented. The positive ion chemistry of the methylsilanes $(CH_3)_nH_{4-n}Si$ (n = 0-3) is briefly considered.

Introduction

Non-branching chain reactions which proceed through ionic intermediates in the gas phase are particularly intriguing since exothermic ion-molecule reactions are usually rapid at thermal energies. In the absence of competing reactions, enormous chain lengths can occur once these processes are initiated. The classic example of such processes is the radiation induced hydrogen-deuterium exchange which leads to formation of HD in mixtures of H_2 and D_2 via sequences of reactions such as indicated by equations 1-3.[2-6] The propagation

$$H_2^+ + H_2 \rightarrow H_3^+ + H \quad (1)$$

$$H_3^+ + D_2 \rightarrow D_2H^+ + H_2 \quad (2)$$

$$D_2H^+ + H_2 \rightarrow H_2D^+ + HD \quad (3)$$

$$H_3^+ + M \rightarrow MH^+ + H_2 \quad (4)$$

steps involve the nearly thermoneutral proton transfer reactions 2 and 3 and their isotopic variants. Rate coefficients measured for these processes indicate that reaction occurs on every collision.[7, 8] Chain lengths of up to 2.4×10^7 have been observed,[6] and the process is interrupted by any species which binds a proton more strongly than hydrogen (e.g., reaction 4 where M = Xe, CH_4, CO, or H_2O).[2-5]

Aside from their intrinsic interest, it is not difficult to imagine that ionic chain reactions might have significant chemical applications. The generation of a single ion may lead to the conversion of 10^7 or more neutral reactants into product with distinctly different chemical properties. Furthermore, if a single molecule interrupts the chain

process, it will lead to a decrease in product yield. Both of these phenomena suggest a chemical amplification effect which might have analytical applications. If the products could be distinguished from the reactants by some physical method, then it would be possible to (1) detect the radiation leading to ionization, (2) detect the initially ionized neutral species in the event that it forms or is itself the chain carrier, or (3) detect a species which interrupts the chain process, thereby leading to a decrease in product yields.

While the energetic requirements for ion generation make gas phase ionic processes somewhat unsuited for chemical synthesis, the occurrence of chain processes might change this situation and be of particular value if the products or reactants are difficult to form in condensed phases or are unstable at elevated temperatures. Even more exciting would be the possibility of gaining isotopic selectivity by controlling the kinetic energy of one isotopic species using ion cyclotron resonance techniques.[9-11] This is rendered closer to a practical reality by the recent demonstration of high resolution ion cyclotron resonance excitation in high density ionized gases (plasmas).[12]

The number of ionic chain reactions which have been characterized are few,[2, 13-17] and we have undertaken the task of identifying additional processes, drawing on the vast body of information concerning the properties and reactions of ions in gases which has become available during the past decade.[9, 16, 18, 19]

Recent studies of substituent effects on the stabilities of ions in the gas phase using the techniques of ion cyclotron resonance

spectroscopy[9-11] (ICR) have proved useful in elucidating relationships between chemical structure, properties, and reactivity.[13-16, 20-27] Carbonium ion stabilities,[13-16] and more recently, siliconium ion stabilities[25-27] in the gas phase can be quantified by the relative heterolytic bond dissociation energy $D(R^+-X^-)$ defined in eq 5 (where X^- = H^-, F^-, Cl^-, Br^-, etc.). Detailed data on carbonium and siliconium

$$RX \rightarrow R^+ + X^- \qquad \Delta H = D(R^+-X^-) \tag{5}$$

ions are available from a variety of mass spectrometric techniques, including low resolution[14, 25] and monoenergetic electron impact,[28] photoionization,[29-33] and ICR studies of X^- transfer reactions (eq 6),[13-16, 24-27] which have advantages over appearance potential

$$R_1^+ + R_2X \rightleftharpoons [R_1XR_2^+]^* \rightleftharpoons R_2^+ + R_1X \tag{6}$$

measurements, where adiabatic thresholds for ion formation are often difficult to discern from the experimental data. Of particular interest are cases where the relative heterolytic bond dissociation energies to F^- and H^- are reversed for a pair of cations R_1^+ and R_2^+.[27] If reactions 7 and 8 are exothermic [requiring that $D(R_1^+-F^-) \geq D(R_2^+-F^-)$ and $D(R_1^+-H^-) \leq D(R_2^+-H^-)$], then the overall process (eq 9) will be

$$R_1^+ + R_2F \rightarrow R_2^+ + R_1F \tag{7}$$

$$R_2^+ + R_1H \rightarrow R_1^+ + R_2H \tag{8}$$

$$R_1H + R_2F \rightarrow R_1F + R_2H \tag{9}$$

exothermic and may occur as a chain reaction proceeding through ionic

intermediates.[13-16] The chain length will be determined by competing processes, which include reactions with impurities. To date only two examples of such processes have been observed using ICR techniques, both involving fluoroalkanes.[13-16]

During the course of recent studies of the fluoromethyl silanes, it became evident that there may be a large number of chain reactions generalized in eq 10 in which Si–H and C–F bonds are interconverted

$$\equiv Si{-}H + \equiv C{-}F \rightarrow \equiv Si{-}F + \equiv C{-}H \qquad (10)$$

to Si–F and C–H bonds via ionic processes. The basis of this expectation can be seen in the data of Figure 1, which presents a schematic representation of $D(R^+{-}H^-)$ and $D(R^+{-}F^-)$ for various carbonium and siliconium ions. The thermodynamic data used to construct Figure 1 (Table I) are the best currently available. The values for $D(R_3Si^+{-}H^-)$ are presently being refined by photoionization mass spectrometry.[33] The different ordering of these ions toward H^- and F^- reference bases can be understood with the aid of the thermochemical cycle of Scheme I and eq 11. Silyl and alkyl radical ionization potentials are quite

$$\begin{array}{ccc} RX & \xrightarrow{D(R^+{-}X^-)} & R^+ + X^- \\ {\scriptstyle D(R{-}X)}\downarrow & & \uparrow{\scriptstyle -EA(X)} \\ R + X & \xrightarrow{IP(R)} & R^+ + X \end{array}$$

Scheme I

$$D(R^+{-}X^-) = D(R{-}X) + IP(R) - EA(X) \qquad (11)$$

comparable for substitutional analogs.[27] Thus, the difference in

FIGURE 1

Scale of hydride affinities $D(R^+-H^-)$ and fluoride affinities $D(R^+-F^-)$ of carbonium and siliconium ions.

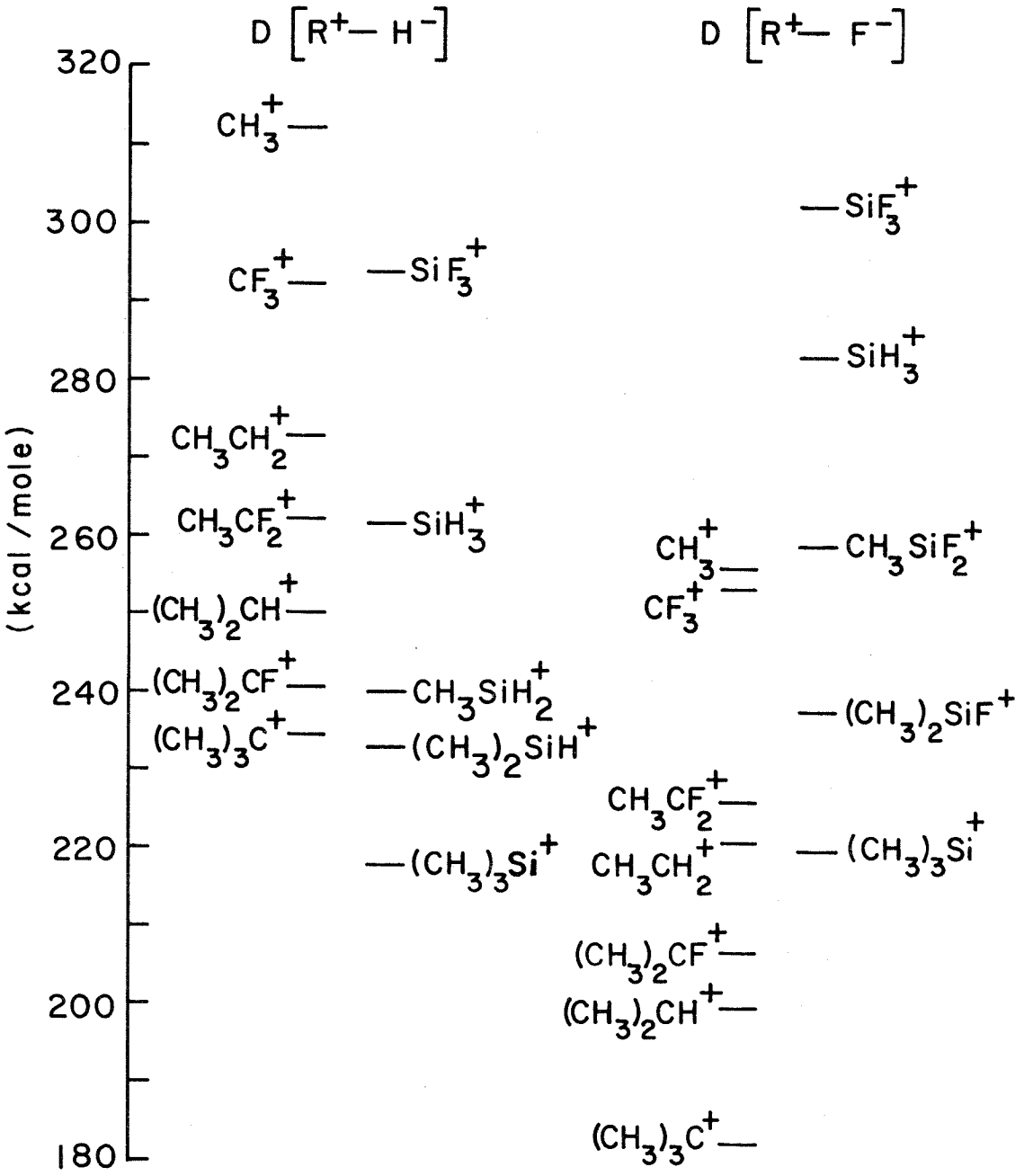
D [R+— H−]
D [R+— F−]
(kcal / mole)
320
300
280
260
240
220
200
180
CH3+—
CF3+—
—SiF3+
CH3CH2+—
CH3CF2+—
—SiH3+
(CH3)2CH+—
(CH3)2CF+—
—CH3SiH2+
(CH3)3C+—
—(CH3)2SiH+
—(CH3)3Si+
—SiF3+
—SiH3+
CH3+—
CF3+—
—CH3SiF2+
—(CH3)2SiF+
CH3CF2+—
CH3CH2+—
—(CH3)3Si+
(CH3)2CF+—
(CH3)2CH+—
(CH3)3C+—

Table I. Comparison of the Best Available Estimates of Thermochemical Properties of Carbon and Silicon Species

R	$\Delta H_f[R]$[a]	$\Delta H_f[R^+]$[a]	$\Delta H_f[RH]$[a]	$\Delta H_f[RF]$[a]	IP[R][b]	D[R–H][c, q]	D[R–F][c, q]	D[R^+–H^-]	D[R^+–F^-]
CH_3	34.0[d]	260.9[g]	- 17.9[k]	- 55.9[d]	9.84[d]	104.0	108.6	312.2[j]	255.5[j]
CH_3CH_2	25.7[d]	218.9[f]	- 20.2[k]	- 62.9[n]	8.38[d]	98.0	106.5	272.5[f]	220.5[f]
$(CH_3)_2CH$	17.6[d]	191.7[f]	- 24.8[k]	- 69.0[m]	7.55[d]	94.5	105.3	249.9[f]	199.4[f]
$(CH_3)_3C$	9.3[e]	169.0[h]	- 32.2[l]	- 74.1[o]	6.93[d]	93.6	102.1	234.4[r]	181.8[r]
$(CH_3)_2CF$	- 26.6[f]	138.0[f]	- 69.0[m]	-129.8[f]	7.14[f]	94.5	121.9	240.4[f]	206.5[f]
CH_3CF_2	- 73.8[f]	108.8[f]	-119.7[n]	-178.2[n]	7.92[f]	98.0	123.1	261.9[f]	225.7[f]
CF_3	-112.2[d]	99.3[i]	-166.3[d]	-223.0[p]	9.17[i]	106.2	129.5	292.0[s]	253.0[s]
SiH_3	45.6[t]	236.3[z]	8.2[t]	-105.0[w]	8.27[v]	89.5	169.3	261.3[r]	282.6[r]
CH_2SiH_2	33.0[t]	202.6[z]	- 4.3[t]	- 99.4[x]	7.37[v]	89.4	151.1[x]	240.1[r]	252.6[x]
$(CH_3)_2SiH$	21.0[t]	182.9[z]	- 16.8[t]	-108.8[x]	7.02[v]	89.9	148.5[x]	232.9[r]	234.6[x]
$(CH_3)_3Si$	2.4[u]	154.8[u]	- 29.6[t]	-126.0[u]	6.61[u]	84.1	147.1	217.6[r]	219.5[u]
$(CH_3)_2SiF$	- 80.1[u]	86.6[u]	-- [x]	-212.0[u]	7.23[u]	-- [x]	150.6	-- [x, y]	237.2[u]
CH_3SiF_2	-166.0[u]	23.7[u]	-- [x]	-296.0[u]	8.23[u]	-- [x]	148.7	-- [x, y]	258.4[u]
SiF_3	-250.0[u]	- 22.7[u]	-283.0[w]	-386.0[u]	9.86[u,aa]	85.1	154.7	293.5[r]	302.0[u]

[a]Heats of formation in kcal/mole at 298°K.

[b]Ionization potentials in eV.

[c]Estimated uncertainties in homolytic bond dissociation energies ± 3 kcal/mole for carbon species and ± 10 kcal/mole for silicon species.

[d]Taken from Ref. 27.

[e]W. Tsang, J. Phys. Chem., 76, 143 (1972).

[f]Taken from Ref. 31.

[g]G. Herzberg and J. Shoosmith, Can. J. Phys., 34, 523 (1956).

[h]Calculated from $\Delta H_f[R^+] = \Delta H_f[R] + IP[R]$ using data in this table.

[i]T. A. Walter, C. Lifschitz, W. A. Chupka, and J. Berkowitz, J. Chem. Phys., 51, 3531 (1969).

[j]Taken from Ref. 14.

Table I. (Continued)

[k]J. D. Cox and G. Pilcher, "Thermochemistry of Organic and Organometallic Compounds", Academic Press, New York, N.Y., 1970.

[l]J. L. Franklin, J. G. Dillard, H. M. Rosenstock, J. T. Herron, K. Draxl, and F. H. Field, "Ionization Potentials, Appearance Potentials and Heats of Formation of Gaseous Positive Ions", NSRDS-NBS 26, Washington, D.C., 1969.

[m]J. R. Lacher, J. Phys. Chem., 60, 1454 (1956).

[n]S. S. Chen, A. S. Rodgers, J. Chao, R. S. Wilhoit, and B. J. Zwolinski, J. Phys. Chem. Ref. Data, 4, 441 (1975).

[o]Estimated using group equivalents method of S. W. Benson, "Thermochemical Kinetics", Wiley, New York, N.Y., 1968.

[p]J. R. Lacher and H. A. Skinner, J. Chem. Soc. A, 1034 (1968).

[q]Calculated from $D[R-X] = \Delta H_f[R] + \Delta H_f[X] - \Delta H_f[RX]$ (where X = H, F) using data in this table.

[r]Calculated from $D[R^+-X^-] = \Delta H_f[R^+] + \Delta H_f[X^-] - \Delta H_f[RX]$ where X = H, F) using data in this table.

[s]Taken from Ref. 17.

[t]P. Potzinger, A. Ritter, and J. Krause, Z. Naturforsch., 30A, 347 (1975).

[u]Taken from Ref. 30.

[v]Calculated from $IP[R] = \Delta H_f[R] + IP[R]$ using data in this table.

[w]D. R. Stull and H. Prophet, "JANAF Thermochemical Tables", 2nd ed., Natl. Stand. Ref. Data. Ser., Natl. Bur. Stand., No. 37 (1971).

[x]No data available, calculated where required by linear interpolation between values given for SiH_3F and $(CH_3)_3SiF$.

[y]From trends observed it is assumed that $D[(CH_3)F_2Si^+-H^-] > D[(CH_3)H_2Si^+-H^-]$ and that $D[(CH_3)_2FSi^+-H^-] > D[(CH_3)_2HSi^+-H^-]$.

[z]Taken from Ref. 33.

[aa]This value appears to be somewhat high, see Ref. 30.

ordering for a particular reference base X^- ($X^- = H^-$ or F^-) reflects primarily differences in homolytic C–X and Si–X bond strengths (Table I). That hydride affinities of carbonium ions are uniformly greater than those of siliconium ions reflects the consistently larger homolytic C–H bond strengths as compared with Si–H bonds. Similarly, the fact that $D(R_3Si^+-F^-)$ values are 30-50 kcal/mol greater than $D(R_3C^+-F^-)$ values for substitutional analogs is as expected from the differences in Si–F and C–F homolytic bond dissociation energies throughout the two series (Table I).[27] The reversal in carbonium and siliconium ion stability ordering in comparing H^- to F^- is then simply a reflection of the reversal in homolytic R–H and R–F bond dissociation energies in the neutral methanes and silanes.

The present paper details in several instances the observation of chain reactions in mixtures of silanes with fluorocarbons. Evidence for one such process, involving mainly the conversion of a mixture of SiH_4 and CF_4 to SiH_3F and CF_3H, has been recently reported by Krause and Lampe,[34, 35] and is particularly applicable to the interpretation of the present results.

Experimental

The theory and instrumentation of ICR mass spectrometry have been previously described.[9-11] This work employed an instrument constructed at Caltech equipped with a 15-inch electromagnet capable of a maximum field strength of 23.4 kG.

CH_3SiD_3 was provided through the courtesy of Professors F. S. Rowland and M. J. Molina. All other chemicals used in this study

were readily available from commercial sources and used without further purification. No impurities were observed in the 70 eV ICR mass spectrum of the compounds examined. Before use, each sample was degassed by repeated freeze-pump-thaw cycles.

Pressures were measured with a Schulz-Phelps type ion gauge calibrated against a MKS Baratron Model 90H1-E capacitance manometer in a manner previously described.[14] The estimated uncertainty in absolute pressures, and thus in all rate constants reported is ± 20%. All experiments were performed at ambient temperature (20-25 °C).

Results and Discussion

Mixture of SiH_4 with CF_4. From the data presented in Figure 1, the exothermic reactions 12 and 13 are expected to occur in a mixture

$$SiH_3^+ + CF_4 \rightarrow CF_3^+ + SiH_3F \quad (12)$$

$$CF_3^+ + SiH_4 \rightarrow SiH_3^+ + CF_3H \quad (13)$$

of SiH_4 with CF_4.[34, 35] These reactions are identical to processes 7 and 8 where R_1^+ is the unsubstituted siliconium ion SiH_3^+ and R_2^+ is the trifluoromethyl carbonium ion CF_3^+, and lead to the overall process 14, in which Si–H and C–F bonds are interconverted to Si–F

$$SiH_4 + CF_4 \rightarrow SiH_3F + CF_3H \quad (14)$$

and C–H bonds just as in eq 10, the overall process being 56.5 kcal/mol exothermic.

The ion chemistry of SiH_4 alone has been extensively investigated in the gas phase.[33, 36-38] The ion-molecule reactions at low pressures (10^{-6} Torr) and 14 eV are characterized by fast hydride transfer processes (eq 15 and 19) forming SiH_3^+, and by condensation reactions to binuclear silicon species (eq 16-18, 20). CF_3^+ produced

$$SiH_2^+ + SiH_4 \rightarrow SiH_3^+ + SiH_3 \quad (15)$$
$$\rightarrow Si_2H_2^+ + 2H_2 \quad (16)$$
$$\rightarrow Si_2H_4^+ + H_2 \quad (17)$$
$$\rightarrow Si_2H_5^+ + H \quad (18)$$

$$SiH_3^+ + {}^*SiH_4 \rightarrow {}^*SiH_3^+ + SiH_4 \quad (19)$$
$$\rightarrow Si_2H_5^+ + H_2 \quad (20)$$

by the electron impact dissociation of CF_4 at 14 eV and low pressures ($\sim 10^{-6}$ Torr) is unreactive towards CF_4.[14]

Figure 2 presents the temporal variation of ion abundance observed in a 1.6:1 mixture of SiH_4 and CF_4 at a total pressure of 1.7×10^{-6} Torr following ionization by a 14 eV, 10 ms electron beam pulse. During the first ~200 ms, SiH_2^+ reacts with SiH_4, forming SiH_3^+ (eq 15), and SiH_3^+ reacts with CF_4 to produce the additional chain centers CF_3^+, SiH_2F^+, and CF_2H^+. After ~ 200 ms an <u>apparent</u> equilibrium is established between the different ion populations. Double resonance experiments[9, 10] verify the occurrence of the coupled reactions shown in Scheme II, with each product ion resulting from several precursor ions as indicated. While the F^- and H^- transfer

FIGURE 2

Temporal variation of CF_3^+, SiH_3^+, CF_2H^+, and SiH_2F^+ signal intensities following a 14 eV, 10 ms electron beam pulse in a 1.6:1 mixture of SiH_4 and CF_4 at 1.7×10^{-6} Torr total pressure.

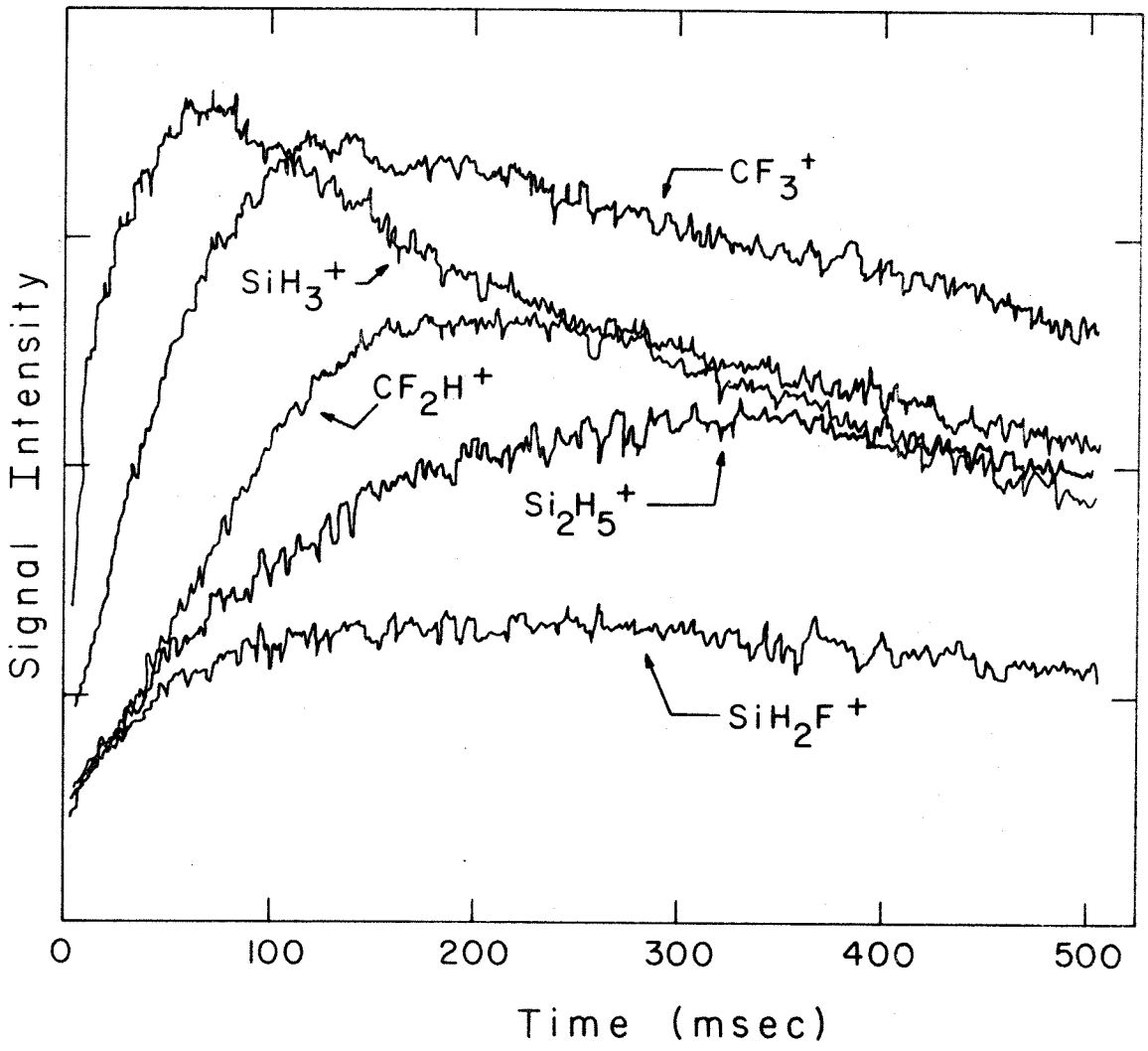
Signal Intensity
CF_3^+
SiH_3^+
CF_2H^+
$Si_2H_5^+$
SiH_2F^+
0
100
200
300
400
500
Time (msec)

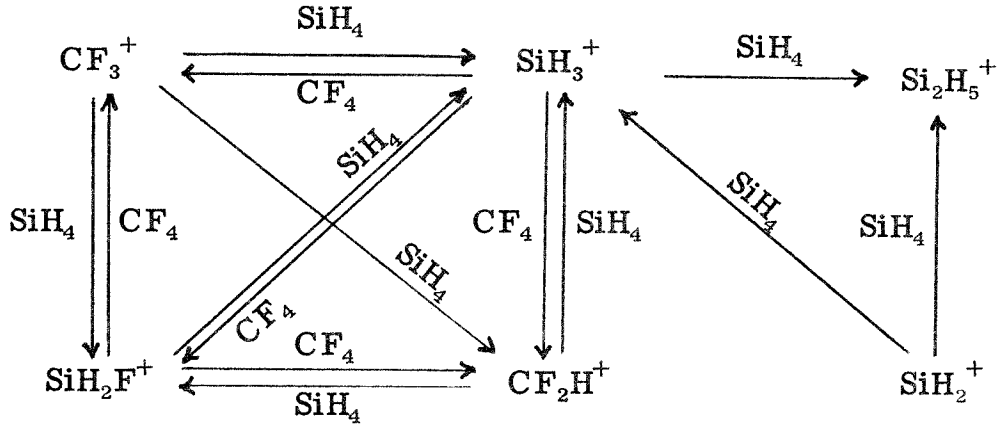

Scheme II

reactions 12, 13, and 21-23 are observed (Scheme II), the remaining

$$SiH_2F^+ + CF_4 \rightarrow CF_3^+ + SiH_2F_2 \quad (21)$$

$$CF_2H^+ + SiH_4 \rightarrow SiH_3^+ + CF_2H_2 \quad (22)$$

$$SiH_2F^+ + SiH_4 \rightarrow SiH_3^+ + SiH_3F \quad (23)$$

reactions involve a more extensive redistribution of fluorine and hydrogen between carbon and silicon centers, as also reported by Krause and Lampe using high-pressure tandem mass spectrometry.[34, 35] The $Si_2H_5^+$ ion terminates the chain processes (Scheme II), and does not react further with CF_4.

The chain reactions presented in Scheme II may be characterized by a kinetic chain length,[39] which is defined by the rate of formation of the individual chain carriers divided by the rate of the chain terminating reactions (eq 20). Taking the average rate constant for formation of the chain carriers as $k = 1.0 \times 10^{-9}$ $cm^3 molecule^{-1} s^{-1}$,[35] and the rate constant for the chain termination reaction 20 as

$k = 2.4 \times 10^{-11}$ $cm^3 molecule^{-1} s^{-1}$,[38] a kinetic chain length of 25.9 is calculated, where the pressures of SiH_4 and CF_4 employed are the same as those in Figure 1. In other words, approximately 26 chain carriers are generated for every molecule of $Si_2H_5^+$ produced, which terminates the chain reactions (Scheme II).

Mixture of $MeSiD_3$ with Me_2CF_2. The gas phase ion chemistry of $MeSiH_3$ has been previously studied at high pressures ($1\text{-}6 \times 10^{-3}$ Torr).[40] Using trapped ion ICR techniques[11] at low pressures (approximately 5×10^{-7} Torr), similar results are obtained. The $MeSiD^+$ fragment ion reacts with $MeSiD_3$ to produce $MeSiD_2^+$ by hydride transfer (eq 24; $k = 7.0 \times 10^{-10}$ $cm^3 molecule^{-1} s^{-1}$). Both the $MeSiD^+$ and

$$MeSiD^+ + MeSiD_3 \rightarrow MeSiD_2^+ + MeSiD_2 \qquad (24)$$

$MeSiD_2^+$ ions react with $MeSiD_3$ to exchange CH_3 for D_2, eq 25 and 26.

$$MeSiD^+ + MeSiD_3 \rightarrow Me_2SiD^+ + SiD_3 \qquad (25)$$

$$MeSiD_2^+ + MeSiD_3 \rightarrow Me_2SiD^+ + SiD_4 \qquad (26)$$

The total rate constant for production of Me_2SiD^+ is $k = 3.4 \times 10^{-10}$ $cm^3 molecule^{-1} s^{-1}$. At long ion trapping times (> 400 ms), a small amount ($< 2\%$) of Me_3Si^+ is produced by reaction 27.

$$Me_2SiD^+ + MeSiD_3 \rightarrow Me_3Si^+ + SiD_4 \qquad (27)$$

The only ion molecule reaction observed in Me_2CF_2 (6×10^{-7} Torr) involves fluoride transfer to the $MeCF_2^+$ fragment ion, producing the more stable Me_2CF^+ carbonium ion (eq 28; $k = 7.9 \times 10^{-10}$ $cm^3 molecule^{-1} s^{-1}$).

$$MeCF_2^+ + Me_2CF_2 \rightarrow Me_2CF^+ + MeCF_3 \qquad (28)$$

Figure 3 presents the temporal variation of relative ion abundance in a 2.1:1 mixture of $MeSiD_3$ and Me_2CF_2 at a total pressure of 1.6×10^{-6} Torr following a 20 eV, 10 ms electron beam pulse. Double resonance experiments[9, 10] indicate that the sequence of reactions represented by Scheme III occurs in this system. Excluding

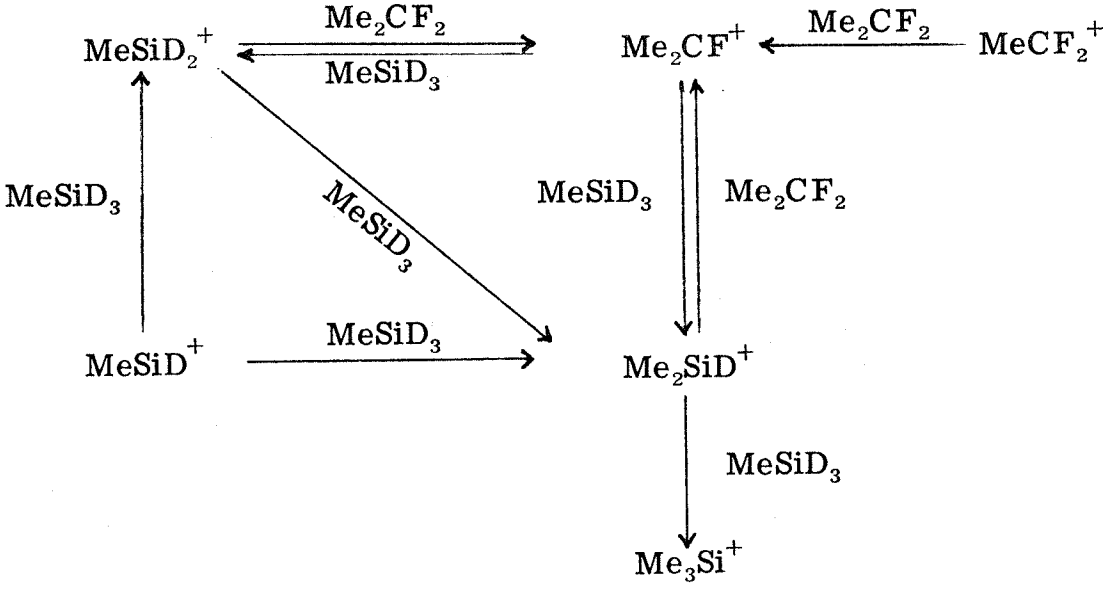

Scheme III

the ion chemistries of $MeSiD_3$ and Me_2CF_2 alone, the $MeSiD_2^+$, Me_2CF^+, and Me_2SiD^+ ions act as chain carriers for process 29, so

$$MeSiD_2^+ \underset{MeSiD_3}{\overset{Me_2CF_2}{\rightleftharpoons}} Me_2CF^+ \underset{Me_2CF_2}{\overset{MeSiD_3}{\rightleftharpoons}} Me_2SiD^+ \qquad (29)$$

that at relatively long ion trapping times (> 400 ms) an equilibrium exists between these three relative ion populations (Figure 3). Reaction

FIGURE 3

Temporal variation of relative ion abundance in a 2.1:1 mixture of $MeSiD_3$ and Me_2CF_2 at a total pressure of 1.6×10^{-6} Torr following a 20 eV, 10 ms electron beam pulse.

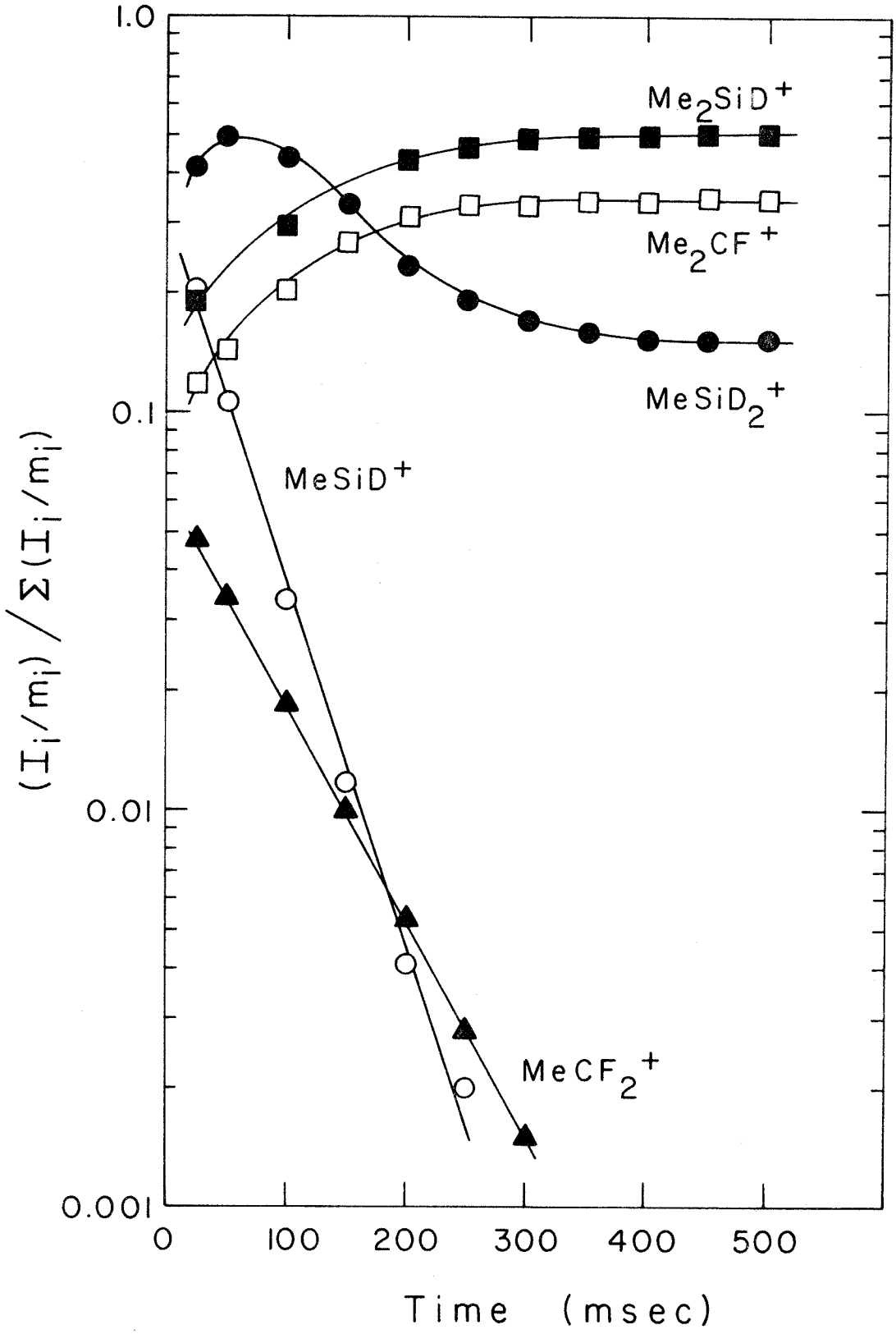
1.0
0.1
0.01
0.001
0
100
200
300
400
500
Time (msec)
$(I_i/m_i) / \Sigma(I_i/m_i)$
Me_2SiD^+
Me_2CF^+
$MeSiD_2^+$
$MeSiD^+$
$MeCF_2^+$

29 suggests a complicated process in which the overall result is the interconversion of Si–D and C–F bonds into Si–F and C–H bonds. The chain reaction is interrupted by the condensation reaction 27 of Me_2SiD^+ to Me_3Si^+.

Mixture of Me_2SiH_2 with Me_2CF_2. The 12 eV mass spectrum of Me_2SiH_2 at 5.2×10^{-7} Torr reveals the following ions; $MeSiH^+$ (21%), $MeSiH_2^+$ (5%), Me_2Si^+ (41%), and Me_2SiH^+ (33%), in good agreement with the previously reported mass spectrum.[41, 42] In the trapped ion mass spectrum of Me_2SiH_2 at the same experimental conditions, reactions 30-35 are observed. Hydride transfer reactions are facile,

$$MeSiH^+ + Me_2SiH_2 \longrightarrow Me_2SiH^+ + MeSiH_2 \quad (30)$$

$$MeSiH_2^+ + Me_2SiH_2 \longrightarrow Me_2SiH^+ + MeSiH_3 \quad (31)$$

$$Me_2Si^+ + Me_2SiH_2 \xrightarrow{96\%} Me_2SiH^+ + Me_2SiH \quad (32)$$

$$Me_2Si^+ + Me_2SiH_2 \xrightarrow{4\%} Me_3Si_2H_2^+ + Me \quad (33)$$

$$Me_2SiH^+ + Me_2SiH_2 \xrightarrow{95\%} Me_3Si^+ + MeSiH_3 \quad (34)$$

$$Me_2SiH^+ + Me_2SiH_2 \xrightarrow{5\%} Me_4Si_2H_3^+ \quad (35)$$

and all produce the Me_2SiH^+ ion (eq 30-32).[42] The Me_3Si^+ ion is generated in reaction 34 by the exchange of CH_3 for H_2.[42] Two reactions which lead to low yields ($< 3\%$ of the total ionization) of binuclear silicon ions (eq 33 and 35) are also observed.

Chain reactions involving four carriers are observed in a mixture of Me_2SiH_2 with Me_2CF_2. Figure 4 presents the temporal variation

FIGURE 4

Temporal variation of Me_2CF^+, Me_2SiH^+, Me_3Si^+, and Me_2CH^+ signal intensities following a 14 eV, 10 ms electron beam pulse in a 6.1:1 mixture of Me_3SiH and Me_2CF_2 at 7.8×10^{-7} Torr total pressure.

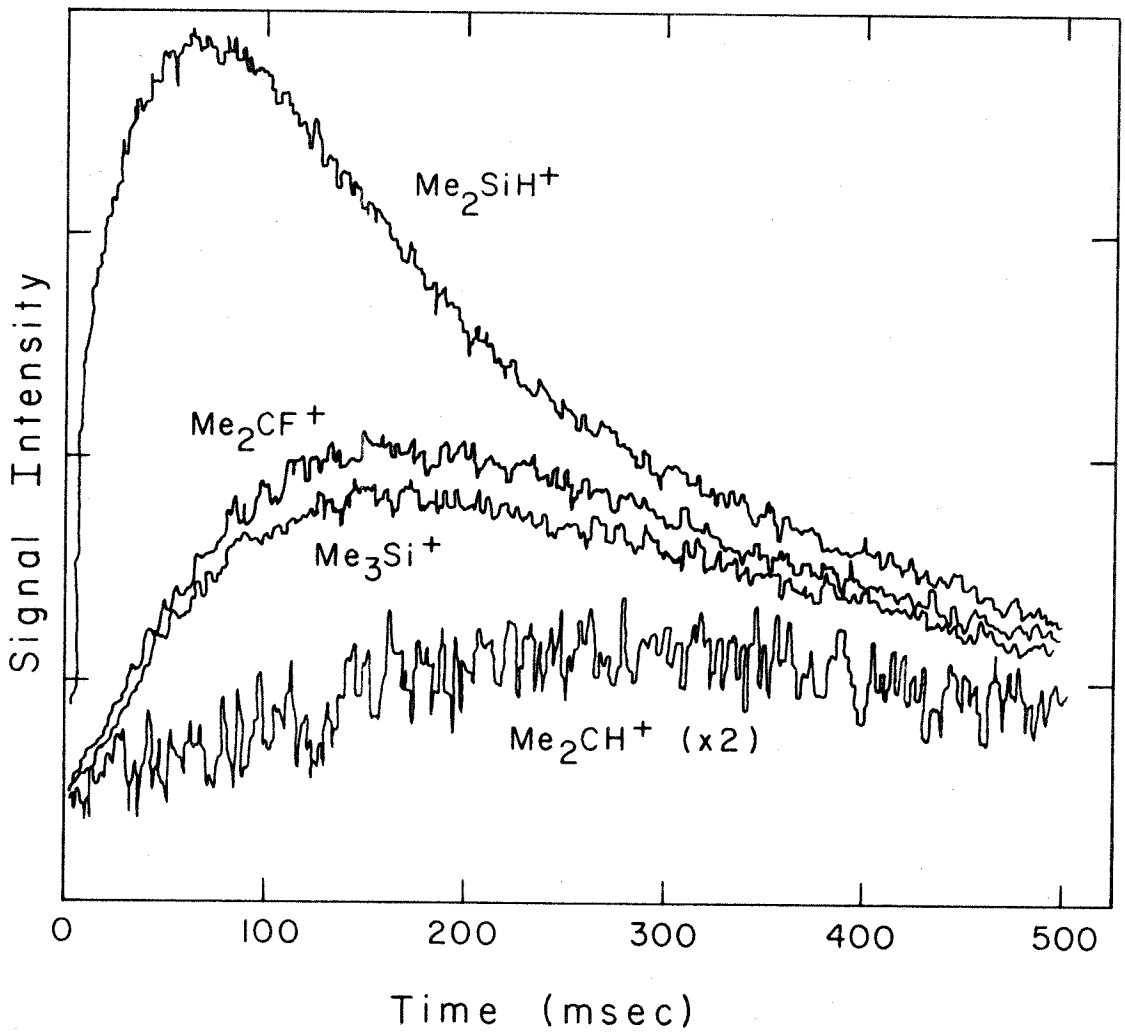
Signal Intensity
Me_2SiH^+
Me_2CF^+
Me_3Si^+
Me_2CH^+ (x2)
0
100
200
300
400
500
Time (msec)

in relative signal intensity in a 6.1:1 mixture of Me_2SiH_2 and Me_2CF_2 at a total pressure of 7.8×10^{-7} Torr following a 14 eV, 10 ms electron beam pulse. The chain reactions occurring in this system are summarized by Scheme IV.

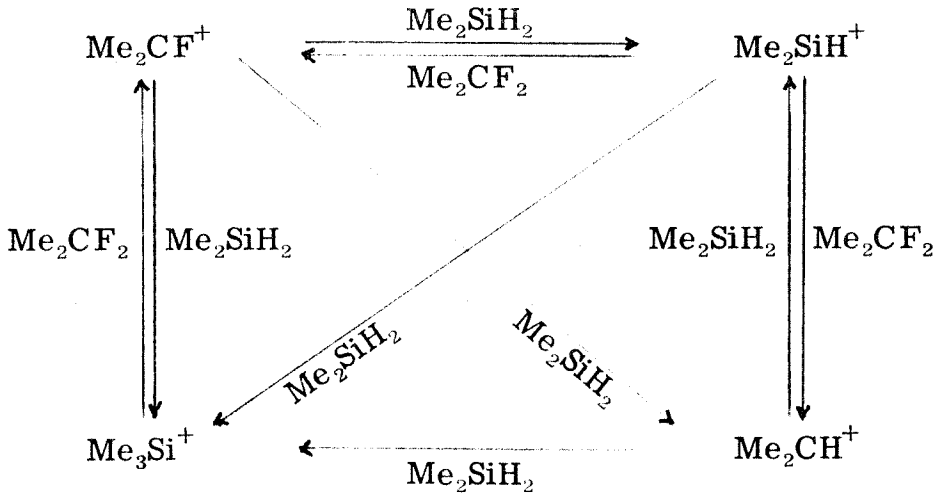

Scheme IV

Mixture of Me_3SiH and Me_2CF_2. Data which reveal a fourth example of ionic chain reactions in the gas phase are presented in Figure 5. In a 1.1:1 mixture of Me_3SiH and Me_2CF_2 at a total pressure of 5.3×10^{-7} Torr, reactions 36 and 37 are observed following a 12 eV,

$$Me_2CF^+ + Me_3SiH \rightarrow Me_3Si^+ + Me_2CFH \quad (36)$$

$$Me_3Si^+ + Me_2CF_2 \rightarrow Me_2CF^+ + Me_3SiF \quad (37)$$

10 ms electron beam pulse. Product ions which result from condensation reactions and which would terminate the chain reactions 36 and

FIGURE 5

Temporal variation of Me_3Si^+ and Me_2CF^+ signal intensities in a 1.1:1 mixture of Me_3SiH and Me_2CF_2 at a total pressure of 5.3×10^{-7} Torr following a 12 eV, 10 ms electron beam pulse.

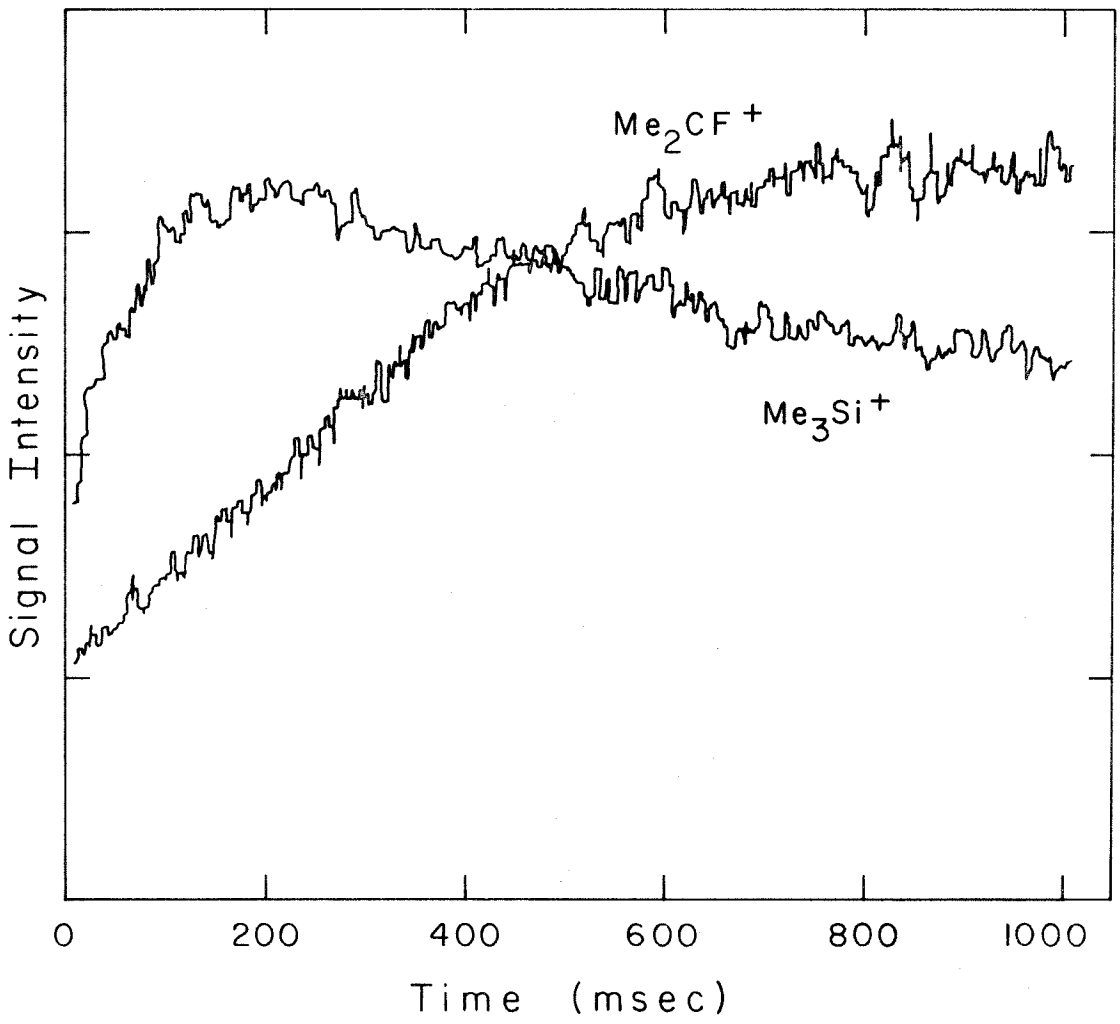
Me2CF+
Me3Si+
Signal Intensity
0
200
400
600
800
1000
Time (msec)

37 are not observed in this mixture, even at long ion trapping times ($\approx$ 2000 ms) and relatively high pressures ($\sim 2 \times 10^{-6}$ Torr). In the pair of coupled reactions 36 and 37, double resonance ion ejection of either ionic species leads to the decay in relative abundance of the other.[13-15, 43] From the data presented in Figure 6, obtained after a delay of 700 ms, the rate of hydride transfer (eq 36) is established as $k = 2.5 \times 10^{-10}$ $cm^3 molecule^{-1} s^{-1}$ and the rate of fluoride transfer (eq 39) as $k = 2.9 \times 10^{-10}$ $cm^3 molecule^{-1} s^{-1}$. As is observed for CF_4 and SiH_4, the overall chain reaction involves interchange of F and H on carbon and silicon centers (eq 38) and is exothermic by 39 kcal/mol.[27,44]

$$Me_3SiH + Me_2CF_2 \rightarrow Me_3SiF + Me_2CFH \qquad (38)$$

Conclusions

As conjectured, the above observations confirm that ionic chain reactions occur in mixtures of fluorocarbons with silanes which interchange fluorine and hydrogen on carbon and silicon centers. The processes are generally not simple since multiple interchanges occur in a single collision.[34, 35] In addition, side reactions frequently inhibit the process by consuming the chain carriers. In the mixture of Me_3SiH with Me_2CF_2, absence of hydrogen bonded to the reactive center of the chain carriers mitigates against multiple interchanges which contribute to the complexity of other systems. It is also noted that the reactions discussed were examined at low pressure where clustering is not prevalent. At higher pressures, formation of clusters by the chain carrier might inhibit the process. Freeman has reported ionic

FIGURE 6

Logarithmic plot of relative signal intensities for Me_3Si^+ and Me_2CF^+ following continuous ejection after 700 ms. The slopes of these lines and the known pressures of the neutral species give the rate constants for H^- and F^- transfer in a mixture of Me_3SiH and Me_2CF_2 (eq 36 and 37, respectively).

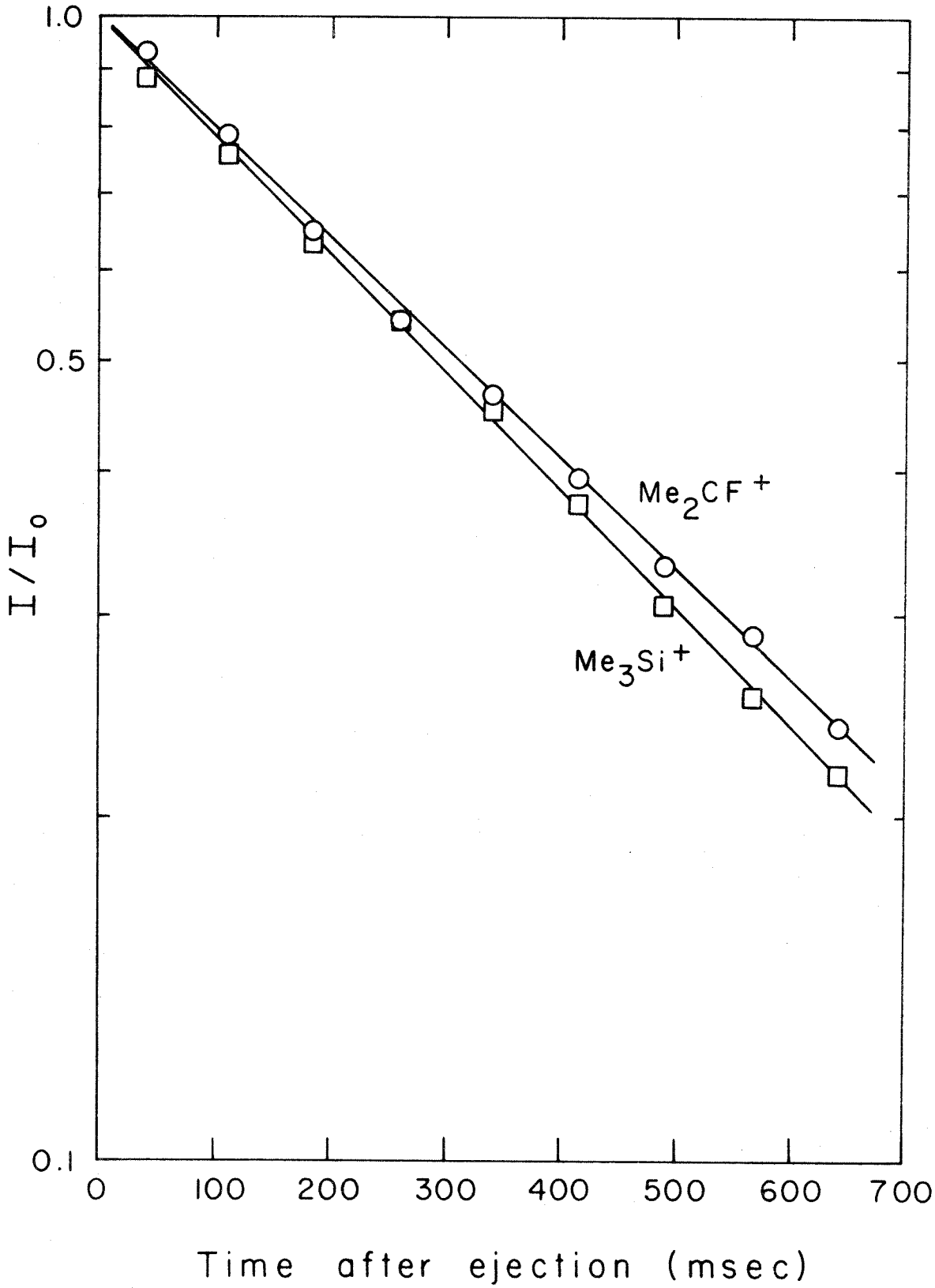
1.0
0.5
0.1
I / I₀
Me₂CF⁺
Me₃Si⁺
0
100
200
300
400
500
600
700
Time after ejection (msec)

chain reactions which exhibit an activation energy at higher pressures, which is generally associated with the breaking up of cluster ions.[2] It would be of interest to examine the chain reactions considered in the present work under radiolytic conditions in both gas and solution phases.[45, 46]

The data in Figure 1 can be used to suggest many other pairs of silanes and fluorocarbons for which ionic chain reactions should occur. The considerations applied to these systems can be generally extended to predict many processes involving mixed halide and hydride transfer between different centers. This is particularly true for most metal ions since metal-halogen bonds are often stronger than carbon-halogen bonds, and metal-hydrogen bonds are almost always weaker than carbon-hydrogen bonds.[47]

Acknowledgment. This research was supported in part by the Energy Research and Development Administration under Grant No. E(04-3)767-8.

References and Notes

(1) Present address: Monsanto Polymer and Petrochemical Company, Petrochemical Research and Development, 800 N. Lindbergh Blvd., St. Louis, Mo. 63166.

(2) For a discussion of the importance of radiation-induced ionic chain reactions in gases, see K. Bansal and G. R. Freeman, Radiat. Res. Rev., 3, 209 (1971).

(3) S. O. Thompson and O. A. Schaefer, J. Am. Chem. Soc., 80, 553 (1958).

(4) O. A. Schaefer and S. O. Thompson, Radiat. Res., 10, 671 (1959).

(5) A. R. Anderson, in "Fundamental Processes in Radiation Chemistry", P. Ausloos, ed., Wiley-Interscience, New York, N.Y., 1968, Chapter 5.

(6) T. Terao and R. A. Back, J. Phys. Chem., 73, 3884 (1969).

(7) J. L. Beauchamp, Adv. Mass Spectrom., 6, 717 (1974).

(8) T. B. McMahon, P. G. Miasek, and J. L. Beauchamp, Int. J. Mass Spectrom. Ion Phys., 21, 63 (1976).

(9) For recent reviews of ion cyclotron resonance spectroscopy, see J. L. Beauchamp, Annu. Rev. Phys. Chem., 22, 527 (1971); T. A. Lehman and M. M. Bursey, "Ion Cyclotron Resonance Spectrometry", Wiley, New York, N.Y., 1976.

(10) B. S. Freiser, T. B. McMahon, and J. L. Beauchamp, Int. J. Mass Spectrom. Ion Phys., 12, 249 (1973).

(11) T. B. McMahon and J. L. Beauchamp, Rev. Sci. Instrum., 43, 509 (1972).

(12) J. M. Dawson, H. C. Kim, D. Arnush, B. D. Fried, R. W. Gould, L. O. Heflinger, C. F. Kennel, T. E. Romesser, R. L. Stenzel, A. Y. Wong, and R. F. Wuerker, Phys. Rev. Lett., 37, 1547 (1976).

(13) T. B. McMahon, R. J. Blint, D. P. Ridge, and J. L. Beauchamp, J. Am. Chem. Soc., 94, 8934 (1972).

(14) R. J. Blint, T. B. McMahon, and J. L. Beauchamp, J. Am. Chem. Soc., 96, 1269 (1974) and references 25-29 contained therein.

(15) J. L. Beauchamp and J. Y. Park, J. Phys. Chem., 80, 575 (1976).

(16) J. L. Beauchamp, in "Interactions Between Ions and Molecules", P. Ausloos, ed., Plenum, New York, N.Y., 1975, pp. 413-444.

(17) W. J. Holtslander and G. R. Freeman, Can. J. Chem., 45, 1661 (1967).

(18) J. L. Franklin, ed., "Ion-Molecule Reactions", Vols. 1 and 2, Plenum Press, New York, N.Y., 1972.

(19) S. G. Lias and P. Ausloos, "Ion-Molecule Reactions. Their Role in Radiation Chemistry", Amer. Chem. Soc., Washington, D.C., 1975.

(20) G. A. Olah and P. v. R. Schleyer, ed., "Carbonium Ions", Vol. I, Interscience, New York, N.Y., 1968, and references contained therein.

(21) W. G. Henderson, D. Holtz, J. L. Beauchamp, and R. W. Taft, J. Am. Chem. Soc., 94, 4728 (1972).

(22) M. Taagepera, W. G. Henderson, R. T. C. Brownlee, D. Holtz, J. L. Beauchamp, and R. W. Taft, J. Am. Chem. Soc., 94, 1369 (1972).

(23) E. M. Arnett, F. M. Jones III, M. Taagepera, W. G. Henderson, J. L. Beauchamp, D. Holtz, and R. W. Taft, J. Am. Chem. Soc., 94, 4727 (1972).

(24) R. D. Wieting, R. H. Staley, and J. L. Beauchamp, J. Am. Chem. Soc., 96, 7552 (1974).

(25) M. K. Murphy and J. L. Beauchamp, J. Am. Chem. Soc., 98, 5781 (1976) and references 13-23 contained therein.

(26) M. K. Murphy, R. R. Corderman, and J. L. Beauchamp, to be submitted for publication.

(27) M. K. Murphy, Ph.D. Thesis, California Institute of Technology, Pasadena, California, 1976.

(28) F. P. Lossing, Bull. Soc. Chim. Belg., 81, 125 (1972); F. P. Lossing and G. P. Semeluk, Can. J. Chem., 48, 955 (1970).

(29) M. Krauss, J. A. Walker, and V. H. Diebler, J. Res. Nat. Bur. Stand., A72, 281 (1968).

(30) G. Distefano, Inorg. Chem., 9, 1919 (1970).

(31) M. K. Murphy and J. L. Beauchamp, J. Am. Chem. Soc., 99, 2085 (1977).

(32) A. D. Williamson, P. R. LeBreton, and J. L. Beauchamp, J. Am. Chem. Soc., 98, 2705 (1976).

(33) R. R. Corderman and J. L. Beauchamp, unpublished results.

(34) J. R. Krause and F. W. Lampe, J. Am. Chem. Soc., 98, 7826 (1976).

(35) J. R. Krause and F. W. Lampe, J. Phys. Chem., 81, 281 (1977).

(36) R. H. Wyatt and J. L. Beauchamp, unpublished results.

(37) T.-Y. Yu, T. M. H. Cheng, V. Kempter, and F. W. Lampe, J. Phys. Chem., 76, 3321 (1972); W. N. Allen, T. M. H. Cheng, and F. W. Lampe, ibid., 66, 3371 (1977).

(38) G. W. Stewart, J. M. S. Henis, and P. P. Gasper, J. Chem. Phys., 58, 890 (1973); J. M. S. Henis, G. W. Stewart, M. K. Tripodi, and P. P. Gasper, ibid., 57, 389 (1972).

(39) F. S. Dainton, "Chain Reactions: An Introduction", Methuen, London, 1966.

(40) P. Potzinger and F. W. Lampe, J. Phys. Chem., 74, 587 (1970); T. M. Mayer and F. W. Lampe, ibid., 78, 2422 (1974).

(41) G. P. van der Kelen, O. Volders, H. van Onckelen, and Z. Eeckhaut, Z. Anorg. Allg, Chem., 338, 106 (1965).

(42) P. Potzinger and F. W. Lampe, J. Phys. Chem., 75, 13 (1971).

(43) R. H. Staley and J. L. Beauchamp, J. Chem. Phys., 62, 1998 (1975).

(44) For a discussion of the problems involved in determination of thermochemical data describing organosilicon compounds and ionic species derived from them, see: S. Tannenbaum, J. Am. Chem. Soc., 76, 1027 (1954); I. M. T. Davidson and I. L. Stephenson, J. Organomet. Chem., 7, P24 (1967); M. F. Lappert, J. B. Pedley, J. Simpson, and T. R. Spaulding, J. Organomet. Chem., 29, 195 (1971).

(45) M. G. Robinson and G. R. Freeman, Can. J. Chem., 51, 1010 (1973).

(46) J. F. Schmidt and F. W. Lampe, J. Phys. Chem., 73, 2706 (1969).

(47) B. deB. Darwent, "Bond Dissociation Energies of Simple Molecules", Nat. Stand. Ref. Data Ser. Nat. Bur. Stand., 31, 1971.

CHAPTER VII

Photoionization Mass Spectrometry of the Methylsilanes $(CH_3)_nH_{4-n}Si$ (n = 0-3)

Reed R. Corderman and J. L. Beauchamp

Contribution No. 5545 from the Arthur Amos Noyes Laboratory of Chemical Physics, California Institute of Technology, Pasadena, California 91125

Abstract

Photoionization efficiency curves for the low energy fragment ions $(P-H)^+$, $(P-H_2)^+$, and $(P-CH_4)^+$ for the series of methyl substituted silanes $(CH_3)_nH_{4-n}Si$ (n = 0 - 3) are reported. Appearance potentials of 12.15 ± 0.05, 11.27 ± 0.10, 10.92 ± 0.05, and 10.30 ± 0.03 eV are determined for the siliconium ion fragments SiH_3^+, $MeSiD_2^+$, Me_2SiH^+, and Me_3Si^+, respectively, arising from H loss. These data are interpreted in terms of the thermochemistry of the various ionic and neutral silicon species, and afford accurate calculation of hydride affinities, $D(R_3Si^+-H^-)$, of 261.3, 240.1, 232.9, and 217.6 kcal/mol for the siliconium ions SiH_3^+, $MeSiD_2^+$, Me_2SiH^+, and Me_3Si^+, respectively. These values are 15-50 kcal/mol lower than the analogous carbonium ions.

Introduction

Recent studies from this laboratory of the positive ion chemistry of methylsilanes utilizing ion cyclotron resonance techniques[1] have provided information regarding the relative stabilities of methyl substituted siliconium ions, $(CH_3)_nH_{3-n}Si^+$ (n = 0 - 3), in the absence of complicating solvation phenomena.[2,3] It was shown that methyl substituents effect variations in siliconium ion stabilities, $H_3Si^+ < MeSiH_2^+ < Me_2SiH^+ < Me_3Si^+$, for hydride ion as the reference base, paralleling trends previously observed in the analogous series of carbonium ions. Further, investigations of hydride transfer reactions between substituted carbonium and siliconium ions have shown that siliconium ions are substantially more stable than their carbon analogues. The more complete ion stability order (with H^- as the reference base), $CH_3^+ < CH_3CH_2^+ < SiH_3^+ < (CH_3)_2CH^+ < CH_3SiH_2^+ < (CH_3)_2SiH^+ < (CH_3)_3C^+ < (CH_3)_3Si^+$, has been established.[2,3]

Accurate carbonium ion heats of formation, obtained principally from high-resolution electron and photon impact mass spectrometry,[4-6] have been used to calculate quantitative hydride affinities of carbonium ions. These values serve to bracket the siliconium ion stabilities within known bounds. Although some thermochemical data describing methylsilyl cations are available from electron impact mass spectral studies,[7,8] the experimental uncertainties in these low resolution experiments make comparison with carbonium ions somewhat unreliable. Photoionization mass spectrometry (PIMS) affords accurate determination of appearance potentials for fragmentation processes,

with threshold resolution greater than conventional electron impact techniques. In the present report photoionization efficiency curves are presented for the low energy siliconium ion fragments produced from photoionization of the methylsilanes, $(CH_3)_nH_{4-n}Si$ (n = 0 - 3). The yield of molecular ions from most of the methylsilanes is so low as to preclude accurate measurement of their ionization potentials in this study.[8] Results from a recent investigation of ions derived from $(CH_3)_4Si$ are utilized in the present work.[9] Heats of formation and hydride affinities of siliconium ions derived from these data permit a detailed evaluation of the effects of methyl-substitution α to carbon and silicon charge centers.

Experimental

The Caltech-Jet Propulsion Laboratory photoionization mass spectrometer used in this study has been described in detail elsewhere.[10] A MgF_2 coated grating blazed at 1200 Å ruled with 1200 lines mm^{-1} was used in first order in the present experiments. The sample pressure (typically 1×10^{-4} Torr) was measured with a MKS Baratron Model 90H1 capacitance manometer. Other pertinent operating conditions include: source temperature, ambient (20-25°C); resolution, 2 Å FWHM; ion energy for mass analysis, 10.0 eV, and repeller field, 0.3 V cm^{-1}. In order to minimize ion-molecule reactions in the ion source, measurements were also made at higher repeller fields (1-2 V cm^{-1}), resulting in shorter ion residence times of ~ 5 μsec. The hydrogen many-line spectrum was utilized in the wavelength range examined (960 - 1300 Å). Ion intensities were

corrected for ^{28}Si (92.2%), ^{29}Si (4.7%), and ^{30}Si (3.1%) isotope contributions.[11] Unless explicitly stated, all ion notations refer to the ^{28}Si isotope.

Samples of SiH_4, Me_2SiH_2, and Me_3SiH are available from commercial sources. $MeSiD_3$ was graciously provided by Professors F. S. Rowland and M. J. Molina. Before use each sample was degassed by repeated freeze-pump-thaw cycles.

Results

SiH_4. Photoionization efficiency curves for the molecular ion and the two low energy fragment ions SiH_3^+ and SiH_2^+ for photon energies between 11.0 eV and 13.0 eV are presented in Figure 1. These are the only ions observed in this energy range. The onset for molecular ion production is obscured near threshold by a structural feature which is very probably vibrational in origin, since at 300°K about 6% of the molecules will be excited into the ν_2 (978 cm^{-1}, doubly degenerate) and ν_4 (910 cm^{-1}, triply degenerate) vibrational modes.[12] Alternatively, autoionization may be occurring to produce the wide band of low photoionization efficiency centered at approximately 1077 Å (11.51 eV). The location of the trough in the photoionization efficiency at approximately 1060±10 Å (11.69±0.10 eV) is in reasonable agreement with the adiabatic ionization potential measured by He(I) photoelectron spectroscopy for silane of 11.66 eV.[13] The photoionization efficiency rises with photon energy as higher vibrational levels of the parent ion ground electronic state are populated.

FIGURE 1

Photoionization efficiency curves for SiH_4^+, SiH_2^+, and SiH_3^+ generated from SiH_4 in the photon energy range 11.0 - 13.0 eV.

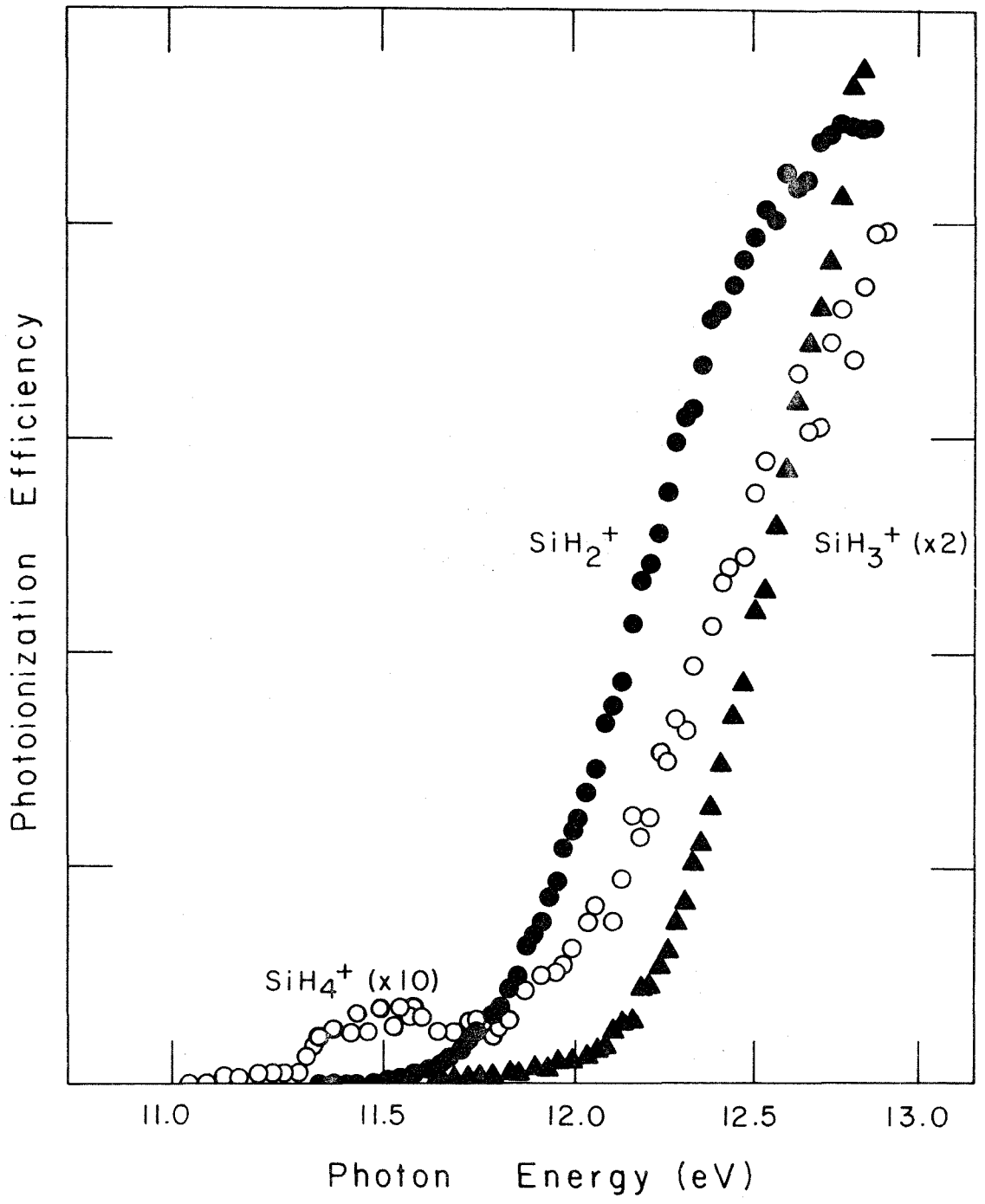
Photoionization Efficiency
SiH2+
SiH3+ (x2)
SiH4+ (x10)
11.0
11.5
12.0
12.5
13.0
Photon Energy (eV)

Fragmentation producing SiH_2^+ by loss of H_2 from the molecular ion (process 1) exhibits an onset at 1050 ± 2 Å, corresponding to an

$$SiH_4 + h\nu \begin{cases} \longrightarrow SiH_2^+ + H_2 & (1) \\ \longrightarrow SiH_3^+ + H & (2) \end{cases}$$

appearance potential of 11.81 ± 0.03 eV. Similarly, the SiH_3^+ ion is produced by fragmentation of the molecular ion (process 2) with an onset at 1020 ± 3 Å, or 12.15 ± 0.05 eV. Table I summarizes the observed photoionization thresholds and ion enthalpies of formation calculated therefrom. Table I includes recent literature values for the various ion heats of formation for comparison with the present results. These have been determined mainly from similar, but less accurate electron impact studies.[7] Also included in Table I are the enthalpies of formation of neutrals utilized in these calculations,[7a] and the adiabatic ionization potentials determined using He(I) photoelectron spectroscopy.[7a]

$MeSiD_3$. Photoionization efficiency curves for $MeSiD_2^+$, $MeSiD^+$, and SiD_2^+ produced by the photoionization of d_3-methylsilane between 10.5 and 12.0 eV photon energies are presented in Figure 2. The photoionization efficiency curve for ions of m/e 49 (not shown) is coincident with, and approximately 3% of, the abundance of the photoionization efficiency curve for $MeSiD_2^+$, and is attributed to $Me^{30}SiD_2^+$. This result indicates that the molecular cation, $MeSiD_3^+$, is not observed, most likely because the transition to the ground state of the ion has a very low probability,[8] analogous to the threshold behavior

Table I. Photoionization Data for Methylsilanes

Molecule	Ion	IP or AP (eV)	$\Delta H^{\circ}_{f_{298}}$ (kcal/mol) present work	literature[a]
SiH_4				8.2
	SiH_4^+	11.69 ± 0.10	277.8	277.3
	SiH_2^+	11.81 ± 0.03	280.4	281.3
	SiH_3^+	12.15 ± 0.05	236.3	238.9
CH_3SiD_3				-4.3
	$CH_3SiD_3^+$	10.7[a]	--	241.8
	CH_3SiD^+	11.16 ± 0.03	253.0	257.9
	$CH_3SiD_2^+$	11.27 ± 0.10	202.6	215.0
	SiD_2^+	11.42 ± 0.03	277.0	278.1
$(CH_3)_2SiH_2$				-16.8
	$(CH_3)_2SiH_2^+$	10.3[a]	--	220.1
	$(CH_3)_2Si^+$	10.58 ± 0.03	227.1	229.5
	CH_3SiH^+	10.74 ± 0.03	248.8	256.4
	$(CH_3)_2SiH^+$	10.92 ± 0.05	182.9	186.9
$(CH_3)_3SiH$				-29.6
	$(CH_3)_3SiH^+$	9.9[a]	--	198.1
	$(CH_3)_2Si^+$	10.14 ± 0.03	222.2	229.8
	$(CH_3)_3Si^+$	10.30 ± 0.03	155.7	160.3
	$(CH_3)_2SiH^+$	10.82 ± 0.10	183.9	187.3
$(CH_3)_4Si$				-42.4[a]
	$(CH_3)_4Si^+$	9.80 ± 0.03[b]	--	183.5[b]
	$(CH_3)_3Si^+$	10.03 ± 0.04[b]	--	154.8[b]

Table I: Continued

[a]Unless otherwise noted, all literature values are from Reference 7a.

[b]Reference 9.

FIGURE 2

Photoionization efficiency curves for $MeSiD^+$, $MeSiD_2^+$, and SiD_2^+ generated from $MeSiD_3$ in the photon energy range 10.5 - 12.0 eV.

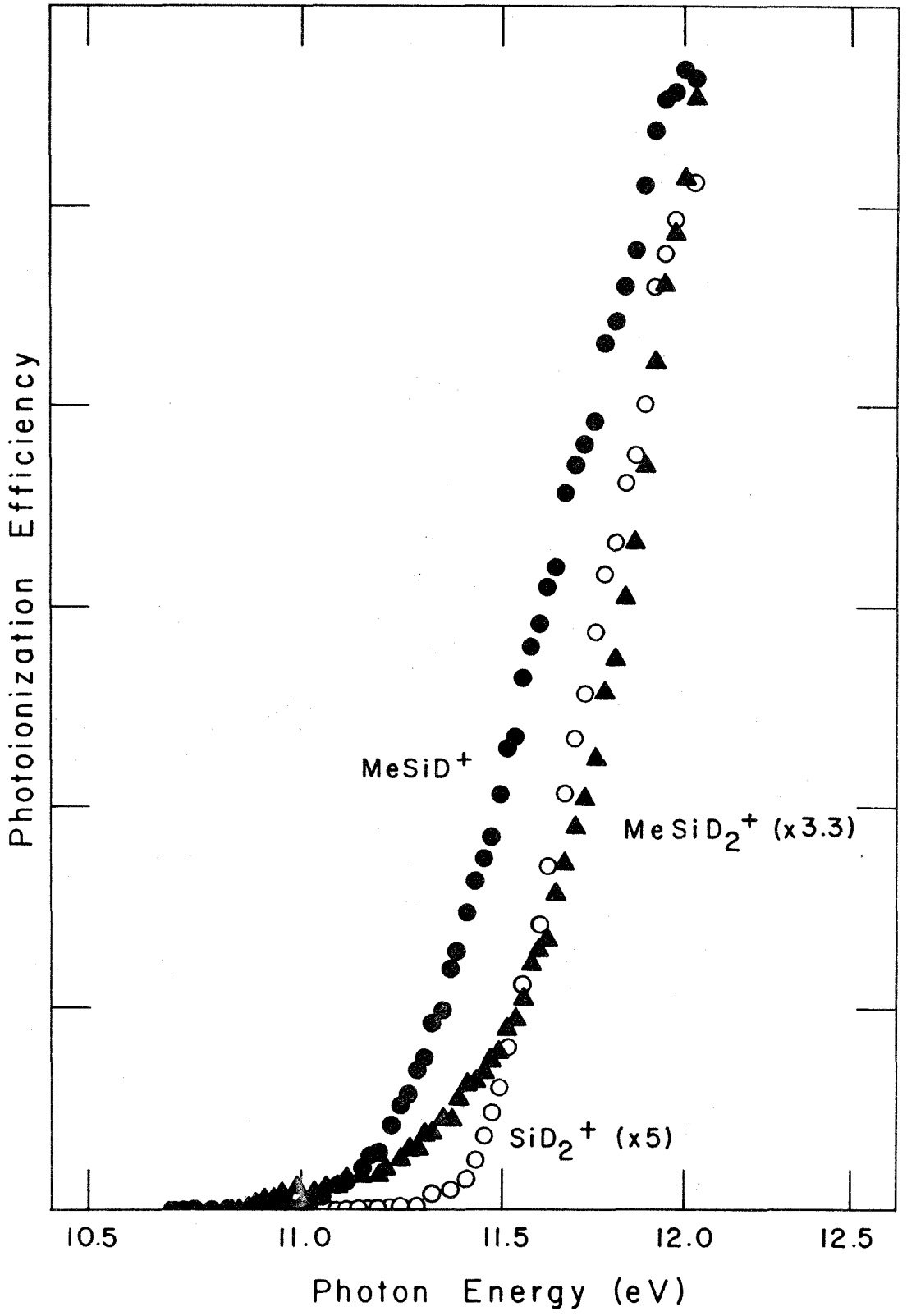
Photoionization Efficiency
MeSiD+
MeSiD2+ (x3.3)
SiD2+ (x5)
10.5
11.0
11.5
12.0
12.5
Photon Energy (eV)

observed for the $C_2H_6^+$ ion from ethane photoionization studies.[5] The lowest energy fragmentation process involves the formation of $MeSiD^+$ with loss of D_2 (eq. 3), which exhibits an onset at 1111 ± 2 Å,

$$MeSiD_3 + h\nu \longrightarrow \begin{cases} MeSiD^+ + D_2 & (3) \\ MeSiD_2^+ + D & (4) \\ SiD_2^+ + CH_3D & (5) \end{cases}$$

or 11.16 ± 0.03 eV. A much more pronounced thermal tail is observed in the photoionization efficiency curve of $MeSiD_2^+$ (eq. 4). The coincidence of the $MeSiD^+$ and $MeSiD_2^+$ curves from 1130 to 1110 Å suggests that the rapid ion-molecule reaction 6 ($k = 9.9 \times 10^{-10}$ cm^3 molecule^{-1} s^{-1})[14] may be partially responsible for the production of $MeSiD_2^+$.

$$MeSiD^+ + MeSiD_3 \rightarrow MeSiD_2^+ + MeSiD_2 \qquad (6)$$

Experiments at high source repeller fields, however, where ion residence times are much reduced, did not appreciably change the appearance of this threshold. Pair process formation of $MeSiD_2^+$ (and D^-) is excluded since this would exhibit a much lower threshold (≈ 1180 Å) than is observed for the direct ionization process (eq. 4). The thermochemical data presented in Table I for $MeSiD_2^+$ is calculated by choosing an onset of 1100 ± 10 Å, or 11.27 ± 0.10 eV. The photoionization efficiency curve for the production of SiD_2^+ by loss of CH_3D from the molecular ion (process 5), exhibits a sharp onset at 1085 ± 2 Å (11.42 ± 0.03 eV).

Me_2SiH_2. Figure 3 presents photoionization efficiency curves for the production of ions from Me_2SiH_2 at photon energies between 10.0 and 12.0 eV. Three ions are observed in this energy range, Me_2Si^+, $MeSiH^+$, and Me_2SiH^+, corresponding to processes 7-9,

$$Me_2SiH_2 + h\nu \longrightarrow \begin{cases} Me_2Si^+ + H_2 & (7) \\ MeSiH^+ + CH_4 & (8) \\ Me_2SiH^+ + H & (9) \end{cases}$$

respectively. As for SiH_4 and $MeSiD_3$, the lowest energy fragmentation process involves loss of H_2 and production of Me_2Si^+, which has an onset at 1172 ± 2 Å (10.58 ± 0.03 eV). At higher energies CH_4 is lost from the molecular ion (eq. 8), resulting in formation of $MeSiH^+$, which exhibits an onset at 1154 ± 2 Å (10.74 ± 0.03 eV). The fragmentation process 9, loss of H from the parent ion, exhibits an onset at 1135 ± 3 Å, yielding 10.92 ± 0.05 eV for the appearance potential of Me_2SiH^+ from dimethylsilane. As in d_3-methylsilane, the molecular cation is not observed.[8]

Me_3SiH. Photoionization efficiency curves for Me_2Si^+, Me_3Si^+, and Me_2SiH^+ generated in trimethylsilane between 9.5 and 11.5 eV photon energies are shown in Figure 4. As for the methylsilanes previously mentioned, the lowest energy fragmentation involves production of Me_2Si^+ by loss of CH_4 from the molecular ion (eq. 10), and

$$Me_3SiH + h\nu \longrightarrow \begin{cases} Me_2Si^+ + CH_4 & (10) \\ Me_3Si^+ + H & (11) \\ Me_2SiH^+ + CH_3 & (12) \end{cases}$$

FIGURE 3

Photoionization efficiency curves for Me_2Si^+, $MeSiH^+$, and Me_2SiH^+ generated from Me_2SiH_2 in the photon energy range 10.0 - 12.0 eV.

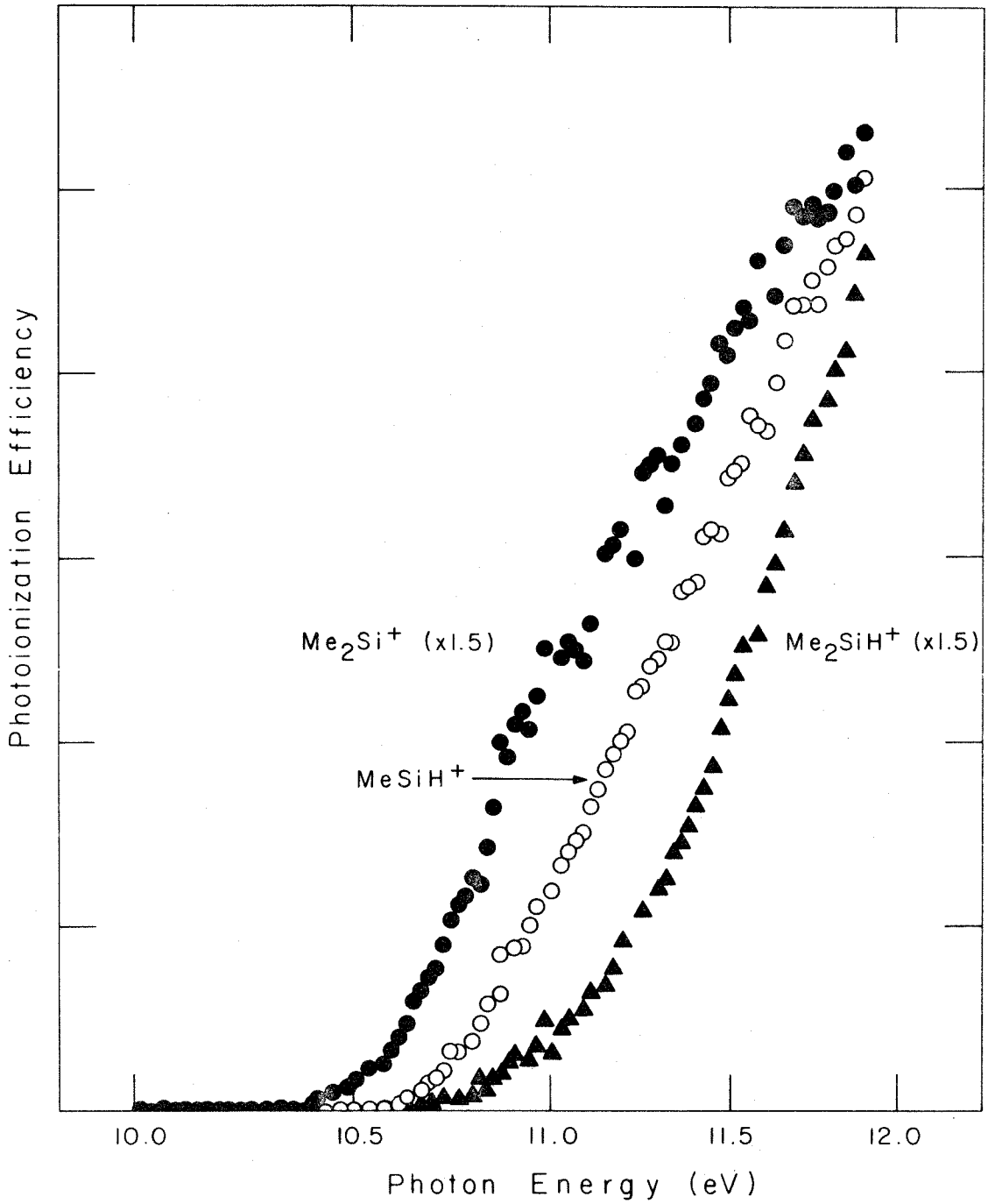
Photoionization Efficiency
Me2Si+ (x1.5)
Me2SiH+ (x1.5)
MeSiH+
10.0
10.5
11.0
11.5
12.0
Photon Energy (eV)

FIGURE 4

Photoionization efficiency curves for Me_2Si^+, Me_3Si^+, and Me_2SiH^+ generated from Me_3SiH in the photon energy range 9.5 - 11.5 eV.

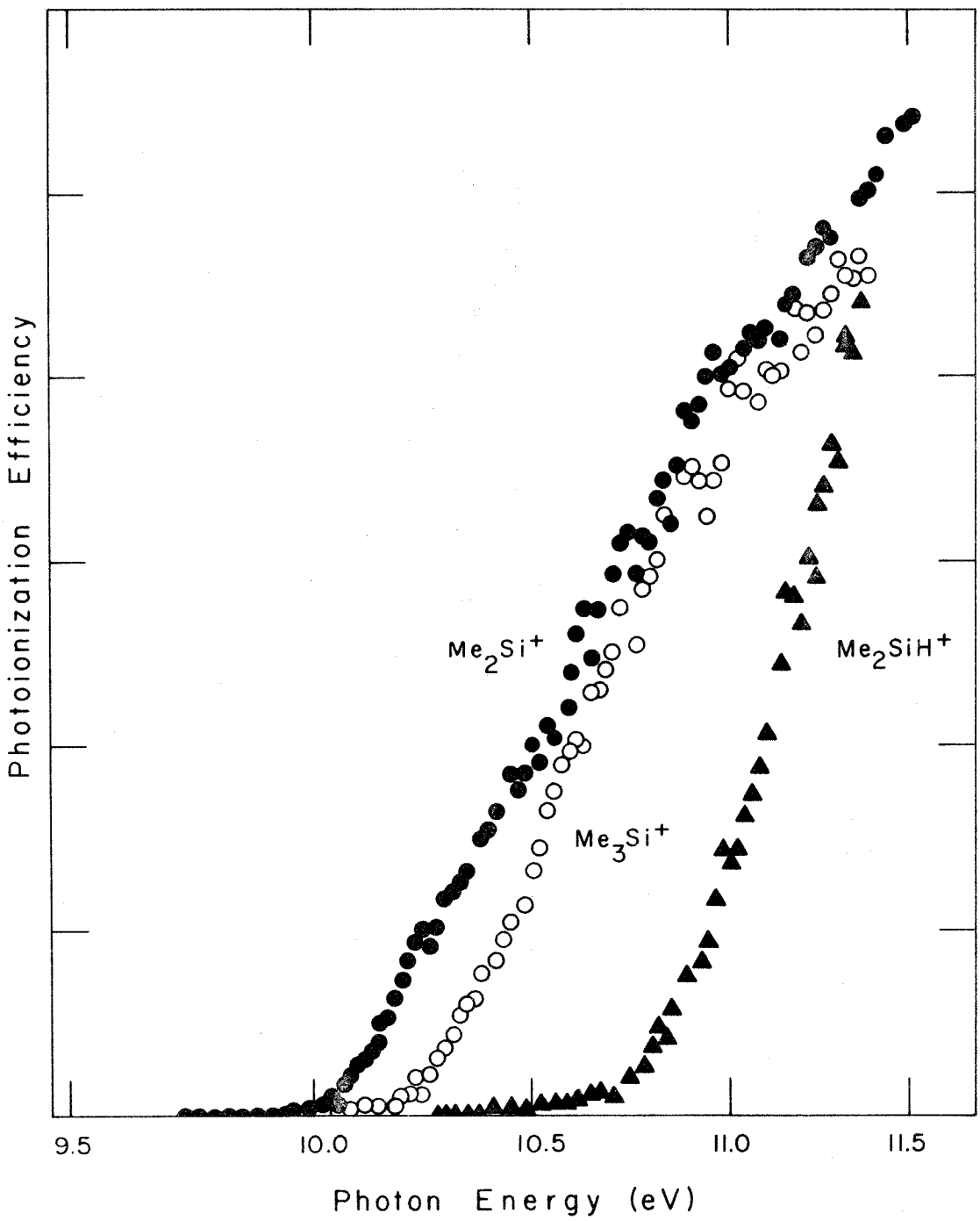
Photoionization Efficiency
Me2Si+
Me2SiH+
Me3Si+
9.5
10.0
10.5
11.0
11.5
Photon Energy (eV)

exhibits a sharp threshold at 1222 ± 2 Å, or 10.14 ± 0.03 eV. The onset for formation of the Me_3Si^+ ion (eq. 11) also displays a sharp threshold at 1204 ± 2 Å, or 10.30 ± 0.03 eV. The threshold for production of Me_2SiH^+ (eq. 12) exhibits a larger thermal tail than either of the thresholds for formation of Me_2Si^+ or Me_3Si^+. The quoted appearance potential for this species in Table I (1151 ± 10 Å, or 10.77 ± 0.10 eV) is obtained by extrapolation of the linearly rising portion of the Me_2SiH^+ photoionization efficiency curve to zero photoionization efficiency. The observed thresholds and derived ion heats of formation are summarized in Table I.

Discussion

The interpretation of observed photoionization thresholds requires consideration of the contribution of thermal internal energy of the neutral to dissociation processes and of the possibility of significant kinetic shifts. These phenomena have been discussed in detail elsewhere;[9,15] we note only that consistency of the present results with implications of hydride transfer reactions of the methylsiliconium ions[2,3] suggests that the measured thresholds are reasonably accurate. Significant kinetic shifts are not expected to be associated with the facile fragmentation processes reported in Table I, which all occur within 1 eV of the neutral methylsilane ionization potential.

The observed photoionization thresholds (Table I) allow calculation of a variety of ion thermochemical properties. Enthalpies of formation of the methylsilane parent neutral molecules, Me_nSiH_{4-n} (n = 0-4), and methylsilyl radicals, Me_nSiH_{3-n} (n = 0-3), are available from a recent

mass spectrometric determination of bond dissociation energies in a variety of organosilicon compounds.[7a] Standard sources of thermochemical data were employed to obtain various other enthalpies of formation required in these calculations.[16,17]

Siliconium Ion Hydride Affinities. Perhaps the most important results of the present study are the values for the hydride affinities, $D(R_3Si^+-H^-)$, of the four siliconium ions, $(CH_3)_nH_{3-n}Si^+$ (n = 0-3), which are calculated using relationship 13 and presented in Table II.

$$D(R_3Si^+-H^-) = \Delta H_f(R_3Si^+) + \Delta H_f(H^-) - \Delta H_f(R_3SiH) \qquad (13)$$

The calculated values exhibit a marked increase with increasing hydrogen substitution in place of methyl.

Related Thermochemical Properties. Included in Table II are estimates of the excess energy required to fragment molecular ions through loss of H_2, H, and CH_3 from the various molecular ions, denoted as $D(R_3Si^+-X)$ (where X = H_2, H, and CH_3). Calculations of the excess energies necessary to induce Si-X bond breaking in the methylsilane molecular ions using eq. 14 require only a knowledge of relative

$$D(R_3Si^+-X) = AP(R_3Si^+) - IP(R_3SiX) \qquad (14)$$
$$(X = H_2,\ H,\ CH_3)$$

ionization thresholds and do not depend on ΔH_f values of the neutral silanes. The calculated values are small, with loss of H_2 the most favorable, and do not exhibit any trend with increasing methyl substitution. Values for $D(H_3Si^+-CH_3)$ and $D(MeH_2Si^+-CH_3)$, for which direct

Table II. Calculated Thermochemical Properties[a]

Ion (R_3Si^+)	$D(R_3Si^+-H^-)$[b]	$D(R_2Si^+-H_2)$[c]	$D(R_3Si^+-H)$[c]	$D(R_3Si^+-CH_3)$[c]	$\Delta H_f(R_3Si)$	$IP(R_3Si)$[h]
H_3Si^+	261.3	2.8	10.6	28.7[e]	45.6[f]	8.25
$(CH_3)H_2Si^+$	240.1	10.6	13.1	16.7[e]	33.0[f]	7.37
$(CH_3)_2HSi^+$	232.9	6.5	14.3	21.2	21.0[f]	7.02
$(CH_3)_3Si^+$	217.6	5.5 (CH_4)[d]	9.2	5.3	8.2[g]	6.40

[a]Heats of formation and bond dissociation energies are in kcal/mol.

[b]Calculated from eq. 13 in the text using data from Table I.

[c]Calculated from eq. 14 in the text using data from Table I.

[d]Calculated for the process $Me_3SiH^+ \rightarrow Me_2Si^+ + CH_4$.

[e]Calculated from eq. 15 in the text using data from Table I.

[f]Reference 7a.

[g]Calculated from $\Delta H_f(Me_3SiH)$ = -29.6 kcal/mol (reference 7a) and $D(Me_3Si-H)$ = 89.9 kcal/mol (reference 18).

[h]Radical ionization potentials are in eV; calculated from eq. 16 in the text and the data in Table I.

measurements of the appearance thresholds of siliconium ion fragments resulting from CH_3 loss are not available, may be calculated approximately from eq. 15, using the enthalpy of formation data given in Table I.

$$D(R_3Si^+-CH_3) = \Delta H_f(R_3Si^+) + \Delta H_f(CH_3) - \Delta H_f(R_3SiH^+)$$
$$(R_3Si^+ = H_3Si^+,\ MeH_2Si^+) \quad (15)$$

Ionization potentials of the methylsilyl radicals are calculated in a straightforward fashion using equation 16. The value of $D(R_3Si-H)$

$$IP(R_3Si) = AP(R_3Si^+) - D(R_3Si-H) \quad (16)$$

used throughout is $D(Me_3Si-H) = 89.9 \pm 2.6$ kcal/mol, recently obtained in a study of the kinetics of the gas phase reaction between iodine and Me_3SiH.[18]

Comparisons of thermochemical data for trisubstituted methylsilane radicals and ions derived in the present study with literature data for the analogous carbon species and Me_3Si are presented in Table III. These data facilitate interpretation of the effects of methyl and hydrogen substitution on carbon and silicon centers. From the calculated hydride affinities, an ion stability order $CH_3^+ < C_2H_5^+ < SiH_3^+ < (CH_3)_2CH^+ < (CH_3)SiH_2^+ < (CH_3)_3C^+ < (CH_3)_2SiH^+ < (CH_3)_3Si^+$ is predicted. This ordering is entirely consistent with the experimentally observed ordering as discussed in the introduction.

In contrast to the greater stabilities of carbonium ions compared with their siliconium analogues when F^- is taken as the reference base,[2] the hydride affinity data included in Table III show a dramatic reversal. With H^- as the reference base, carbonium ions are consistently less

Table III. Comparison of Thermochemical Properties of Silicon and Carbon Species[a]

	$\Delta H_f(R_3C)$	$\Delta H_f(R_3Si)$[b]	$IP(R_3C)$[c]	$IP(R_3Si)$[b,c]	$\Delta H_f(R_3C^+)$	$\Delta H_f(R_3Si^+)$[d]	$D(R_3C^+-H^-)$[e]	$D(R_3Si^+-H^-)$[b]
H_3M	34.8[f]	45.6	9.82[i]	8.27	261.3	236.3	312.4	261.3
$(CH_3)H_2M$	25.7[g]	33.0	8.30[j]	7.36	217.1	202.6	270.5	240.1
$(CH_3)_2HM$	17.6[g]	21.0	7.55[k]	7.02	191.7	182.9	249.7	232.9
$(CH_3)_3M$	9.3[h]	8.2	6.93[k]	6.36	169.1	154.8	234.7	217.6

[a]Heats of formation and bond dissociation energies are in kcal/mol.

[b]Data from Table II.

[c]Radical ionization potentials are in eV.

[d]Data from Table I.

[e]Calculated from $D(R^+-H^-) = \Delta H_f(R^+) + \Delta H_f(H^-) - \Delta H_f(RH)$, using data in this table, $\Delta H_f(H^-) = 33.2$ kcal/mol (reference 16), and $\Delta H_f(R_3CH)$ from Reference 17.

[f]Reference 7a.

[g]J. A. Kerr, Chem. Rev., 66, 465 (1966).

[h]W. Tsang, J. Phys. Chem., 76, 143 (1972).

[i]W. A. Chupka and C. Lifshitz, J. Chem. Phys., 48, 1109 (1968).

[j]F. A. Houle and J. L. Beauchamp, accepted for publication in Chem. Phys. Lett.

[k]F. P. Lossing and G. P. Semeluk, Can. J. Chem., 48, 955 (1970).

stable than the substitutionally analogous silicon ions. The different ordering of carbonium and siliconium ion stabilities towards H^- can be understood with the aid of eq. 17. Since the silyl and alkyl radical

$$D(R^+ - X^-) = D(R-X) + IP(R) - EA(X) \qquad (17)$$

ionization potentials are quite comparable for substitutional analogs, the result that hydride affinities of the various carbonium ions are uniformly larger than those of siliconium ions reflects the consistently larger homolytic C–H bond strengths, $D(C-H) \approx 98$ kcal/mol, as compared to Si–H bond strengths, $D(Si-H) \approx 90$ kcal/mol.[18] The incremental decreases in hydride affinities effected by successive methyl substitution are consistently larger for carbonium ions than siliconium. Furthermore, there is a regular attenuation of the methyl group stabilizing effect observed for carbonium but not siliconium hydride affinities. These differences in methyl substituent effects suggest that π stabilization of the charge center by methyl groups is relatively more effective for carbon charge centers than for silicon, presumably due to poorer spatial overlap of occupied substituent orbitals with Si^+ 3p orbitals as compared with C^+ 2p orbital vacancies in the ions.

Acknowledgments

This research was supported in part by the Energy Research and Development Administration under Grant No. E(04-3) 767-8 and represents one phase of research carried out at the Jet Propulsion Laboratory, California Institute of Technology under Contract No. NAS7-100, sponsored by the National Aeronautics and Space Administration. The PIMS instrumentation was made possible by a grant from the President's Fund of the California Institute of Technology.

References and Notes

(1) For recent reviews of ion cyclotron resonance spectroscopy see J. L. Beauchamp, Annu. Rev. Phys. Chem., 22, 527 (1971); T. A. Lehman and M. M. Bursey, "Ion Cyclotron Resonance Spectrometry", Wiley, New York, N.Y., 1976.

(2) M. K. Murphy and J. L. Beauchamp, J. Am. Chem. Soc., in press.

(3) R. R. Corderman, M. K. Murphy, and J. L. Beauchamp, unpublished results.

(4) (a) F. P. Lossing, Bull. Soc. Chim. Belg., 81, 125 (1972); (b) F. P. Lossing and G. P. Semeluk, Can. J. Chem., 48, 955 (1970).

(5) B. Steiner, C. F. Giese, and M. A. Inghram, J. Chem. Phys., 34, 189 (1971); W. A. Chupka and J. Berkowitz, ibid., 47, 2921 (1967).

(6) A. D. Williamson, P. R. LeBreton and J. L. Beauchamp, J. Am. Chem. Soc., 98, 2705 (1976).

(7) (a) P. Potzinger, A. Ritter, and J. Krause, Z. Naturforsch., 30A, 347 (1975); (b) J. R. Krause and P. Potzinger, Int. J. Mass Spectrom. Ion Phys., 18, 303 (1975).

(8) G. P. van der Kelen, O. Volders, H. van Onckelen, and Z. Eeckhaut, Z. Anorg. Allg. Chem., 338, 106 (1965).

(9) M. K. Murphy and J. L. Beauchamp, J. Am. Chem. Soc., 99, 2085 (1977).

(10) R. R. Corderman, P. R. LeBreton, S. E. Buttrill, A. D. Williamson, and J. L. Beauchamp, J. Chem. Phys., 65, 4929 (1976); P. R. LeBreton, A. D. Williamson, J. L. Beauchamp, and W. T. Huntress, J. Chem. Phys., 62, 1623 (1975); A. D. Williamson, Ph.D. Thesis, California Institute of Technology (1975).

(11) R. C. Weast, Ed., "Handbook of Chemistry and Physics", 51st ed., Chemical Rubber Co., Cleveland, Ohio, 1970, p. B-252.

(12) G. Herzberg, "Infrared and Raman Spectra of Polyatomic Molecules", D. Van Nostrand Co., Princeton, N.J., 1955.

(13) B. P. Pullen, T. A. Carlson, W. E. Moddeman, G. K. Schweitzer, W. E. Bull, and F. A. Grimm, J. Chem. Phys., 52, 768 (1970).

(14) T. M. Mayer and F. W. Lampe, J. Phys. Chem., 78, 2422 (1974).

(15) W. A. Chupka, J. Chem. Phys., 30, 191 (1959); ibid., 54, 1936 (1971); T. Walter, C. Lifshitz, W. A. Chupka, and J. Berkowitz, ibid., 51, 3531 (1969); M. L. Vestal in "Fundamental Processes in Radiation Chemistry", P. Ausloss, Ed., Wiley Interscience, New York, N.Y., 1968.

(16) D. R. Stull and H. Prophet, "JANAF Thermochemical Tables", 2nd ed., Natl. Stand. Ref. Data Ser. Natl. Bur. Stand., No. 37 (1971).

(17) J. D. Cox and G. Pilcher, "Thermochemistry of Organic and Organometallic Compounds", Academic Press, New York,

N.Y., 1970.

(18) R. Walsh and J. M. Wells, J. Chem. Soc. Faraday Trans. I, 72, 100 (1976).